INFLUENCE OF LIGHTWEIGHT EXPANDED PERLITE AND VERMICULITE ON THE PROPERTIES OF GROUND GRANULATED BLAST FURNACE SLAG AND FLY ASH-BASED MORTAR

TIE TZER SHENG

FACULTY OF ENGINEERING
UNIVERSITI MALAYA
KUALA LUMPUR

2022

INFLUENCE OF LIGHTWEIGHT EXPANDED PERLITE AND VERMICULITE ON THE PROPERTIES OF GROUND GRANULATED BLAST FURNACE SLAG AND FLY ASH-BASED MORTAR

TIE TZER SHENG

DISSERTATION SUBMITTED IN FULFILMENT OF THE REQUIREMENTS FOR THE DEGREE OF MASTER OF ENGINEERING SCIENCE

FACULTY OF ENGINEERING
UNIVERSITI MALAYA
KUALA LUMPUR

2022

UNIVERSITI MALAYA

ORIGINAL LITERARY WORK DECLARATION

Name of Candidate : **Tie Tzer Sheng**

Matric No : **17050910/1 (KGA170020)**

Name of Degree : **Master of Engineering Science**

Title of Project Paper / Research Report / Dissertation / Thesis ("this Work"):
Influence of lightweight expanded perlite and vermiculite on the properties of ground granulated blast furnace slag and fly ash-based mortar

Field of Study : **Structural Engineering & Materials**

I do solemnly and sincerely declare that:

1) I am the sole author / writer of this Work;
2) This Work is original;
3) Any use of any work in which copyright exists was done by way of fair dealing and for permitted purposes and any excerpt from, or reference to or reproduction of any copyright work has been disclosed expressly and sufficiently and the title of the Work and its authorship have been acknowledged in this Work;
4) I do not have any actual knowledge nor do I ought reasonably to know that the making of this work constitutes an infringement of any copyright work;
5) I hereby assign all and every rights in the copyright to this Work to the University of Malaya ("UM") who henceforth shall be owner of the copyright in this Work and that any reproduction or use in any form or by any means whatsoever is prohibited without the written consent of UM having been first had and obtained;
6) I am fully aware that if in this course of making this Work I have infringed any copyright whether intentionally or otherwise, I may be subject to legal action or any other action as may be determined by UM.

Candidate's Signature Date: 20/12/2021

Subscribed and solemnly declared before,

Witness's Signature Date: 6/1/2022

Name :
Designation :

INFLUENCE OF LIGHTWEIGHT EXPANDED PERLITE AND VERMICULITE ON THE PROPERTIES OF GROUND GRANULATED BLAST FURNACE SLAG AND FLY ASH-BASED MORTAR

ABSTRACT

The production of cement is highly energy-intensive and contributes to 7% of total worldwide CO_2 emission which can cause the environmental problem and threaten to the earth's atmosphere. Adopting supplementary cementitious materials (SCM) can help to reduce the dependency on cement in moving towards the use of sustainable construction materials. Increasing calls for more efficient construction materials also encourages the use of lightweight materials. Hence, this research is carried out to investigate the influence of lightweight aggregate, namely expanded perlite (EP) and expanded vermiculite (EV), in terms of the key and functional properties of ground granulated blast furnace slag (GGBS) and fly ash-blended mortar. As mechanical strength is not the prime consideration in mortar, high volume of the lightweight aggregate (>50%) as sand replacement was promoted. Likewise, SCM such as GGBS and fly ash is also utilized as substantial amount of partial cement replacement (>30%) for the sustainability of the mortar. The framework of this research was categorized into two phases, where Phase I focuses on the determining the combination of materials (SCM and lightweight aggregate) to obtain suitable mix based on targeted density (1400kg/m^3 to 1600kg/m^3) and 28 days strength (≥ 5.17MPa). The mortars mixed with 50% lightweight fine aggregate (EP or EV) with or without the use of 30% SCM (GGBS or fly ash) could achieve the targeted density and strength. Based on this, the mortars are categorized as Mortar Type N with Density Class D1.6, while the mortars mixed with 50% EP as sand replacement can be

categorized as soft mortar due to higher flow diameter (≥200mm) than EV mortar. Response surface methodology (RSM) was also found to be useful to provide the mathematical prediction equation for density and strength and optimize the mix design of the lightweight mortar. The mortars which achieved targeted density and strength were then selected for further investigation in Phase II. In Phase II, the key properties (flow, water retention, density, compressive strength and water sorptivity) and functional properties (sound absorption and solar reflectance) of the selected mortars were evaluated. All selected mortars mixed with the lightweight aggregates (50% EP or EV) with or without 30% SCM showed high water retention (≥91%), while mortars with EP showed the highest flow diameter. In overall, among the investigated mortars, the lightweight mortar mixed by 30% GGBS as cement replacement with 50% EP as sand replacement presented the best combination as it had adequate fresh properties (flow = 232mm and water retention = 92%), achieved the targeted density (1460kg/m^3) and strength (5.8MPa), lowest sorptivity (0.947mm.min$^{-0.5}$), exhibited good sound absorption coefficient (α = 0.26 and NRC = 0.17) and high solar reflectance index (SRI = 0.63). Compared to conventional mortar, the mix is good for echo sound or noise absorption and imparts addition features such as solar heat or solar light reflection when applied as building material.

Keywords: Lightweight mortar, lightweight aggregate, supplementary cementitious materials, responses surface methodology (RSM), key properties, functional properties.

PENGARUH EXPANDED PERLITE DAN VERMICULITE TERHADAP SIFAT-SIFAT DALAM MORTAR CAMPURAN DENGAN GROUND GRANULATED BLAST FURNACE SLAG DAN FLY ASH

ABSTRAK

Pengeluaran simen berintensifkah tenaga dan menyumbang kepada 7% daripada jumlah pelepasan CO_2 di seluruh dunia yang boleh menyebabkan masalah persekitaran dan mengancam atmosfera bumi. Penggunaan supplementary cementitious materials (SCM) dapat membantu mengurangkan kebergantungan pada simen untuk bergerak ke arah penggunaan bahan binaan lestari. Meningkatkan permintaan untuk bahan binaan yang lebih cekap juga mendorong penggunaan bahan ringan. Oleh itu, kajian ini dijalankan untuk mengkaji pengaruh agregat ringan dinamakan expanded perlite (EP) dan expanded vermiculite (EV), dari segi sifat utama dan sifat fungsional dalam mortar campuran dengan ground granulated blast furnace slag (GGBS) dan fly ash. Oleh kerana kekuatan mekanikal yang tinggi bukanlah pertimbangan utama dalam kajian ini, jumlah agregat ringan yang tinggi (>50%) sebagai penggantian pasir dipromosikan. Begitu juga, SCM seperti GGBS dan fly ash digunakan sebagai sejumlah besar penggantian simen separa (>30%) untuk kelangsungan mortar. Kerangka kajian ini dikategorikan kepada dua fasa, Fasa I memfokuskan pada penentuan kombinasi bahan (SCM dan agregat ringan) untuk mendapatkan campuran yang sesuai berdasarkan kepadatan yang disasarkan (1400kg/m^3 hingga 1600kg/m^3) dan kekuatan 28 hari (≥5.17MPa). Mortar yang dicampurkan dengan agregat halus ringan 50% (EP atau EV) dengan atau tanpa penggunaan 30% SCM (GGBS atau fly ash) dapat mencapai ketumpatan dan kekuatan yang disasarkan. Berdasarkan ini, mortar dikategorikan sebagai Mortar Jenis N dengan

ketumpatan Kelas D1.6, manakala mortar bercampur dengan 50% EP sebagai pengganti pasir boleh dikategorikan sebagai mortar lembut kerana diameter aliran yang lebih tinggi (≥ 200mm) daripada EV mortar. Response Surface Methodology (RSM) juga didapati berguna untuk memberikan persamaan ramalan matematik untuk ketumpatan dan kekuatan dan mengoptimumkan reka bentuk campuran mortar ringan. Mortar yang mencapai ketumpatan dan kekuatan yang disasarkan kemudian dipilih untuk kajian lebih lanjut dalam Fasa II. Di Fasa II, sifat utama (aliran, pengekalan air, ketumpatan, kekuatan mampatan dan daya serap air) dan sifat fungsional (penyerapan bunyi dan pantulan solar) dari mortar yang dipilih telah dinilai. Semua mortar dipilih bercampur dengan agregat ringan (50% EP atau EV) dengan atau tanpa 30% SCM menunjukkan pengekalan air yang tinggi (≥91%), manakala mortar dengan EP menunjukkan diameter aliran tertinggi. Secara keseluruhan, antara mortar yang disiasat, mortar ringan yang campur sebanyak 30% GGBS sebagai pengganti simen dengan 50% EP sebagai penggantian pasir menunjukkan kombinasi yang terbaik kerana jenis campuran ini mempunyai sifat segar yang mencukupi (aliran = 232mm dan pengekalan air = 92%), mencapai ketumpatan sasaran (1460kg/m3) dan kekuatan (5.8MPa), daya serapan terendah ($0.947 mm.min^{-0.5}$), menunjukkan pekali serapan bunyi yang baik (α = 0.26 dan NRC = 0.17) dan indeks pemantulan suria yang tertinggi (SRI = 0.63). Berbanding dengan mortar konvensional, campuran ini bagus untuk bunyi gema atau penyerapan hingar dengan memberikan ciri-ciri tambahan seperti haba suria atau pantulan cahaya suria apabila campuran ini digunakan untuk bahan binaan. Oleh itu, penggunaan buih akustik tambahan atau bahan penebat haba boleh diminimumkan.

Kata kunci: Mortar ringan, agregat ringan, supplementary cementitious materials, responses surface methodology (RSM), sifat utama, sifat fungsional

ACKNOWLEDGEMENTS

First of all, I would like to take this opportunity to express my gratefulness and thankfulness to both of my supervisors, Ir. Ts. Dr. Mo Kim Hung and Associate Professor Dr. Ubagaram Johnson Alengaram for their guidance, limitless support and willingness to share their knowledge for me to kick start for this research, Their efforts, encouragement, patience, valuable suggestions and comments have motivated me to have a positive thinking when went through the overall research process until I complete my master study.

In addition, I wish to express my deepest appreciate to all of my friends who always assist and gave their ultimate support to me especially when I carried out laboratory work. I also need to express my special thanks to all the laboratory technicians for their assistance in ensuring the successful completion of my experiments. I offer my kindest regards and blessing to all of those who had supported me for this research.

Last but not least, I would like to express my sincere gratitude to my parents who giving me the strength, motivation, patience and financial support to complete my master study successfully.

Research Is Creating New Knowledge

TABLE OF CONTENT

ABSTRACT ... iii

ABSTRAK ... v

TABLE OF CONTENT ... viii

LIST OF FIGURES ... xii

LIST OF TABLES ... xiv

LIST OF SYMBOLS ... xvi

LIST OF ABBREVIATIONS ... xviii

CHAPTER 1: INTRODUCTION ... 1

1.1 Background ... 1

1.2 Problem Statement ... 3

1.3 Research objective ... 6

1.4 Scope of work ... 6

1.5 Research Significance ... 7

CHAPTER 2: LITERATURE REVIEW ... 8

2.1 General ... 8

2.2 SCM and its influence ... 9

2.2.1 GGBS ... 9

2.2.1.1 Effect of GGBS on flow/workability in cement-based products ... 10

2.2.1.2 Effect of GGBS on strength in cement-based products ... 11

2.2.2 Fly ash ... 12

2.2.2.1 Effect of fly ash on flow/workability in cement-based products ... 13

2.2.2.2 Effect of fly ash on strength in cement-based products ... 14

2.3 Lightweight aggregate and its influence ... 16

2.3.1 Expended vermiculite (EV) ... 16

2.3.1.1 Effect of EV on flow/workability 17

2.3.1.2 Effect of EV on density 18

2.3.1.3 Effect of EV on strength 18

2.3.2 Expanded perlite (EP) 19

2.3.2.1 Effect of EP on flow/workability 20

2.3.2.2 Effect of EP on density 20

2.3.2.3 Effect of EP on strength 21

2.4 Fresh properties of lightweight cement mortar/concrete 22

2.4.1 Flow/workability 22

2.4.2 Water retention 23

2.5 Hardened properties of lightweight cement mortar/concrete 24

2.5.1 Density 24

2.5.2 Strength 25

2.5.3 Water sorptivity 27

2.6 Functional properties of non-traditional concrete 29

2.6.1 Sound absorption 29

2.6.2 Solar reflectance 33

2.6.3 Summary 36

CHAPTER 3: MATERIALS AND TEST METHODS 38

3.1 Research flow chart 38

3.2 General 39

3.3 Raw materials 39

3.3.1 Binder (Cement and SCM) 39

3.3.2 Fine and lightweight aggregate 40

3.4 Mix proportion, mix procedure and sample preparation 41

3.5 Phase I 42

3.5.1 Compressive strength 43
3.5.2 Response surface methodology (RSM) 44
3.6 Phase II 46
3.6.1 Water retention 47
3.6.2 Water sorptivity 48
3.6.3 Sound absorption 49
3.6.4 Solar Reflectance 50
CHAPTER 4: RESULTS AND DISCUSSION 55
4.1 General 55
4.2 Phase I 55
4.2.1 Flow diameter 55
4.2.2 Density 59
4.2.3 Compressive Strength 62
4.2.4 RSM modelling and analysis 65
4.2.4.1 GGBS mortar with EP as sand replacement 68
4.2.4.2 GGBS mortar with EV as sand replacement 72
4.2.4.3 Fly ash mortar with EP as sand replacement 75
4.2.4.4 Fly ash mortar with EV as sand replacement 79
4.2.4.5 Validation of experiment 83
4.3 Phase II 84
4.3.1 Fresh properties (flow diameter and water retention) 85
4.3.2 Density 87
4.3.3 Compressive strength 88
4.3.4 Sorptivity 91
4.3.5 Sound absorption 93
4.3.6 Solar reflectance 96

CHAPTER 5: CONCLUSION & RECOMMENDATIONS 101

5.1 Conclusion 101

5.2 Recommendations.. 103

REFERENCE 104

LIST OF PUBLICATION.. 119

LIST OF FIGURES

Figure 1.1: Schematic diagram of lightweight mortar in terms of functional properties.. 5

Figure 2.1: Expanded vermiculite (Koksal et al., 2015). 17

Figure 2.2: Expanded perlite (Rashad, 2016a). 19

Figure 2.3: Linear correlation between density and compressive sterngth for lightweight mortar (Lanzon Torres and Garcia-Ruiz, 2009). 26

Figure 2.4: Sound absorption coefficient of concrete paving block containing various amount of crumb rubber (Ling et al., 2010). 30

Figure 2.5: Illustration of trapped air in crumb rubber concrete (Bashar et al., 2012). .. 31

Figure 2.6: Sound absorption of specimen containing various BA contents (Leiva et al., 2012). (PC = pervious concrete, SC = standard concrete). 32

Figure 2.7: Concrete without (left) and with cenosphere (right) (Tiwari et al., 2004). .. 33

Figure 2.8: Schematic diagram of pyranometer measurement (Akbari et al., 2008). 34

Figure 3.1: Research flow chart. 38

Figure 3.2: Size distribution of fine sand, EP and EV. 41

Figure 3.3: Cube samples were cast into steel mould. 44

Figure 3.4: Apparatus for water retention test. 48

Figure 3.5: Sound absorption samples used in Phase II. 50

Figure 3.6: Impedance tube measurement based on ISO10534-2. 50

Figure 3.7: White colour surface. 52

Figure 3.8: Black colour surface. 52

Figure 3.9: Setup of pyranometer with cylindrical curtain shade. 53

Figure 3.10: RGB analysis for sample F30-EP50. 54

Figure 4.1: Flow value of GGBS mortar containing EV and EP as sand replacement... 55

Figure 4.2: Flow value of fly ash mortar containing EV and EP as sand replacement... 56

Figure 4.3: 28-day density of GGBS-blended mortar. 59

Figure 4.4: 28-day density of fly ash-blended mortar. 59

Figure 4.5: 28-day strength of GGBS-blended mortar. 63

Figure 4.6: 28-day strength of fly ash-blended mortar. 63

Figure 4.7: Contour plot and response surface of flow, density and strength for GGBS mortar with EP. 71

Figure 4.8: Contour plot and response surface of flow, density and strength for GGBS mortar with EV. 75

Figure 4.9: Contour plot and response surface of flow, density and strength for fly ash mortar with EP. 79

Figure 4.10: Contour plot and response surface of flow, density and strength for fly ash mortar with EV. 83

Figure 4.11: Flow value of selected samples. 85

Figure 4.12: Water retention value of selected samples. 86

Figure 4.13: Crack pattern of lightweight mortars. 89

Figure 4.14: Appearance of mortars after completion of sorptivity test. 92

Figure 4.15: Sound absorption coefficient for Phase II samples. 95

Figure 4.16: Appearance of the mortar samples in solar reflectance test. 98

Figure 4.17: Comparison between SRI value from RGB histogram analysis with protocol measurement. 98

LIST OF TABLES

Table 2.1: Composition requirement of GGBS (BS EN 15167-1: 2006) 9

Table 2.2: Chemical composition of GGBS 9

Table 2.3: Chemical composition of fly ash 13

Table 2.4: Chemical composition of vermiculite (Rashad, 2016b) 16

Table 2.5: Strength reduction variation of EV mortars 19

Table 2.6: Chemical composition for EP 20

Table 2.7: Strength reduction variation of EP sample 22

Table 2.8: Representative values of solar reflectance 35

Table 3.1: Chemical composition of GGBS and fly ash 40

Table 3.2: Combination mix for Phase I 43

Table 3.3: Additional replacement levels of materials for RSM analysis 45

Table 3.4: Factors and factor levels adopted for RSM 46

Table 3.5: Factor combinations as per face-centered composite for all mixes 46

Table 3.6: Combination mix for Phase II 47

Table 4.1: Differences of flow value between Phase I samples with control mortar 57

Table 4.2: Differences of density between Phase I samples with control mortar 61

Table 4.3: Differences of strength between Phase I samples with control mortar 64

Table 4.4: Actual and predicted values for GGBS mortar with EP 66

Table 4.5: Actual and predicted values for GGBS mortar with EV 67

Table 4.6: Actual and predicted values for fly ash mortar with EP 67

Table 4.7: Actual and predicted values for fly ash mortar with EV 68

Table 4.8: Analysis of variance (ANOVA) for flow, density and strength for GGBS with EP samples by RSM model 69

Table 4.9: Analysis of variance (ANOVA) for flow, density and strength for GGBS with EV samples by RSM model 72

Table 4.10: Analysis of variance (ANOVA) for flow, density and strength for fly ash with EP samples by RSM model 76

Table 4.11: Analysis of variance (ANOVA) for flow, density and strength for fly ash with EV samples by RSM model 80

Table 4.12: Validation of the responses surface model for different types of samples .. 84

Table 4.13: Comparison result between experimental data and RSM analysis 84

Table 4.14: Differences in density between Phase II with Phase I and RSM prediction 88

Table 4.15: Difference of strength between Phase II with Phase I 89

Table 4.16: Average value of sorptivity coefficient with the standard deviation 91

Table 4.17: NRC for selected mortar samples 96

LIST OF SYMBOLS

a : Mass of dry mortar mixture, used for preparing whole batch of mortar (g)

A, B : Independent variables

CO_2 : Carbon Dioxide

CR : Crumb rubber

D : RSM Prediction

D_f : Degrees of freedom

Diff. : Differences (%)

E : Residual

EP : Expanded perlite

EV : Expanded vermiculite

F30-EP50 : 30% cement replaced by fly ash and 50% replaced by expanded perlite

GGBS : Ground granulates blast furnace slag

G30-EV50 : 30% cement replaced by ground granulated blast furnace slag and 50% sand replaced by expanded vermiculite

G30-EV50 : 30% cement replaced by ground granulated blast furnace slag and 50% sand replaced by expanded vermiculite

Hz : Hertz

I : Absorption (mm)

I_H : 1st time incoming horizontal global solar irradiance

I'_H : 2nd time incoming horizontal global solar irradiance

R : Water retention value (%)

R_b : Reflected solar irradiance from black cloth

R_t : Reflected solar irradiance from uncovered sample

R_w : Reflected solar irradiance from white cloth

R^2 : Coefficient of determination between the dependent variable and the fitted values

U : Mass of rigid mould (g)

V : Mass of 5 unused dry filter paper (g)

W : Mass of rigid mould, with fresh mortar (g)

W_1 : The weight of dried cubic mortar (g)

W_2 : The weight of cubic mortar after absorbed by water (g)

X : Mass of 5 wet filter paper (g)

$\overline{X}$: Mean square

y : predicted response

y_1 : Mass of water added to the prepared mortar (g)

Z : Mass of water present (g)

z_1 : Mass of absorbed water (g)

α : Sound absorption coefficient

β_0 : Intercept

β_1, β_2 : Linear effect coefficients

β_{11}, β_{12} : Quadratic effect coefficient

β_{12} : Interaction effect coefficient

e : exponential function

$\sum X$: Sum of square

LIST OF ABBREVIATIONS

ANOVA	: Analyses of the variance
ASTM	: American Standard for Testing and Materials
BA	: Bottom ash
C	: Experiment results
CA	: Coarse aggregates
COV	: Coefficient of variation
C-S-H	: Calcium silicate hydrate
ISO	: International Organization for Standardization
ITZ	: Interfacial transition zone
NRC	: Noise reduction coefficient
PC	: Pervious concrete
PSD	: Particle size distribution
Residual SD	: Residual standard deviation
RGB	: Red, green and blue histogram
RSM	: Response surface methodology
SC	: Standard concrete
SCM	: Supplementary cementitious materials
SRI	: Solar reflectance index
SSD	: Saturated surfaced dry
XRF	: X-ray fluorescence

CHAPTER 1: INTRODUCTION

1.1 Background

Mortar for masonry construction can be classified into two major categories, namely, rendering mortar and masonry (bedding) mortar (Mortar Industry Association, 2015). The former is applied in external or internal renderings on wall, ceiling, and partitions, whereas bedding mortar is used to lay and bind construction units such as bricks or blocks. Mortar is formed by using cement as a binder which hardens and adheres with sand through hydration process. Most commonly, Portland cement mortar and lime mortar are used in construction industry. However, the usage mortars in construction industry directly will add on the demand of cement production especially in developing countries. The total output of cement globally in year 2012 was about 3.6 billion tons (Zhang et al., 2013). The amount was increased by more than 4 billion tons in year 2014 (Ofosu-Adarkwa et al., 2020) and it is expected that the demand of cement in global will rise by up to 400% in year 2050 (Damtoft et al., 2008).

Cement manufacturing is a major contributor of greenhouse gases, especially for CO_2 emission (Ali et al., 2011; Amato, 2013). The cement industry is responsible for approximately 7% of total worldwide CO_2 emission and the cement subsector consumes about 12-15% of the total industrial energy use (Ali et al., 2011). This is due to the raw materials in the production of cement and burning fuels needed to maintain high temperature in cement kiln. Hence, adopting cement as the binder in either mortar or concrete indirectly causes environmental problems and threaten the earth's atmosphere. As the trend is moving towards sustainability in the construction industry, the environmental impact of cement in cement products needs to be reduced.

Supplementary cementitious materials (SCM) such as ground granulated blast furnace slag (GGBS), fly ash, silica fume and metakaolin are commonly used in mortar or concrete (Yang et al., 2014; Srivastava et al., 2018). Due to the hydraulic properties and fineness nature of GGBS, the use of GGBS as cement replacement in mortar or concrete can density the cement matrix and resulted in compressive strength and durability improvement (Oner and Akyuz, 2007; Xie et al., 2019). Similarly for the use of fly ash as cement replacement, the rich silica content of fly ash contributed on the pozzolanic reaction for mortar or concrete (Muthusamy et al., 2021) resulting a better compressive strength due to additional calcium silica hydrate (C-S-H) produced in the cement matrix at later ages.

Moreover, the use of SCM as cement replacement is also beneficial to the environment by reducing the carbon footprint. Radwan et al. (2021a) reported that CO_2 emission was reduced about 18% to 20% when maximum of 20% fly ash or GGBS was used as cement replacement. High volume cement replacement by 50% with either fly ash or GGBS can reduce the CO_2 emission by up to 47 %. Likewise, CO_2 emission reduction as high as 66% was reported when 70% cement was replaced by the SCM (fly ash and GGBS) (Radwan et al., 2021b).

Besides that, recently, there has been several research which investigated the use of lightweight aggregate such as expanded vermiculite (EV) (Koksal et al., 2015; Rashad, 2016b), expanded perlite (EP) (Sengul et al., 2011; Rozycka and Pichor, 2016; Rashad, 2016a; Lu et al., 2018), expanded polystyrene (Ferrandiz-Maz et al., 2014) and expanded granulated cork (Borges et al., 2018) in mortar or concrete production. The aim is to enhance the energy efficiency of building in terms of reducing self-weight, improving sound and thermal insulation of the construction materials. For example, the inclusion of lightweight aggregate as sand replacement in mortar or concrete is able to reduce the overall self-weight of the building structure due to lower specific gravity. Compared to sand, platy and sponge-like structure of EV and open pores surface of EP are also beneficial for sound and thermal insulations in the mortar or concrete (Rashad, 2016a; Rashad, 2016b). This is because numerous air voids can be formed in the matrix which can act as an insulator to absorb the sound or noise from surrounding and hinder the transmission of heat energy. Hence, it can minimize the dependency on soundproof or thermal insulation materials in the building, ensuring the comfort of occupants in the building, as well as reducing electricity consumption required to cool the building spaces.

Apart from these, combining the use of SCM such as GGBS with lightweight aggregate in mortar or concrete could be potential alternative to improve the energy efficiency of building. Compared to the used of Portland cement, the off-white colour of GGBS can whiten the appearance of mortar or concrete. Generally, white surface of mortar or concrete is not only good in aesthetic, it can lower the surface temperature experienced by the building by naturally reflecting the solar heat from the building's surface. Gradually, less energy is needed to cool down the interior of the building.

1.2 Problem Statement

To minimize the environmental pollution from cement production, many of the researchers explored the use SCM such as GGBS (Cerulli et al., 2003; Thakur et al., 2016) and fly ash (Chindaprasirt et al., 2005; Christy and Tensing, 2010) as cement replacement in the mix for the mortar or concrete products. GGBS is a by-product from the manufacturing process of iron in the blast furnace. The selection of GGBS as SCM for mortar or concrete is due to the similar cementitious properties as cement. However, adopting GGBS as cement replacement in mortar or concrete can cause low early strength compared to using only cement. This is due to the slow hydraulic reaction of GGBS and the strength of GGBS mortar or concrete is only accelerated at the later ages. However, this later age effect cannot compensate for the strength loss when high volume of GGBS (>50%) is used to replace cement. This is mainly because of the greater effect of cement content dilution with GGBS which is more significant (Thakur et al., 2016). Hence, past researchers reported that optimum strength could be obtained for mortar (Chin et al., 2020) or concrete (Oner and Akyuz, 2007; Thakur et al., 2016; Chowdary et al., 2017; and Xie et al., 2020) when around 30% to 50% of cement was replaced by GGBS.

Fly ash is another type of industrial by-product used as SCM for mortar or concrete due to the silica content. In general, adopting fly ash as cement replacement for mortar or concrete can induce pozzolanic reaction and produce additional calcium silicate hydrate (C-S-H) product, thus increasing the overall strength. However, due to the slow pozzolanic reaction of fly ash, the early strength of mortar or concrete is typically lower compared to GGBS. It was reported that the reduction of 28 days compressive strength for mortar (Chindaprasirt et al., 2005; Christy and Tensing, 2010; He et al., 2019) or concrete (Duran-Herrera et al, 2011; Huang et al, 2013) was obtained when more than 50% of fly ash was used. The pozzolanic reaction is similarly offset by the cement content dilution when high volume of cement was replaced by fly ash. Hence, it is clear that the use of SCM such as GGBS and fly ash as high-volume cement replacement still has its drawbacks in normal cement mortar or concrete.

Nowadays, researchers began to explore the use of alternative aggregate in mortar or concrete to promote better and improved building energy efficiency. Majority of previous works discussed on the use of lightweight aggregate for the improvement in the thermal performance of mortar or concrete besides the evaluation of its mechanical properties (Sengul et al., 2011; Ferrandiz-Maz et al., 2014; Koksal et al., 2015; Rozycka and Pichor, 2016; Rashad, 2016a; Lu et al., 2018). Although usage of lightweight aggregate can reduce the mechanical properties of mortar/concrete, the inherently porous nature of lightweight aggregate increased the porosity content which can decreased the functional thermal conductivity as more air was present in the pores. Such lightweight aggregate concrete product helps in reducing heat transmission, improving the thermal comfort of occupants in the building structure. However, there is lack of work which discusses on other functional properties like sound absorption and solar reflectance for lightweight mortar or concrete (Figure 1.1). These functional properties can also be linked to the building's energy efficiency and comfort of the occupants.

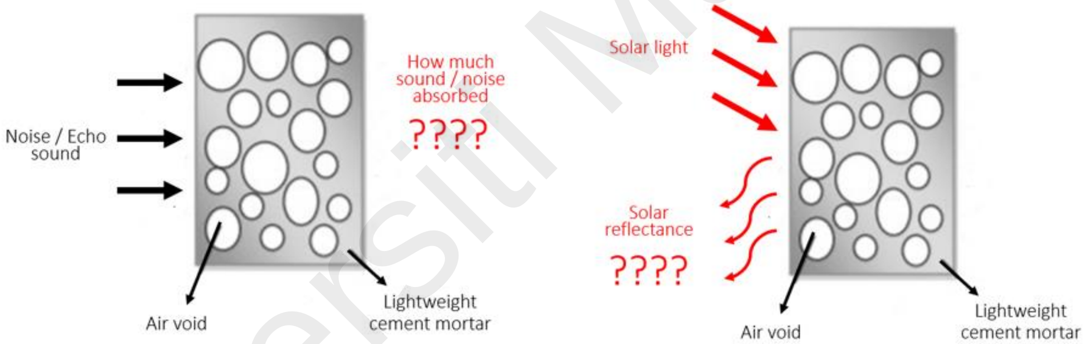

Figure 1.1: Schematic diagram of lightweight mortar in terms of functional properties.

Although the use of high volume of SCM and lightweight aggregate may be detrimental for the strength of cement mortar, unlike concrete, there is only need of sufficient strength, which is typically low, for mortar application. Hence, the usage of high contents of these materials (SCM and lightweight aggregate) in cement mortar is justifiable. This research therefore aims to evaluate the influence of using high volume of commercially available SCM (GGBS and fly ash) and lightweight aggregate (EV and EP) in the country towards the key and functional properties of the produced lightweight cement mortar. The selection of EV and EP as lightweight aggregate in this study was mainly due to the similar properties and commercially available in the country.

1.3 Research objective

This research was conducted to assess the properties of lightweight cement mortar utilizing SCM. The main research objectives are:

1. To determine the optimum combination of high volume SCM (GGBS and fly ash) and lightweight fine aggregate (EV and EP) in cement mortar.
2. To evaluate the influence of SCM (GGBS and fly ash) and lightweight fine aggregate (EV and EP) on the key properties of cement mortar.
3. To assess the functional properties (sound absorption and solar reflectance) of the lightweight cement mortar containing SCM.

1.4 Scope of work

The scope of this research is to investigate the influence of combining SCM (GGBS and fly ash) as cement replacement with the selected commercially available lightweight fine aggregate (EP and EV) that are available in the country as sand replacement in cement mortar. With this, the replacement levels of 30%, 50% and 70% were selected as cement replacement. For sand replacement, partial (50%) and full amount (100%) of EP or EV were evaluated in this research. The overall framework for this study is categorized into two phases, namely Phase I and Phase II. Phase I focus on determining the combination of materials (SCM and lightweight aggregate) to produce suitable mix based on the targeted density (to achieve density in the range of 1400 kg/m^3

to 1600kg/m^3) and 28 days strength (to achieve minimum strength of 5.17MPa) for lightweight cement mortar. A total of 30 types of mixtures were prepared in this study. Response surface methodology (RSM) was used to provide the mathematical prediction equations and optimize the mix design based on the selected properties (density and strength) of the lightweight cement mortar. Based on Phase I, a total of 6 mixtures achieved the targeted density and strength. Hence, these mixtures were prepared for Phase II. In Phase II, the key properties of cement mortar, such as flow, water retention, density, compressive strength and water sorptivity were evaluated. Furthermore, the functional properties such as sound absorption and solar reflectance of the lightweight cement mortar are also analyzed in Phase II. This is done to assess the possibility of imparting these added-value functional properties by using the lightweight cement mortar.

1.5 Research Significance

This research aims to explore an alternative and eco-friendly lightweight cement mortar which can exhibit the required performance as those expected of normal mortar. Besides able to reduce usage of cement (and the associated environmental impact) with high volume SCM, the inclusion of the lightweight aggregate is believed to be able to impart additional features such as aesthetic (bright or white appearance), sound absorption and solar reflectance functions to the cement mortar. This shall introduce a more useful construction for improving the energy efficiency of building with enhanced comfort for occupants of the buildings.

CHAPTER 2: LITERATURE REVIEW

2.1 General

By-products refer to the waste substances or objects that are produced from manufacturers. It generally acts as the secondary or incidental products proposed by industries with aim to reduce the wastes pollution and enhance greening environment. Industrial by-products such as GGBS and fly ash are widely used as SCM commercially in the cement industry. These types of by-products generally possess hydraulic and pozzolanic characteristics, respectively. Hence, adopting these by-products as cement replacement in cement mortar may alter the key properties. EP and EV also appears to be the latest alternative lightweight fine aggregate with aim to improve the functional characteristics of cement mortar due to the low self-weight, high porosity content, good thermal and acoustic properties of lightweight aggregate.

With these, the sub-sections below summarize the related literature regarding the effect of using high volume GGBS and fly ash as SCM in mortar or concrete. The influence of lightweight aggregate (EP and EV) in terms of fresh and hardened properties of mortar or concrete is also evaluated. The key properties (flow, water retention, density, compressive strength and water sorptivity) for lightweight aggregate mortar or concrete are also discussed in this chapter. The functional properties of sound absorption and solar reflectance for modified cement-based materials from the literature are also detailed.

2.2 SCM and its influence

2.2.1 GGBS

GGBS is a by-product from the manufacturing of iron. It is obtained from the blast furnace of iron ore, limestone and coke under high temperature of 1500° C (Hawileh et al., 2017). The iron ore from blast furnace is reduced to iron and the remaining materials from slag will float on top of it. The slag is then being tapped off as molten liquid which consist of the characteristics of alumina, silica, calcium oxide and magnesium oxide. The molten slag is allowed to be quenched under high pressure of water jet with aim to obtain the granulated slag. The quenching of these particles is then be dried and ground into fine powder to form the GGBS. Table 2.1 shows the minimum requirement of GGBS composition according to BS EN 15167-1:2006, whereas Table 2.2 summarizes the chemical composition for GGBS based on literature.

Table 2.1: Composition requirement of GGBS (BS EN 15167-1: 2006)

Characteristics	Test method	Requirement
Magnesium oxide	EN 196-2	≤ 18.0%
Sulfide	EN 196-2	≤ 2.0%
Sulfate	EN 196-2	≤ 2.5%
LOI	EN 196-2	≤ 3.0%
Chloride	EN 196-2	≤ 0.10%

Table 2.2: Chemical composition of GGBS

Chemical composition (%)	Chen and Liu (2008)	Hawileh et al. (2017)	Tavasoli et al. (2018)	Prasath Kumar et al. (2019)
SiO_2	26.40	34.90	26.50	34.90
Al_2O_3	8.00	14.00	7.10	10.20
Fe_2O_3	1.60	0.60	3.00	0.38
CaO	40.30	39.80	58.00	42.70
MgO	4.60	6.00	-	6.74
SO_3	3.20	0.07	1.30	0.66
Na_2O	-	0.46	-	0.51

2.2.1.1 Effect of GGBS on flow/workability in cement-based products

The fresh properties of cement-based materials can be assessed by flowability or workability in terms of flow or slump value. For example, the workability of lightweight concrete mixed by coconut shell (Prasath Kumar et al., 2019), oil palm shell (Shafigh et al., 2013) and expanded clay (Chen and Liu, 2008) as coarse aggregate replacement were increased about by 4% to 36% when maximum of 30% GGBS was used as cement replacement. The improvement of workability was mainly attributed to the grading and smooth texture of GGBS than cement. In addition, the use of GGBS in lightweight concrete is able to increase the workability by reducing the initial hydration of cement (Xie et al., 2019).

In the case of normal concrete, it was highlighted that the use of 50% GGBS as cement replacement presented an increase in the slump value (Thakur et al., 2016; Tavasoli et al., 2018). The obtained slump was about 20% higher than that of the corresponding controls without GGBS. By increasing the GGBS content up to 85%, it was reported that the slump of GGBS concrete can be increased by about 100% higher than conventional concrete (Wainwright and Rey, 2000). The increased in slump value was probably due to the higher chemical modulus of GGBS concrete than conventional concrete (Wainwright and Rey, 2000). The smooth and finer GGBS could be another factor which increased the entrainment of air in the concrete matrix and subsequently increased the volume of paste (Wainwright and Rey, 2000; Siddique and Bennacer, 2012; Thakur et al., 2016).

In contrast, other researchers highlighted that the flow/slump value of normal mortar or concrete was decreased by about 16% when GGBS in the range of 30% to 40% was used as cement replacement (Ling and Poon, 2004; Chowdary et al., 2017). The reduction of flow/slump value was attributed to the use of water-cement ratio which is insufficient for hydration as the fineness of GGBS increased the total surface area per unit volume in the mixture. Hence, it was proposed to increase the water-cement ratio up to 0.60 in the mixture to avoid for the loss in flow/slump value when GGBS content was increased (Lim et al., 2012).

2.2.1.2 Effect of GGBS on strength in cement-based products

In terms of 28 days compressive strength, it was reported that the use of maximum 40% GGBS as cement replacement in lightweight concrete improved the strength by about 6% to 30% (Mo et al., 2015b; Kumar et al., 2019; Sindhuja et al., 2020). For example, Mo et al. (2015c) reported that the compressive strength of oil palm shell concrete was improved by about 6% when 20% of cement was replaced by GGBS. Kumar et al. (2019) reported similar trend as the obtained compressive strength was increased by about 15% to 20% when maximum of 20% GGBS was used in coconut shell concrete. Sindhuja et al. (2020) revealed that the used of 40% GGBS in lightweight expanded clay concrete improved the compressive strength up to 30%. Similarly for the case in normal concrete, past researchers revealed that not more than 50% GGBS as cement replacement increased the compressive strength in the range of 19% to 94% compared to the corresponding conventional concrete (Oner and Akyuz, 2007; Thakur et al., 2016; Tanwar et al., 2021). The improvement in compressive strength for normal or lightweight concrete was mainly attributed to the fineness nature of GGBS particles than cement which improved the packing density and densified the overall cement matrix (Oner and Akyuz, 2007; Thakur et al., 2016; Xie et al., 2019). In addition, the SiO_2 content of GGBS was able to react with calcium hydroxide to form additional C-S-H gels and this caused the strength improvement of normal or lightweight concrete (Kumar et al., 2019; Tanwar et al., 2021).

However, some literatures highlighted that the 28 days compressive strength of lightweight concrete showed reduction trend when more than 50% of cement was replaced by GGBS. Strength reduction in the range of 12% to 26% was found for oil palm shell concrete when more than 50% of GGBS was used as cement replacement (Shafigh et al., 2013; Mo et al., 2015a; Mo et al., 2015b; Mo et al., 2016). Researchers found similar trend for normal concrete when further increase of the cement replacement by GGBS in the range of 50% to 85%, where the reduction of 28 days compressive strength as high as 37% was obtained (Wainwright and Rey, 2000; Thakur et al., 2016; Xie et al, 2020). The reduction of strength for normal or lightweight concrete was attributed due to the high GGBS (>50% replacement) content which was governed by the cement content dilution effect (Oner and Akyuz, 2007; Shafigh et al., 2013; Thakur et al., 2016; Chowdary et al., 2017; Xie et al., 2020). Hence, it can be summarized that the optimum level of GGBS for maximizing strength is up to 50% of cement replacement, depending on the different proportions and types of cement-based materials.

2.2.2 Fly ash

Fly ash is another type of industrial by-products which is produced from the combustion of pulverized coal in thermal power plants. When the pulverized coal is ignited in the combustion chamber, the carbon and volatile materials are burned off. However, some of the mineral impurities of clay, shale and feldspars, are fused in suspension and carried out of the combustion chamber in the exhaust gases. As the exhaust gases cool, the fused materials solidify into spherical glassy particles and called as fly ash (Elmrabet et al., 2019). Most of the fly ash particles are in solid spheres and some are in hollow cenospheres. Typically, a minimum of 50% fly ash has particle sizes between 1μm to 100μm with surface area and specific gravity within range 300–500m^2/kg and 1.9-2.8, respectively (Rashad, 2015). Table 2.3 summarizes the chemical composition of fly ash based on literature. Fly ash generally can be classified into Class C and Class F. Class C fly ash is high-calcium fly ash due to its higher CaO content (>18%) compared to Class F fly ash (≤18%) according to ASTM C618. As compared to Class F fly ash, Class C fly ash is able to exhibit additional hydraulic ability but lesser pozzolanic activity.

Table 2.3: Chemical composition of fly ash

Chemical composition (%)	Chen and Liu (2008)	Shafigh et al. (2013)	Kurt et al. (2015)	Elmrabet et al. (2019)
SiO_2	54.90	64.40	47.50	52.32
Fe_2O_3	6.90	4.00	16.60	4.86
CaO	8.70	1.00	6.60	5.82
MgO	1.80	0.66	4.65	1.41
Al_2O_3	25.80	20.90	15.95	27.27
SO_3	0.60	0.30	3.94	2.01
K_2O	-	1.20	1.96	1.00
Na_2O	0.30	0.32	1.74	-

2.2.2.1 Effect of fly ash on flow/workability in cement-based products

In terms of lightweight concrete, it was reported that the flow was increased by 15% to 25% when maximum of 40% fly ash was used as cement replacement in concrete which incorporated pumice aggregate (Kurt et al, 2015) and expanded clay (Chen and Liu, 2008) as coarse aggregate replacement. Similarly, it was highlighted that the slump of oil palm clinker concrete increased up to 65% when 40% to 50% of cement was replaced by fly ash (Shafigh et al., 2016; Ghazali et al., 2021). Shannag (2011) noticed that the use of 10% fly ash (by weight) in volcanic tuff/pumice concrete increased the slump up to 13% compared to the control sample. In conventional concrete, it was also found that the workability of fly ash concrete was increased in the range of 23% to 54% (Siddique, 2004; Sahmaran and Yuman, 2007; Yoon et al., 2014; Shaikh and Supit, 2015; Gholampour and Ozbakkaloglu, 2017) when a maximum of 60% cement was replaced by fly ash. Whereas for conventional mortar, the flow increased up to 9% when 30% to 45% of fly ash was used as cement replacement (Cheerarot and Jaturapitakkul, 2004; Nguyen et al., 2018). The increment of flow or slump value in either lightweight concrete or conventional concrete/mortar was mainly attributed to the spherical shape and smooth surface of fly ash than cement. In contrast, Herki et al. (2013) revealed that the workability of lightweight concrete mixed by waste polystyrene as aggregate replacement showed decreasing trend when the fly ash content was increased up to 40%. The reduction of workability was contributed by the high carbon content of fly ash which increased the demand of water. In addition, due to the fine content of fly ash which tended to agglomerate in the mixture, Shafigh et al. (2016) highlighted that additional water was required for the mixed to achieve workable lightweight concrete when more than 50% of cement was replaced by fly ash.

2.2.2.2 Effect of fly ash on strength in cement-based products

In terms of 28 days strength, researchers reported that the use of 30% fly ash as cement replacement in lightweight concrete incorporated with coconut shell (Prakash et al., 2019) or pumice aggregate (Tanyildizi and Coskun, 2008) as coarse aggregate replacement resulted in the reduction in strength by about 7% to 14%, respectively. Further increase in the fly ash content up to 50% in expanded clay (Chen and Liu, 2008) or oil palm shell concrete (Shafigh et al., 2016; Ghazali et al., 2021; Muthusamy et al., 2021) could increase the strength loss in the range of 13% to 47%. Similarly for the conventional concrete, the strength of fly ash concrete decreased linearly when high volume of fly ash (>50%) was adopted (Siddique, 2004; Sahmaran and Yaman, 2007; Yoon et al., 2014). For example, the reduction of concrete strength was about 23% to 57% (Ganesh Babu and Saradhi Babu, 2004; Siddique, 2004; Sahmaran and Yaman, 2007; Yoon et al., 2014; Gholampour and Ozbakkaloglu, 2017) when maximum of 50% cement was replaced by fly ash.

In the case of conventional mortar, it was revealed that about 34% of strength loss was obtained when maximum of 50% fly ash was used as cement replacement (He et al., 2019). The main reason of strength reduction in cement-based materials containing fly ash was due to the slow pozzolanic reaction of fly ash which requires longer time to take place and enhance the strength. As high volume of cement was replaced by fly ash, the amount of calcium hydroxide from cement become lesser and this caused the failure of fly ash to generate additional C-S-H in the mixture. In addition, past researchers pointed out that the reduction of later strength could be due to the curing method. The lack of water present during air curing may hinder the pozzolanic reactions for C-S-H production (Muthusamy et al., 2021). Hence, the strength loss was increased when high volume of fly ash was used in cement-based materials.

However, the literature highlighted the different findings on compressive strength when not more than 50% of fly ash was used as cement replacement in conventional mortar or concrete. For example, the compressive strength of cement mortar is close to the control (Sun et al., 2021) or even higher than control (about 12%) (Hsu et al., 2018) when finer particles (5690 cm^2/g - 9632 cm^2/g) of fly ash was used as cement replacement in the range of 20% to 45%. Whereas for the case of self-consolidating concrete, the 28 days compressive strength was increased by about 30% when maximum of 20% cement was replaced by fly ash (Sabet et al., 2013). The increment in strength was probably due to the finer particles of fly ash which is able to demonstrate filling effect in the self-consolidating concrete mixture and the pozzolanic activity could be induced effectively by optimizing the use of fly ash in the mixture.

2.3 Lightweight aggregate and its influence

2.3.1 Expended vermiculite (EV)

Vermiculite is a natural mica-like mineral which formed under natural condition such as hydrothermal alteration of biotite, weathering or phlogopite. The chemical composition of vermiculite is given in Table 2.4. EV (Figure 2.1) can be formed when heat under high temperature of 650-950˚C through the exfoliation process (Rashad, 2016b). EV exhibits advantageous properties such as low thermal conductivity (0.04-0.12W/mK), low bulk density (10-11 times less than its original volume before heating), endurance and chemical inertness compared to conventional aggregate (Schackow et al., 2014; Koksal et al., 2015). The appearance of EV is typically golden-yellow or brown in color.

Table 2.4: Chemical composition of vermiculite (Rashad, 2016b)

Chemical properties	Composition (wt%)
SiO_2	37-42
MgO	12-14
Al_2O_3	10-13
Fe_2O_3	5-17
H_2O	8-18
FeO	1-3

Figure 2.1: Expanded vermiculite (Koksal et al., 2015).

2.3.1.1 Effect of EV on flow/workability

The effect on fresh properties for mortar is greatly influenced by the content and type of aggregate used. For example, it was reported that the flow of fly-ash based geopolymer mortars was reduced by about 11% when 30% of sand was replaced by EV (Gencel et al., 2021). The reduction of flow was attributed to the porous structure of EV which absorbed more water during the fresh mixture. Hence, additional water needs to be added to achieve a workable mortar. However, Karatas et al. (2019) revealed that the flow of self-compacting cement mortar or fly ash-based geopolymer mortar was increased by about 2% when maximum of 30% EV was used as sand replacement. Further increase in the sand replacement by EV up to 60% in cement mortar could increase the flow value by about 11% to 24% (Koksal et al., 2015; Mo et al., 2018). This was probably due to the lower fines content of EV (size less than 0.15mm) than sand which reduced the water demand for fresh mortar (Mo et al., 2018). In addition, it was highlighted that the particles size of EV in the range of 0 to 5mm enhanced the air content in the cement matrix and resulted in the increase in the flow value compared to conventional mortar (Rashad, 2016b; Karatas et al., 2019).

2.3.1.2 Effect of EV on density

The type of aggregates used in mortar or concrete is one of the factors that affect the density. By using lightweight aggregate such as EV, the density of cement mortar was decreased by about 11% (Karatas et al., 2019) and 26% (Mo et al., 2018), respectively when maximum of 60% sand (by volume) was replaced by EV. The density of mortar was also found to reduce by about 37% when the EV/cement ratio was increased from 3 to 7 (Koksal et al., 2020). Similarly in the case of concrete, there was a 12% reduction in density when maximum of 10% (by weight) sand was replaced by EV (Abdul Rahman and Bahu, 2016). The reduction of density in mortar or concrete sample was mainly due to the lightweight (specific gravity of about 1.17) and porous structure of EV than sand which increased the porosity in the mixture.

2.3.1.3 Effect of EV on strength

When using EV as sand replacement, it was noticed that the strength of the mortar exhibited a decreasing trend when the replacement level of sand was increased. For example, 28 days compressive strength for fly ash-based geopolymer mortar was decreased by about 13% when maximum of 30% sand (by volume) was replaced by EV (Gencel et al., 2021). Similarly, the strength reduction was about 31% (Schackow et al., 2014), 52% (Karatas et al., 2019) and 64% (Mo et al., 2018), respectively when 40% to 65% of sand (by volume) was replaced by EV in cement mortar. Strength loss as high as 72% was obtained when maximum of 10% (by weight) EV was adopted for sand replacement in cement-lime mortar (Silva et al, 2010). The increase of strength loss was attributed to the porous and soft structure with fine particle size of EV which created more porous structure in the mixture (Silva et al, 2010; Schackow et al., 2014; Mo et al., 2018). In addition, high volume of EV content as sand replacement in the mixture may increase the strength loss due to insufficient of water for hydration process (Gencel et al., 2021). Hence, strength loss for mortar was increased when high volume of EV was used as sand replacement (Table 2.5).

Table 2.5: Strength reduction variation of EV mortars

Specimen	EV content (%)	Strength reduction (%)
Mortar (Gencel et al., 2021)	30 (by volume)	13
Mortar (Schackow et al., 2014; Karatas et al., 2019; Mo et al., 2018)	40 to 65 (by volume)	31-64
Mortar (Silva et al, 2010)	10 (by weight)	72

2.3.2 Expanded perlite (EP)

Perlite is a glassy volcanic rock which consists of the composition of alumina and silicon oxide. Perlite is formed by the hydration of obsidian. Expanded perlite (Figure 2.2) is produced from the raw perlite rock and it is applied as a valuable lightweight material. It occurs naturally and expands greatly from 4 to 20 times than its original volume under high temperature between 900ºC to 1200ºC. EP possess the properties of high porosity, chemical inertness as well as exhibiting excellent thermal and acoustic properties (Sengul et al., 2011; Rozycka and Pichor, 2016; Rashad, 2016a, Allameh-Haery et al., 2017). Table 2.6 summarizes the chemical composition for EP based on literature.

Figure 2.2: Expanded perlite (Rashad, 2016a).

Table 2.6: Chemical composition for EP

Chemical composition (%)	Turkmen and Kantarci (2007)	Silva et al. (2010)	Rozycka and Pichor (2016)
SiO_2	71.0 -75.0	76.5	70.0
Al_2O_3	12.0 - 16.0	13.4	14.0
CaO	0.2 - 0.5	1.3	3.0
Na_2O	2.9 – 4.0	3.0	-
FeO	1.0 – 3.0	1.2	-
MgO	-	0.3	0.2

2.3.2.1 Effect of EP on flow/workability

Similar as EV, the inclusion of high-volume EP as sand replacement in mortar or concrete generally increased the flow/workability properties. For example, the flow value of cement mortar was increased by 16.5% when EP content as high as about 7% (by weight) was used in mortar mix (Lanzon and Garcia-Ruiz, 2008). In terms of concrete, the slump of high strength concrete was increased by about 41% when a maximum of 30% EP (by volume) was used as sand replacement (Karakoc and Demirboga., 2010). Further increase in the sand replacement by EP in the range of 35% to 50% by volume in lightweight concrete also showed similar trend as the slump value obtained was increased up to 93% compared to that for conventional concrete (Bakhtiyari et al., 2014; Oktay et al., 2015). The increase of flow or slump value was probably related to the increase in air content in the mortar or concrete matrix (Oktay et al., 2015; Rashad, 2016a).

2.3.2.2 Effect of EP on density

In terms of the mortar/concrete's density, many research works highlighted that the density reduced greatly when the content of EP was increased in the mixture. The reduction of mortar density was about 28% when maximum of 5% perlite (by weight) was used as sand replacement (Silva et al., 2010). Whereas for concrete, it was similarly reported that the density of self-compacting concrete or high strength concrete was reduced by up to 9% when a maximum of 10% (by weight) or 30% (by volume) of EP was used as sand replacement (Turkmen and Kantarci, 2007; Karakoc and Demirboga., 2010; Gandage et al., 2013). Further increase in the sand replacement by EP (between 40% to 80% by volume) in concrete increased the density reduction in the range of 32% to 65% (Sengul et al., 2011; Oktay et al., 2015; Rozycka et al., 2016). The reduction of density in mortar or concrete was mainly contributed by the low specific gravity of EP (Gandage et al., 2013). The high-water absorption (Silva et al., 2010) and porous structure of EP than sand (Sengul et al., 2011; Oktay et al., 2015; Rozycka et al., 2016) could be other reasons which caused the density reduction.

2.3.2.3 Effect of EP on strength

In cement mortar, more than 85% of strength loss was reported when adopting about 7% (by weight) EP powder (Lanzon and Garcia-Ruiz, 2008) or maximum of 5% (by weight) of EP (Silva et al., 2010) as sand replacement. In high strength concrete, the compressive strength was reduced by about 33% when maximum of 30% EP was used (Karakoc and Demirboga., 2010; Karakoc et al., 2012). The strength reduction as high as 62% to 85% was obtained when EP content was increased in the range of 40% to 60% (Sengul et al., 2011; Oktay et al., 2015). Whereas the strength loss of concrete was further increased up to 96% when more than 80% of sand was replaced by EP (Sengul et al., 2011). The strength reduction in mortar or concrete was mainly attributed to the porous and weak structure, low specific gravity with higher water absorption of EP than sand, all of which increased the overall number of internal cavities in the mixture (Silva et al., 2010; Karakoc and Demirboga., 2010; Sengul et al.,2011; Karakoc et al., 2012; Oktay et al., 2015; Rozycka and Pichor; 2016). Hence, the strength loss of mortar or concrete was increased when the replacement level of sand increased (Table 2.7).

Table 2.7: Strength reduction variation of EP sample

Specimen	EP content (%)	Strength reduction (%)
Concrete (Karakoc and Demirboga., 2010; Karakoc et al., 2012)	30 (by volume)	33
Concrete (Sengul et al., 2011; Oktay et al., 2015)	40 to 60 (by volume)	62 to 85
Concrete (Sengul et al., 2011)	> 80 (by volume)	> 96
Mortar (Lanzon and Garcia-Ruiz, 2008; Silva et al, 2010)	5 to 7 (by weight)	> 85

2.4 Fresh properties of lightweight cement mortar/concrete

2.4.1 Flow/workability

In terms of the fresh properties for lightweight aggregate mortar or concrete, it was reported that increased usage of crumb rubber as sand replacement showed the reduction in trend in the flow or slump value. For example, the flow or workability of crumb rubber mortar or concrete was decreased by about 3% when a maximum of 6% sand (by weight) was replaced by crumb rubber (Bisht and Ramana, 2017; Claudio et al., 2020). As compared to the control mortar or concrete, further increase in the crumb rubber content up to 50% (by volume) increased the flow or slump loss up to 59% (Kou et al., 2009; Lv et al., 2015; Yu and Zhu, 2016; Si et al., 2018; Zahid Hossain et al., 2019). The reduction in flow or workability for crumb rubber mortar or concrete was mainly attributed to the irregular or lamellar shape which increased the total surface area (Lv et al., 2015; Yu and Zhu, 2016; Bisht and Ramana, 2017; Si et al., 2018; Claudio et al., 2020). The porous properties of crumb rubber than sand could be another factor which caused the slump value to decrease as the overall blend cannot be mixed properly due to the lack of water to overcome the interparticle friction (Zahid Hossain et al., 2019). Hence, by utilizing high volume of crumb rubber as sand replacement in mortar or concrete, superplasticizer or additional water is needed to maintain the similar workability as the control.

2.4.2 Water retention

Based on ASTM C91/C91M-18, the minimum water retention requirement for mortar mix is about 70%. For mortars with low water retention properties (<70%), the cement hydration in the mix may be adversely affected due to the shortage of water. Hence, this may influence the strength of mortar and surface crack may appear easily when the mortar is used for rendering purpose. By studying the effect of lightweight aggregate in mortar, it was reported that the water retention was increased up to 79.6% (Braga et al., 2012) and 89.2% (Neno et al., 2014), respectively when maximum of 5% (by weight) or 20% (by volume) of lighter weight fine recycled concrete aggregate was used as sand replacement. Similarly for the case of expanded clay which was used to fully replace sand in fly ash mortar, the water retention as high as 97.9% could be obtained (Carrajola et al, 2021). This was attributed to the porous structure of the aggregates (recycled concrete aggregate and expanded clay) which absorb more water than sand and this could be beneficial for continuous cement hydration process. In addition, the larger surface area of lightweight aggregate than sand tends to keep the absorbed water in the mixture (Penacho et al., 2014; Lucas et al., 2016). Specifically, the water retention for mortar as high as 75% was obtained when maximum of 50% sand was replaced by materials such as fine glass waste aggregates (Penacho et al., 2014) and sanitary ware waste (Lucas et al., 2016), which are lighter and more porous than normal sand.

2.5 Hardened properties of lightweight cement mortar/concrete

2.5.1 Density

In general, the use of lightweight aggregate as sand replacement in mortar or concrete could reduce the density/structural dead load and beneficial in the field of building and construction (Lanzon Torres and Garcia-Ruiz, 2009; Coppola et al., 2018). Lightweight aggregates such as expanded polystyrene, EP, expanded glass and hollow microspheres (Lanzon Torres and Garcia-Ruiz, 2009), crumb rubber (Kou et al., 2009; Lv et al., 2015; Yu and Zhu, 2016; Si et al., 2018; Zahid Hossain et al., 2019) and expanded clay (Munoz-Ruiperez et al., 2016) are commonly proposed by researchers in cement mortar. Compared to conventional mortar, the density of mortar mixed with expanded polystyrene as sand replacement exhibited the highest reduction (about 28%) when 0.59% (by weight) of expanded polystyrene was used. This was followed by EP, expanded glass and hollow microspheres, which was about 10%, 6% and 5% respectively (Lanzon Torres and Garcia-Ruiz, 2009). Similarly for the use of 50% crumb rubber (by volume) as sand replacement in mortar, it was reported that the density reduction was increased up to 25% (Yu and Zhu, 2016). Whereas in the case of concrete, the literature highlighted that not more than 16% reduction in density when maximum of 5.5% by weight (Bisht and Ramana, 2017) or 50% by volume of lightweight crumb rubber (Kou et al., 2009; Lv et al., 2015; Bashar and Musa, 2018; Zahid Hossain et al., 2019) were adopted as sand replacement. The density reduction as high as 45% was obtained when fully replacing sand with crumb rubber in concrete (Ampol et al., 2018). The reduction in density for crumb rubber mortar or concrete was mainly contributed by the low specific gravity (less than 1.2) and porous structure of lightweight aggregate compared to sand (specific gravity ≈ 2.6) which increased the internal cavities in mortar or concrete matrix (Kou et al., 2009; Lv et al., 2015; Bisht and Ramana, 2017; Ampol et al., 2018; Claudio et al., 2020).

This was in line with literatures when lightweight expanded clay was used as sand replacement in mortar or concrete. Due to the porous structure of expanded clay than sand, the density of masonry mortar was decreased by about 20% when maximum of 50% expanded clay was adopted (Munoz-Ruiperez et al., 2016). Further increase in the expanded clay content in mortar (more than 75%) caused the density reduction in the range of 32% to 60% (Munoz-Ruiperez et al., 2016; Manuel et al., 2020). When fully replacing sand with expanded clay in concrete, density reduction as high as 22% could be obtained (Rickard et al., 2016). Hence, it can be summarized that density reduction of mortar or concrete was obtained when high volume of sand was replaced by lightweight aggregates.

2.5.2 Strength

Figure 2.3 depicts the linear correlation between density and compressive strength of lightweight mortar mixed by expanded polystyrene, EP, expanded glass and hollow microspheres as sand replacement (Lanzon Torres and Garcia-Ruiz, 2009). The higher the density, the better the strength of mortar. However, the density of mortar or concrete is mainly governed by the type of sand or aggregate used. For example, it was reported that the 28 days compressive strength of concrete was decreased by 18% when maximum of 5.5% (by weight) crumb rubber was used as sand replacement (Bisht and Ramana, 2017). Compared to conventional concrete, the literature highlighted that the compressive strength of lightweight concrete decreased by up to 47% when maximum of 45% crumb rubber was used as sand replacement (Kou et al., 2009; Si et al., 2018; Bashar and Musa, 2018; Zahid Hossain et al., 2019; Xie et al., 2019). The further increase in the crumb rubber content up to 50% in concrete induced the strength loss up to 60% (Lv et al., 2015).

Similarly for the case of crumb rubber mortar, the strength loss was increased up to 78% when maximum of 50% sand was replaced (Yu and Zhu, 2016).

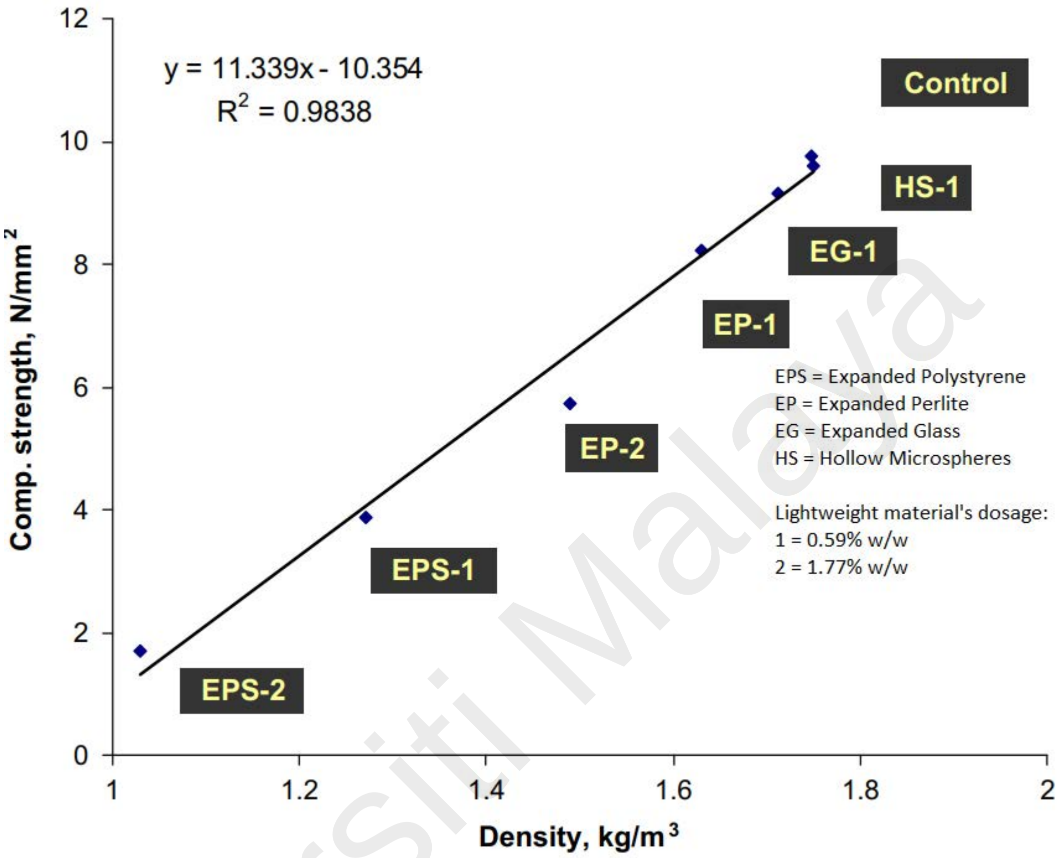

Figure 2.3: Linear correlation between density and compressive sterngth for lightweight mortar (Lanzon Torres and Garcia-Ruiz, 2009).

By fully replacing sand with crumb rubber in cement mortar, Ampol et al. (2018) noticed that strength loss as high as 93% was obtained. The increased in strength loss for crumb rubber mortar or concrete was mainly attributed to the use of crumb rubber which had the ability to repel water and possibly generate more unconnected pores in the mixture (Claudio et al., 2020). In addition, due to the properties of crumb rubber which had low elastic modulus and lower stiffness than sand, adopting high volume of crumb rubber as sand replacement in mortar or concrete could create weak bonding between crumb rubber and cement paste (Ampol et al., 2018; Si et al., 2018; Zahid Hossain et al., 2019; Xie et al., 2019). Hence, it increased the porosity in mortar or concrete and resulted in low strength when high volume of crumb rubber was adopted.

In the case of expanded clay mortar, the literature highlighted similar trends in terms of the 28 days compressive strength. For example, it was revealed that the strength of expanded clay mortar was reduced in the range of 44% to 74% when more than 75% of sand was replaced by expanded clay (Rickard et al., 2016; Munoz-Ruiperez et al., 2016; Munoz-Ruiperez et al., 2018; Manuel et al., 2020). The reduction in strength was mainly attributed to the porous structure of expanded clay compared to sand which increased the overall porosity content in the mixture.

2.5.3 Water sorptivity

The tendency of mortar to absorb and transmit water in non-saturated state can be demonstrated through sorptivity test. Theoretically, sorptivity is one of the important parameters which related to the pore structure, permeability, access the surface quality and durability of mortar sample. In general, the sorptivity of mortar or concrete is greatly influenced by the density, water absorption and type of cement or aggregate used. For example, literature reported that by fully replacing sand with pre-soaked lightweight expanded clay in concrete (water-cement ratio ≈ 0.40), the sorptivity coefficient was slightly higher (0.13mm/min$^{0.5}$) than conventional concrete (<0.09mm/min$^{0.5}$) (Tommy et al., 2006; Liu et al., 2010). Similarly, Chung et al. (2021) noticed that by fully replacing sand with pre-soaked expanded clay in concrete, the sorptivity coefficient was about 43% higher compared to concrete mixed with expanded glass. The increased in sorptivity coefficient was mainly attributed to the porosity content of expanded clay (23% to 42%) which was higher compared to the expanded glass or sand (17% to 28%) (Liu et al., 2010;

Chung et al., 2021). Hence, the interconnectivity of pores in the mixture was increased and resulted in higher sorptivity coefficient than the corresponding expanded glass concrete or conventional concrete.

This is also in line with the literature where maximum of 25% lightweight crumb rubber (by volume) was used as sand replacement in concrete. Specifically, it was highlighted that the sorptivity coefficient of crumb rubber concrete was about 36% to 47% higher than conventional concrete (Gesoglu and Guneyisi, 2011; Sugapriya and Ramkrishnan, 2018). This was probably due to the nature of crumb rubber which repels water. Thus, weak bonding between crumb rubber particle with mixture was formed and this caused the increase in void content or porosity. Similar case was mentioned by literature when lightweight polyethylene terephthalate aggregate was used as sand replacement in cement mortar (Choi et al., 2009). In detail, the sorptivity coefficient of cement mortar was increased by about 52% when maximum of 75% sand was replaced by polyethylene terephthalate aggregate. This was attributed to the high porosity content with the low density of polyethylene terephthalate aggregates (1390kg/m^3) than sand which caused the mortar to absorb more water.

In contrast, the use of 40% prewetted lightweight expanded shale as sand replacement reduced the sorptivity coefficient by about 43% compared to conventional mortar (Elsharief et al.,2005). This may be attributed to the difference in pores characteristics between prewetted expanded shale mortar and the conventional mortar. As the sorptivity is directly proportional to the velocity of capillary rise, the prewetted expanded shale mortar possessed smaller capillary pores due to the denser interfacial transition zone (ITZ). Even though the expanded shale particle had larger pores, the pores were not continuous and were sealed off by the dense paste surrounding the aggregate.

This was similarly pointed out by Henlensiefken et al. (2009) as the reduction of sorptivity coefficient as high as 50% was obtained when maximum of 23.7% saturated expanded shale was used as sand replacement in mortar. This was due to the improvement of ITZ in the mixture, as the saturated expanded shale will not be re-saturated again even though the de-percolation of the ITZ around the sand occurred in conventional mortar and led to the higher sorptivity value compared to saturated expanded shale mortar.

In lightweight expanded clay concrete, it was reported that the sorptivity coefficient was decreased by 13% to 50% when maximum of 10% (by weight) silica fume was used as cement replacement (Muhammad and Chen, 2019; Muhammad et al., 2019). This decrease in sorptivity coefficient was due to the use of silica fume which can densify the microstructure and reduce the porosity of the expanded clay concrete.

2.6 Functional properties of non-traditional concrete

2.6.1 Sound absorption

This section summarizes the literatures available about the sound absorption properties of cement-based materials which incorporate heterogenous materials such as crumb rubber, bottom ash and more.

Rubberized concrete is a lightweight aggregate concrete that utilizes crumb rubber as sand replacement. The specific gravity of crumb rubber (about 0.9 to 1.2) is significantly lower than that for sand (about 2.65). Thus, the unit weight of rubberized concrete can be reduced significantly, indicating a potential improvement in the acoustic properties of concrete (Sukontasukkul, 2009; Ling et al., 2010; Bashar et al., 2012). For example, the best sound absorption characteristics (Noise Reduction Coefficient, NRC = 0.12) was obtained when maximum of 30% crumb rubber was used as sand replacement in concrete (Ling et al., 2010). For the concretes mixed with 10% and 20% of crumb rubber, the NRC was only about 0.07 and 0.09, respectively (Figure 2.4). This was attributed to the increased porosity of the concrete. Lower density of crumb rubber concrete reduces the friction losses within the pore structure. Hence, crumb rubber content enhances the sound absorption properties of the concrete.

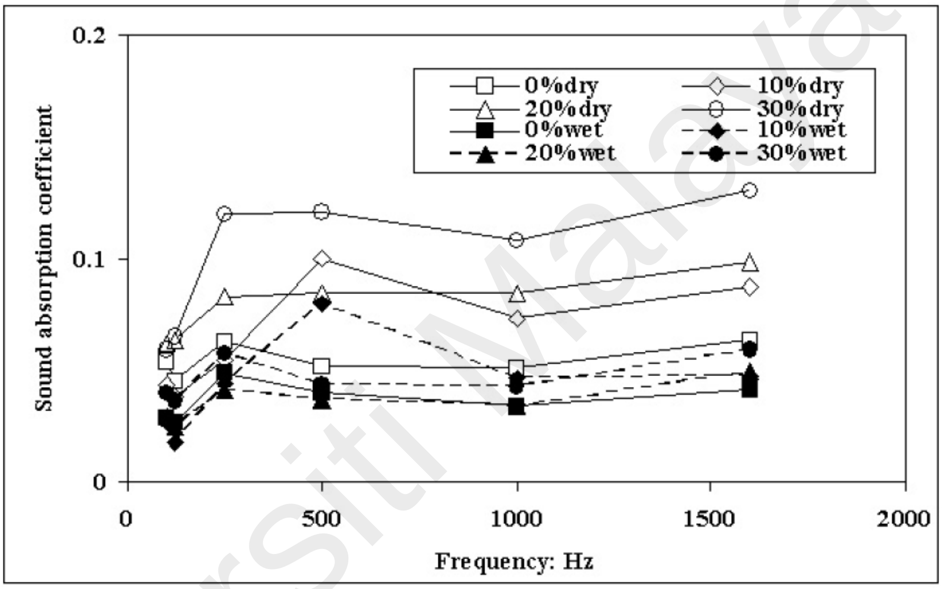

Figure 2.4: Sound absorption coefficient of concrete paving block containing various amount of crumb rubber (Ling et al., 2010).

By adopting high volume of crumb rubber (up to 50%) in concrete block, a greater porosity in concrete was formed due to the trapped air between cement paste and the aggregates surface (Figure 2.5) (Bashar et al., 2012). Hence, NRC value as high as 0.12 was reported for concrete mixed with 50% of crumb rubber, whereas NRC of 0.07 conventional concrete. There are similar positive results of sound absorption reported by other researchers when incorporating crumb rubber as sand replacement in concrete (Pastor et al., 2014; Ghizdavet et al., 2016; Medina et al., 2016). For example, Holmes et al. (2014) reported that the finer the particle size of sand, the greater is the sound absorption of the lightweight aggregate concrete. This was due to the larger surface area of finer size of crumb rubber aggregate. As a comparison, the sound absorption was improved by almost 6 times with the use of 1-3mm size of crumb rubber compared to the crumb rubber size of 10-19mm.

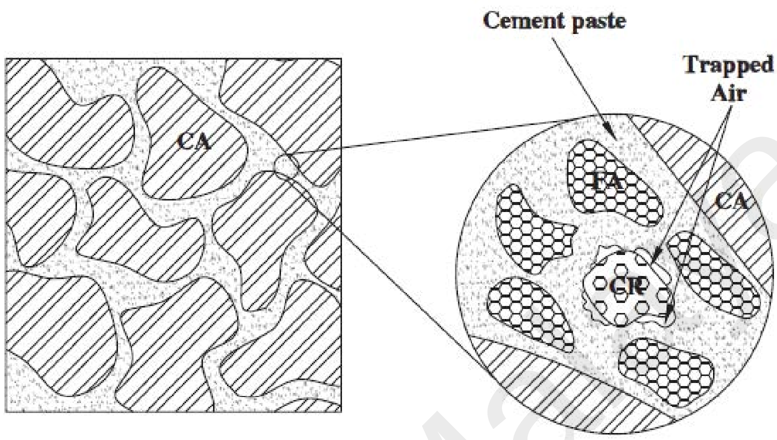

** CA denote as coarse aggregates and CR denote crumb rubber

Figure 2.5: Illustration of trapped air in crumb rubber concrete (Bashar et al., 2012).

Bottom ash (BA) is another type of lighter weight aggregate used with the aim to reduce the density of mortar or concrete and improve the acoustic absorption (Leiva et al., 2012; Arenas et al., 2013; Arenas et al., 2015). Literatures have highlighted that the density of the concrete can be reduced by about 67% when increasing the amount of BA up to 60% (Leiva et al., 2012). This was attributed to the highly porous BA which also has lower specific gravity than sand. Therefore, the acoustic performance of concrete improved when the amount of BA aggregate blended in the concrete was increased (Figure 2.6). Furthermore, the sound absorption coefficient achieved in the concrete with 60% BA aggregate (NRC = 0.25) was similar as pervious concrete. In detail, research works commented that the average sound absorption coefficient of pervious concrete prepared with BA aggregate improved with higher content of BA due to the sound energy loss through friction on the surface of BA being higher than that of normal aggregate

(Ngohpok et al., 2018). Whereas, literature reported that the incorporation of 80% of BA aggregate in concrete improved the acoustic absorption coefficient (NRC = 0.59) (Arenas et al., 2013). Hence, the higher amount of BA aggregates contributed to better acoustic absorption coefficient due to the porous nature of the BA aggregate.

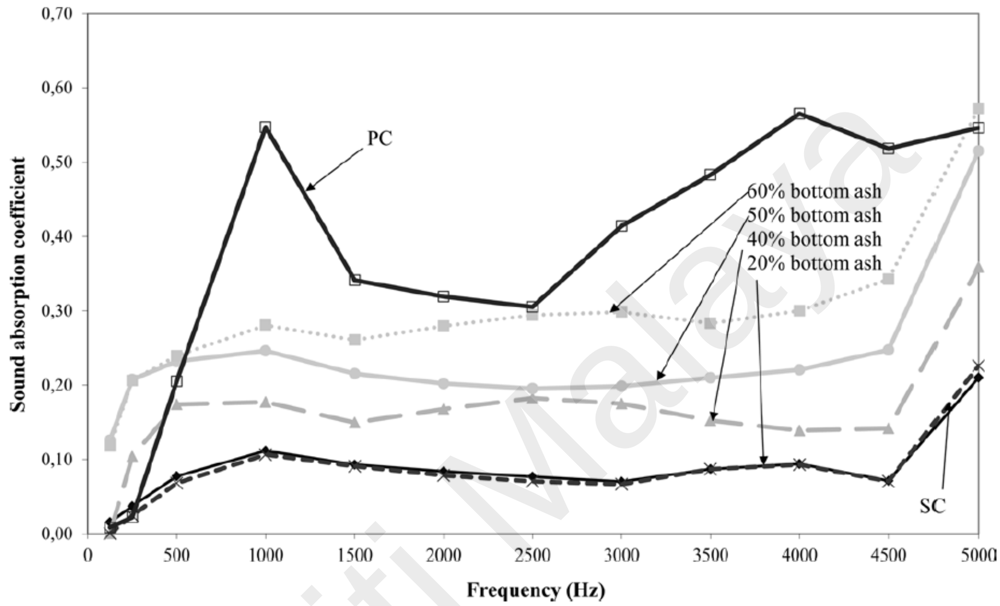

Figure 2.6: Sound absorption of specimen containing various BA contents (Leiva et al., 2012). *(PC = pervious concrete, SC = standard concrete)*.

On the other hand, the inclusion of maximum of 40% (by volume fraction) lightweight cenospheres (size ranging between 10 and 300μm) in asphalt concrete yielded higher sound absorption (α = 0.3 within frequency range of 1000 – 1600Hz) and NRC (0.14), respectively, than that of the control mix without cenospheres (α = 0.1 and NRC = 0.07) (Tiwari et al., 2004). However, the sound absorption coefficient and noise reduction value reduced when more than 40% of cenospheres was included in the asphalt concrete. This was possibly attributed to the filling effect of the cenospheres whereby the cenospheres could easily slip into the voids and filled in the voids within the concrete (Figure 2.7).

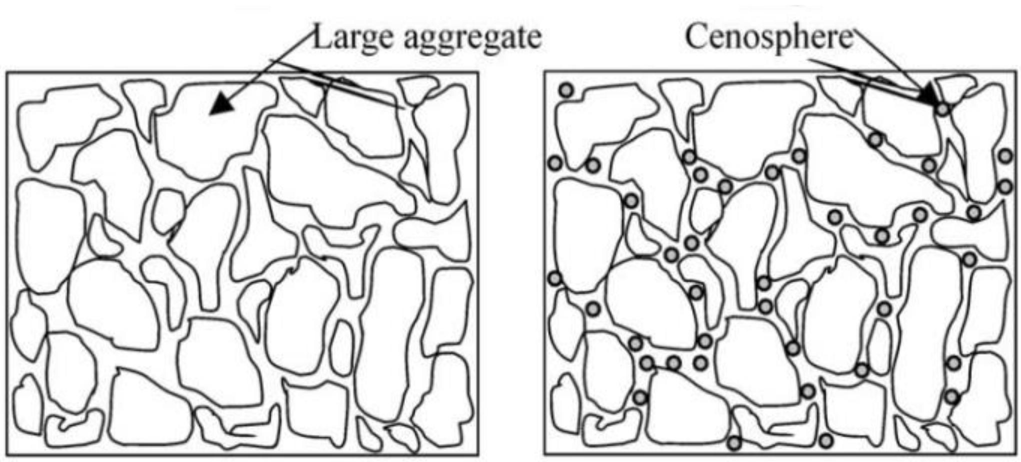

Figure 2.7: Concrete without (left) and with cenosphere (right) (Tiwari et al., 2004).

When considering the impact in sound reduction, it was reported that cement mortar prepared with expanded clay, expanded cork and polystyrene aggregates exhibited superior performance than normal aggregate mortar (Branco and Godinho, 2013). This is because these lightweight aggregates particularly have good effect for sound reduction due to the lower stiffness of aggregate which has high energy dissipation ability.

2.6.2 Solar reflectance

Solar reflectance is defined as the ratio of the incident solar energy which is reflected by the tested surface. Likewise, the solar reflectance can be measured based on the scale of 0 to 1, where '0' indicates non-reflectivity and '1' indicating that all of the solar energy striking a surface is reflected back into the atmosphere (Medgar and Martha, 2007). Hence, light-coloured materials theoretically have higher solar reflectance than black-coloured materials.

Reflectance can be measured in the laboratory or in the field procedures. Usually, the measurement in the laboratory is applicable to determine the solar reflectance of materials itself, while field measurement is suitable to determine the solar characteristics of final product. From the literature, the practical considerations for solar reflectance measurement include pyranometer setup, albedometer measurement (Yan and Lee, 2017) and spectrophotometer or reflectometer measurement (Levinson et al., 2010).

Reflectance measurement by pyranometer (Figure 2.8) is a field procedure described in Standard ASTM E1918 (Pisello, 2015). The measurement of reflectance according to this standard are reliable on the large surface areas (A> $1m^2$). The pyranometer measurement can be used to measure the clear sky global solar reflectance of a horizontal or low-sloped surface (slope < 2:12) during the central hours of the day. However, the measuring technique of pyranometer may potentially be compromised by the presence of shadows, background and instrument error and levelling differences due to the field portable equipment. Hence, a modified version of the standard (E1918A Theory) was proposed by Akbari et al. (2008) to overcome these issues.

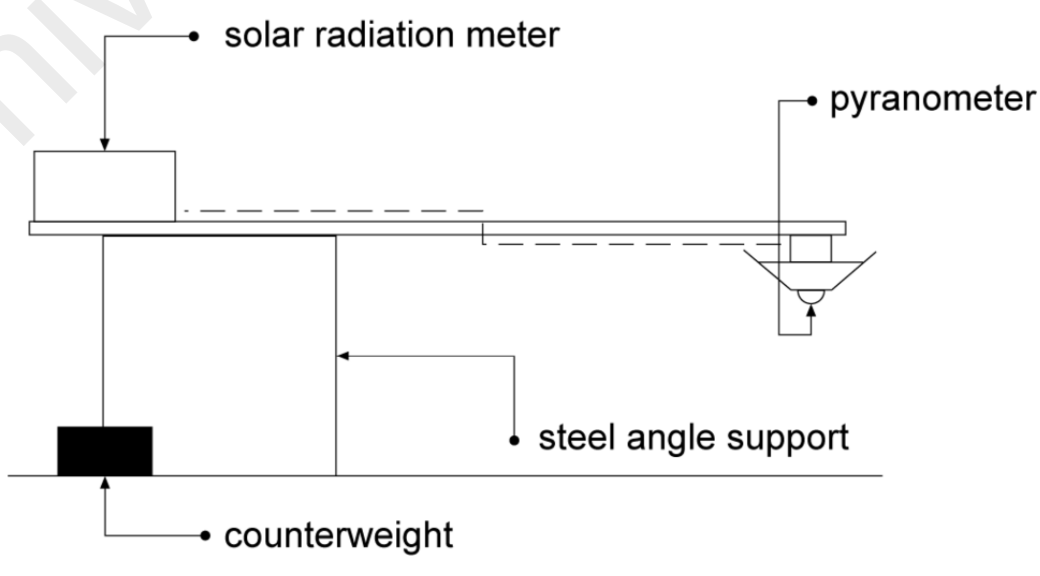

Figure 2.8: Schematic diagram of pyranometer measurement (Akbari et al., 2008).

The technique of albedometer can be used to determine the solar reflectance on small scale sample according to standard E1918A Theory. For example, sample scale of 400cm^2 (Yan and Lee, 2017) and 900cm^2 (Chen et al., 2019) was highlighted in previous research works to determine the solar reflectance value of the modified tile sample and asphalt mixture slab, respectively. The solar reflectance result obtained for white concrete tiles was as high as 0.75 (Pisello, 2015). This result was close to the findings of Kultur and Turkeri (2012) (approximate 0.80) during a sunny day. However, the results obtained by Yan and Lee (2017) for concrete white flat tile (without add any admixture) was about 71 to 82W/m^2 (minimum incoming solar radiation was about 800W/m^2) within 10am to 2pm in summer day. Table 2.8 summarizes solar reflectance values by researchers based on different types and colour of building materials. Obviously, white colour surface of tile/concrete is more effective in increasing the solar reflectance value than those in darker colour.

Table 2.8: Representative values of solar reflectance

Material	Reference	Solar Reflectance
Black coating / bitumen	Pisello (2015)	0.04 – 0.08
Clay tile (red)	Kultur and Turkeri (2012)	0.16 – 0.45
	Pisello (2015)	0.28 – 0.44
Clay tile (grey)	Pisello (2015)	0.18 – 0.33
Clay tile (white)	Kultur and Turkeri (2012)	0.60 – 0.80
	Pisello (2015)	0.70 – 0.80
Concrete tile (white)	Kultur and Turkeri (2012)	0.65 – 0.80
	Pisello (2015)	0.60 – 0.75
White cement concrete	Reza and Boriboonsomsin (2015)	0.87
OPC + GGBS concrete	Hilal and Peiman (2016)	0.52
Granite rock concrete	Levinson and Akbari (2002)	0.34

In terms of concrete, Levinson and Akbari (2002) pointed out that white cement concrete showed higher albedo value (ranging between 0.58 and 0.79) than grey cement concrete (ranging between 0.19 and 0.50) as the bright-coloured surface of white cement concrete was able to reflect more solar radiation. As the surface temperature of concrete is related to the solar radiation when exposed under the sun, the higher the solar radiation (or lower solar reflectance), the higher of the surface temperature is obtained. Nickholas Anting et al. (2014) utilized waste tile (light grey colour) as the coating materials for asphalt pavement (Figure 2.9) and noticed that the surface temperature of coated asphalt pavement was reduced up to maximum 8.5% compared to asphalt pavement without coating. This was due to the bright colour of coating material which promoted high reflectance properties, thereby reducing the amount of solar heat absorbed and resulting in low surface temperature. On the other hand, it was reported that adding 0.3% to 0.8% of polypropylene fibre in lightweight foamed concrete could help to reduce the surface temperature of concrete by up to 4.3% (Jhatial et al., 2020a and 2020b). This was attributed to the hydroponic nature of polypropylene fibre retained more water which have the ability to create more air voids and resulted in delay for solar heat transfer in the matrix. Hence, the thermal conductivity value was reduced and resulted in lower surface temperature compared to foamed concrete without polypropylene fibre. Jhatial et al. (2020c) reported that the thermal conductivity of foamed concrete reduced from 0.82W/mK to 0.47 W/mK when 30% of palm oil fuel ash (POFA) and 5% eggshell powder was used as cement replacement. However, due to the blackish colour of POFA than cement, the surface temperature of POFA foamed concrete was about 3% higher compared to foamed concrete without POFA.

2.6.3 Summary

Due to the environmental impact of conventional cement mortar or concrete, past research have highlighted the use of SCM as partial cement replacement while lightweight aggregate such as vermiculite, perlite, crumb rubber and oil palm shell were explored as aggregate replacement to improve the functional properties. Nevertheless, the combination of SCM as partial cement replacement and lightweight aggregate, such as expanded perlite and vermiculite has yet to be fully developed. Hence, there is a need to explore the knowledge in terms of key and function properties for mix with these combined materials.

In terms of the key properties, the literature revealed that the use of lightweight expanded clay aggregate and recycle fine aggregate shown reduction in mechanical strengths and higher values of water retention and sorptivity coefficient compared to the use of sand in cement mortars. This was mainly due to the porous structure of lightweight aggregate which increased the pores in the mixtures. Therefore, the use of EV or EP may post similar properties and hence these key properties of mortar should be ascertained, particularly in combination with the use of SCM as partial cement replacement.

In terms of functional properties, most research in cement-based materials are only focused on the thermal conductivity due to the porous structure of lightweight aggregate. In fact, the combination of lightweight aggregate with SCM in cement-based materials could enhance other functional properties such as sound absorption and solar reflectance which are lacking in research. Hence, this could be another interesting research gap which can be addressed so that construction buildings can maximize the benefits of these functional properties.

CHAPTER 3: MATERIALS AND TEST METHODS

3.1 Research flow chart

Figure 3.1 summarizes the research flow chart adopted in this study.

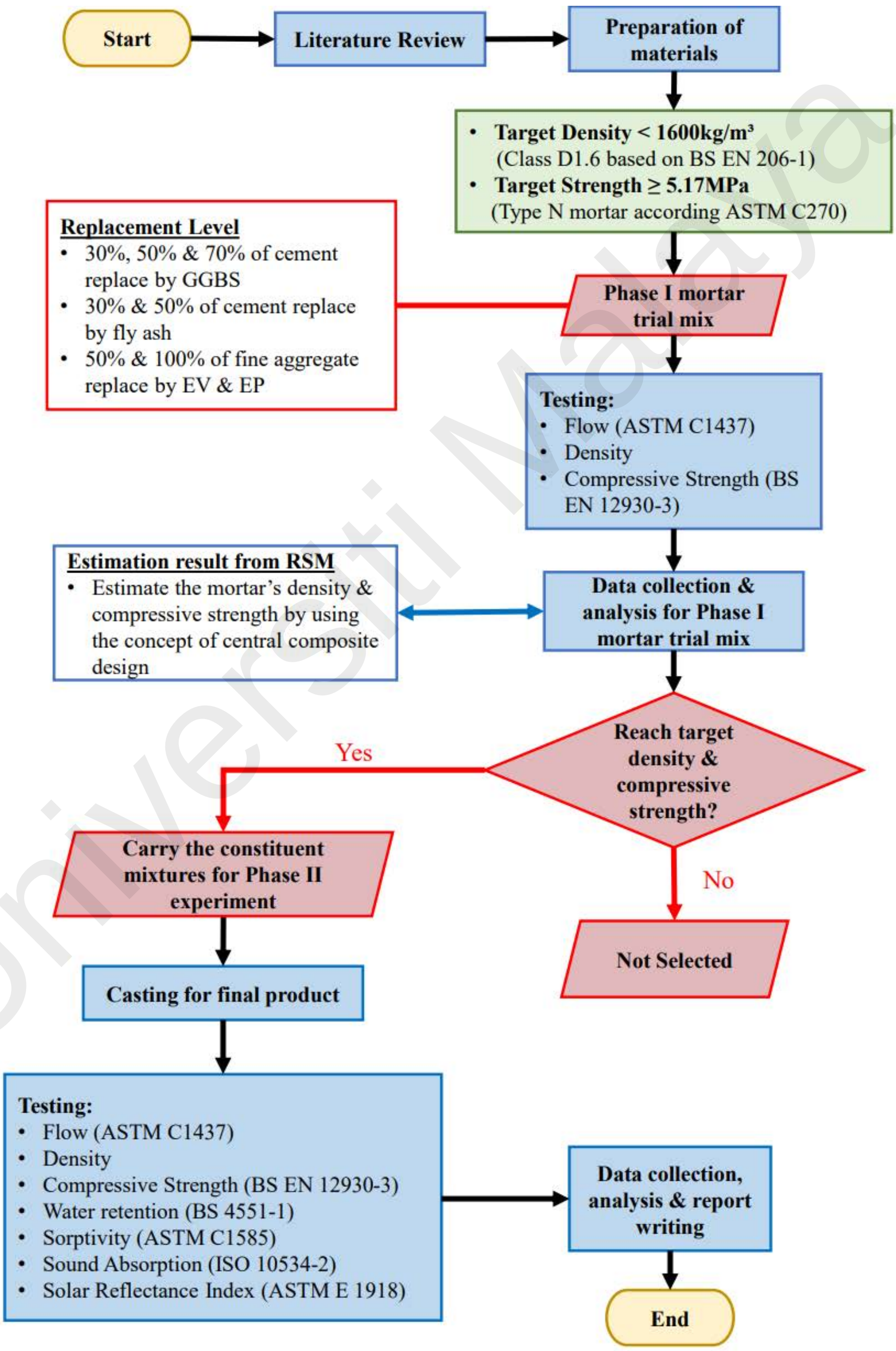

Figure 3.1: Research flow chart.

3.2 General

This section describes the procedures and tests methods carried out to achieve the research objectives. This research is separated into two major phases, namely Phase I and Phase II. Phase I is focused on the determination of adequate mix of SCM (GGBS and fly ash) with the combination of either EP or EV as sand replacement based on trials to achieve the target density in the range of 1400 to 1600kg/m^3 (categorized as Class D1.6 based on BS EN 206-1) and target minimum 28th day strength of 5.17MPa (Categorized as Type N Mortar according to ASTM C270) for mortar. The flow, water retention, density, compressive strength, water sorptivity, sound absorption and solar reflectance test for selected mortar samples were carried out in Phase II.

3.3 Raw materials

3.3.1 Binder (Cement and SCM)

The white Portland cement of type CEM I 52.5N was used as the main binder for the mortars prepared in this research. The specific gravity of the cement was obtained from the cement manufacturer, which was about 3.15. The SCM used in this study were GGBS and fly ash. The major chemical compositions of GGBS and fly ash were evaluated by X-ray fluorescence (XRF) spectrometry analysis and the results are presented in Table 3.1. Similarly, the specific gravity of GGBS and fly ash were obtained from the manufacturer, which was about 2.9 and 2.5, respectively. The particles size of GGBS and fly ash was determined by the particle size distribution (PSD) test and the d_{50} was 14.90µm and 7.45µm, respectively.

Table 3.1: Chemical composition of GGBS and fly ash

Chemical composition (%)	GGBS	Fly Ash
Al_2O_3	11.80	16.07
SiO_2	33.33	35.14
CaO	40.71	15.28
Na_2O	0.27	3.06
MgO	6.10	8.08
P_2O_5	0.02	0.25
SO_3	5.92	2.43
K_2O	0.32	1.10
TiO_2	0.65	0.69
MnO	0.28	0.19
Fe_2O_3	0.35	17.32

3.3.2 Fine and lightweight aggregate

In this research, local mining sand was used for mortar sample. Two different types of lightweight fine aggregate, namely EP and EV were selected as sand replacement. The specific gravity of sand, EP and EV were determined through pycnometer test based on BS EN 1097-6. The obtained specific gravity was 2.65, 0.70 and 1.01, respectively. Whereas, the 30-min water absorption of sand, EP and EV was 1.10%, 142% and 102% respectively. The maximum particle size of SSD sand, EP and EV was 2.36mm and the gradation is presented in Figure 3.2.

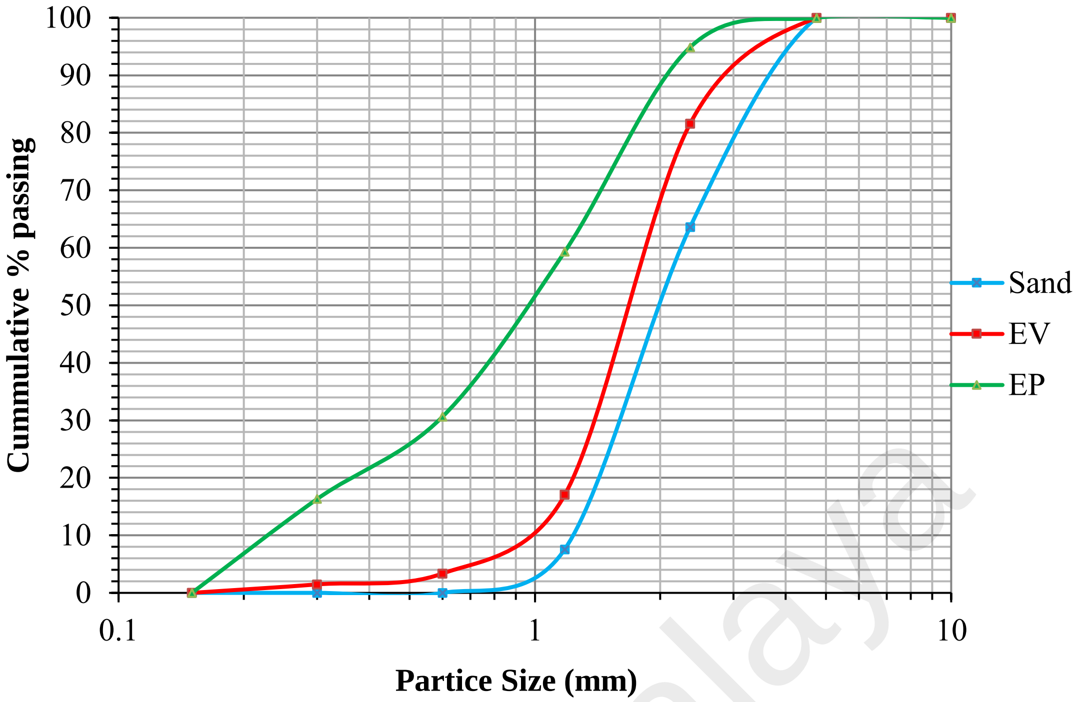

Figure 3.2: Size distribution of fine sand, EP and EV.

3.4 Mix proportion, mix procedure and sample preparation

The aim of the research study is to identify the ideal combination of materials (achieve target density and strength) to produce lightweight mortar. Hence, the mixture composed of binder: sand: water in the ratio 1: 3: 0.5 was selected. The mixing water was used directly from pipe water in laboratory. To account for the water absorption of EP and EV during mixing, both EP and EV are soaked in water for 30 minutes prior to mixing to avoid reducing the effective water/cement ratio (Silva et al., 2010; Sengul et al., 2011; Lu et al., 2018). During mixing, the sand was mixed first, followed by the SCM (either GGBS or fly ash) and white cement. After that, water was added gradually to the dry mixture and mixed with high speed. In order to assess the workability of the fresh mortar mix, the consistency of the mortar was conducted through flow table test according to ASTM C1437.

3.5 Phase I

The cement replacement levels by GGBS were 30%, 50% and 70% (by mass) respectively, whereas 30% and 50% (by mass) of fly ash were adopted as cement replacement for comparison. The 70% fly ash is not used in this research due to very low strength obtained, especially in lightweight mortar. EP and EV were used as sand replacement at 50% and 100% replacement levels (by volume). In Phase I, a total of 30 mixtures were prepared as shown in Table 3.2. The nomenclature of mixtures represents the type and amount of cement and sand replacement. For example, G30-EV50 denotes 30% of cement was replaced by GGBS and 50% of sand replaced by EV, while F30-EP50 denotes 30% of cement replaced by fly ash with partial replacement of sand by EP.

Table 3.2: Mix composition for Phase I

Sample	Replacement content (%)			
	GGBS (by mass)	Fly ash (by mass)	EP (by volume)	EV (by volume)
Control	-	-	-	-
G0-EV50	-	-	-	50
G0-EP50	-	-	50	-
G0-EV100	-	-	-	100
G0-EP100	-	-	100	-
G30-0	30	-	-	-
G30-EV50	30	-	-	50
G30-EP50	30	-	50	-
G30-EV100	30	-	-	100
G30-EP100	30	-	100	-
G50-0	50	-	-	-
G50-EV50	50	-	-	50
G50-EP50	50	-	50	-
G50-EV100	50	-	-	100
G50-EP100	50	-	100	-
G70-0	70	-	-	-
G70-EV50	70	-	-	50
G70-EP50	70	-	50	-
G70-EV100	70	-	-	100
G70-EP100	70	-	100	-
F30-0	-	30	-	-
F30-EV50	-	30	-	50
F30-EP50	-	30	50	-
F30-EV100	-	30	-	100
F30-EP100	-	30	100	-
F50-0	-	50	-	-
F50-EV50	-	50	-	50
F50-EP50	-	50	50	-
F50-EV100	-	50	-	100
F50-EP100	-	50	100	-

3.5.1 Compressive strength

For each mix, 6 cube samples with size of 50mm x 50mm x 50mm were cast into steel mould and kept in laboratory condition for 24 hours (Figure 3.3). After that, the mortar samples were de-moulded and air curing was adopted in this study. The cube samples were tested for compressive strength based on BS EN 12390-3 at the age of 7 and 28 days.

Figure 3.3: Cube samples were cast into steel mould.

3.5.2 Response surface methodology (RSM)

RSM is a collection of mathematical and statistical techniques for modelling and analyzing of problems in which a response is influenced by several variables (Kumar and Baskar, 2014; Rooholamini et al., 2018). In this study, RSM was adopted to estimate the properties of mortar, namely density and compressive strength as the responses based on the materials that were used. Hence, the statistical software "Design-Expert version 11.1.2.0" was used to generate the experimental design and statistical analyzation. Face-centered central composite response surface design with $\alpha = 1$ was used in this study (Kumar and Baskar, 2014). By using the central composite design concept in RSM analysis, additional mixtures containing 35% of GGBS and 25% of fly ash in lightweight cement mortar were prepared as presented in Table 3.3. The content of SCM (GGBS or fly ash) was coded as A and amount of sand replacement by EP or EV was coded as B; both were selected as the factors and studied based on the 2 different types of properties for mortar as its response variables. The factors and factor levels were shown in Table

3.4. The experiment runs were summarized as shown in Table 3.5. Equation 3.1 shows the full quadratic model in terms of coded factors:

$$y = \beta_0 + \beta_1 A+\beta_2 B+\beta_{12} AB+ \beta_{11} A^2+ \beta_{22} B^2 + \varepsilon \quad \text{………………. Eq. 3.1}$$

Where;

y	= predicted response
β_0	= Intercept
β_1, β_2	= Linear effect coefficients
β_{11}, β_{12}	= Quadratic effect coefficient
β_{12}	= Interaction effect coefficient
A, B	= Independent variables
ε	= Residual

Table 3.3: Additional replacement levels of materials for RSM analysis

Sample	Replacement content (%)			
	GGBS (by mass)	**Fly ash (by mass)**	**EP (by volume)**	**EV (by volume)**
G35-0	35	-	-	-
G35-EV50	35	-	-	50
G35-EP50	35	-	50	-
G35-EV100	35	-	-	100
G35-EP100	35	-	100	-
F25-0	-	25	-	-
F25-EV50	-	25	-	50
F25-EP50	-	25	50	-
F25-EV100	-	25	-	100
F25-EP100	-	25	100	-

Table 3.4: Factors and factor levels adopted for RSM

Mixture types	Factor	Code	Factor level (%)		
			-1 (Low)	0 (Intermediate)	1 (High)
GGBS mortar with	GGBS	A	0	35	70
EP substitution	EP	B	0	50	100
GGBS mortar with	GGBS	A	0	35	70
EV substitution	EV	B	0	50	100
Fly ash mortar with	Fly ash	A	0	25	50
EP substitution	EP	B	0	50	100
Fly ash mortar with	Fly ash	A	0	25	50
EV substitution	EV	B	0	50	100

Table 3.5: Factor combinations as per face-centered composite for all mixes

Run	Code Factor		Actual Factors Replacement (%)	
	A	B	GGBS / Fly ash	EP / EV
1	0	0	35 / 25	50 / 50
2	0	1	35 / 25	100 / 100
3	-1	-1	0 / 0	0 / 0
4	1	0	70 / 50	50 / 50
5	0	-1	35 / 25	0 / 0
6	-1	0	0 / 0	50 / 50
7	1	-1	70 / 50	0 / 0
8	1	1	70 / 50	100 / 100
9	-1	1	0 / 0	100 / 100
10	0	0	35 / 25	50 / 50
11	0	0	35 / 25	50 / 50
12	0	0	35 / 25	50 / 50
13	0	0	35 / 25	50 / 50

3.6 Phase II

Table 3.6 summarizes the total mixtures prepared in Phase II. These mixtures were selected based on the achieved target density (in the range of 1400 to 1600kg/m^3) and strength (minimum strength of 5.17MPa) from Phase I. Similar as Phase I, the flow table test, density and compressive strength were determined in Phase II. Hence, cube samples with size of 50mm x 50mm x 50mm were casted and kept in laboratory condition for 24 hours. After that, the mortar samples were de-moulded and air cured until the age of testing. Then, the 28 days compressive strength was carried out based on BS EN 12390-

3. In addition, the water retention, sorptivity, sound absorption and solar reflectance of the selected samples were carried out in this phase.

Table 3.6: Combination mix for Phase II

Sample	Replacement content (%)			
	GGBS (by mass)	Fly ash (by mass)	EP (by volume)	EV (by volume)
Control	-	-	-	-
G0-EV50	-	-	-	50
G0-EP50	-	-	50	-
G30-EV50	30	-	-	50
G30-EP50	30	-	50	-
F30-EP50	-	30	50	-

3.6.1 Water retention

Water retention test was conducted based on BS 4551-1. It can be defined as the mass of water retained in the mortar after the suction treatment by using filter paper as the substrate. The role of controlling water retention of mortar is to ensure that there is no excessive loss of water through evaporation before setting and hardening. To conduct this experiment, a set of rigid mould (100mm internal diameter with 25mm depth) with 2kg mass and filter paper were prepared as shown in Figure 3.4. Fresh mortar was mixed and filled into the rigid mould and the excess mortar on top of the mould was removed before the weight was measured. The weight of 5 dry filter papers were then measured and placed on top of fresh mortar before the fresh mortar was covered by a rigid plate. The mould with fresh mortar and filter papers inside were then inverted and 2kg mass was placed on the inverted base of the mould. After 5 minutes, the mass was removed from the mould and the mould was inverted again. The mass of water present, Z was computed by Equation 3.2. The mass of water absorbed by the filter papers were determined by Equation 3.3 and finally Equation 3.4 was used to calculate the water retention value, R.

Figure 3.4: Apparatus for *water retention test.*

$$Z = \frac{y_1.\ (W-U)}{a+y_1} \quad \text{………………………………. Eq. 3.2}$$

Mass of absorbed water, $Z_1 = X - V$ ……….. Eq. 3.3

$$R = \frac{Z - Z_1}{Z} \times 100\% \quad \text{……………………..……. Eq. 3.4}$$

Where,

y_1 = Mass of water added to the prepared mortar (g)

a = Mass of dry mortar mixture, used for preparing whole batch of mortar (g)

U = Mass of rigid mould (g)

V = Mass of 5 unused dry filter paper (g)

W = Mass of rigid mould, with fresh mortar (g)

X = Mass of 5 wet filter paper (g)

Z = Mass of water present (g)

3.6.2 Water sorptivity

Sorptivity is the measurement of capillary rise absorption rate and based on ASTM C1585. Three 50mm cubic mortars were dried in oven (temperature ≈ 105 ± 5ºC) before carrying out the sorptivity test. To conduct this test, the dried cubes samples were weighed. After that, the dried samples were placed inside a tray with water level not more than 5mm above the base of the sample. A timer was initiated from the moment the exposed dried sample's surface came into contact with water. The weight of cubic sample after absorbed by water in the time period of 1, 5, 10, 20, 30, 60, 120 minutes was measured and recorded. The initial rate of water absorption was computed based on Equation 3.5 and the sorptivity coefficient of sample was determined from the slopes of curves (linear regression) registered between time versus initial rate of absorption.

$$\text{Absorption, I (mm)} = \frac{W_2 - W_1}{surface\ area\ of\ water\ penetrated} \quad \text{.... Eq. 3.5}$$

where,

W_1 = The weight of dried cubic mortar (g)

W_2 = The weight of cubic mortar after absorbed by water (g)

3.6.3 Sound absorption

Sound absorption can be defined as the incident of sound that strikes a material and it was not reflected to atmosphere but absorbed through the entrapped air within the internal structure of the sample. In this study, three samples with size of 34.4mm diameter and 100mm depth were prepared (Figure 3.5) and the concept of transfer function method was applied for impedance tube measurement based on ISO 10534-2 (Figure 3.6). The frequency used in this research was in the range between 0 to 4000Hz. NRC was then computed based on the average sound absorption coefficient at selected frequencies of 250Hz, 500Hz, 1000Hz and 2000Hz (Arenas et al., 2013; Palomar et al., 2015).

Figure 3.5: Sound absorption samples used in Phase II.

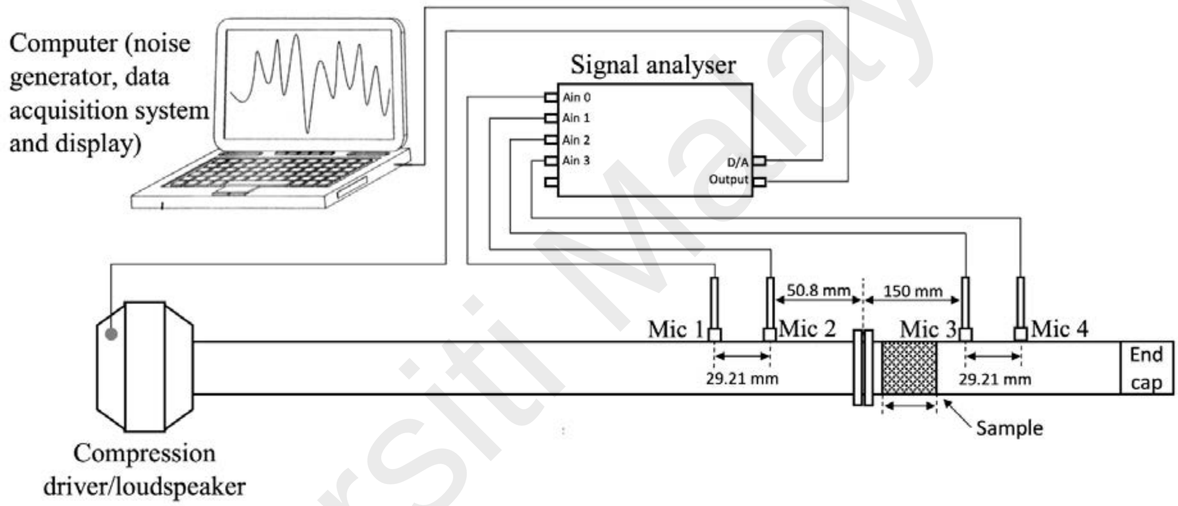

Figure 3.6: Impedance tube measurement based on ISO10534-2.

3.6.4 Solar Reflectance

Solar reflectance index (SRI) is a measurement of the constructed surface's ability to reflect solar heat. The value of SRI of '0' for standard black colour surface and SRI of '1' for standard white colour surface. For this research, a modified method based on E1918A Theory (Akbari et al., 2008) was adopted to determine the incoming and reflection solar radiation.

To conduct this experiment, the field measurement protocol of solar reflectance test was adopted. White and black color cloths with size of 4m square were used as control sample as shown in Figure 3.7 and Figure 3.8 (Sailor et al, 2006). A cylindrical shaded curtain (covered by black cloth to avoid secondary reflection) with 600mm diameter and 500mm in height was designed and used in this protocol. A pyranometer device was then positioned on top of cylindrical curtain and it was connected to the data logger as shown in Figure 3.9. Firstly, the sample with size 300mm x 300mm x 25mm was covered by small white cloth and it was placed inside shaded cylinder box to avoid any environmental disturbance. The pyranometer was faced upwards to measure incoming horizontal global solar irradiance, I_H. After that, the pyranometer was faced downwards to measure the reflected solar irradiance, R_w from the sample cover by white cloth. Next, black cloth was used to replace the white cloth and the reflected solar irradiance, R_b was recorded. Then, the black cloth was removed and the reflected solar irradiance, R_t for the uncovered sample was recorded. Finally, the pyranometer was faced upwards and the incoming solar radiation was measured for the second time, I'_H. The measurement of I_H, R_w, R_b, R_t and I'_H for sample was repeated for every 15 minutes interval within 10am to 2pm. The measurement of incoming and reflectance solar radiations at each interval was completed within 10 minutes to minimize measurement error. Similar procedures were repeated for control sample to determine its reflectance value.

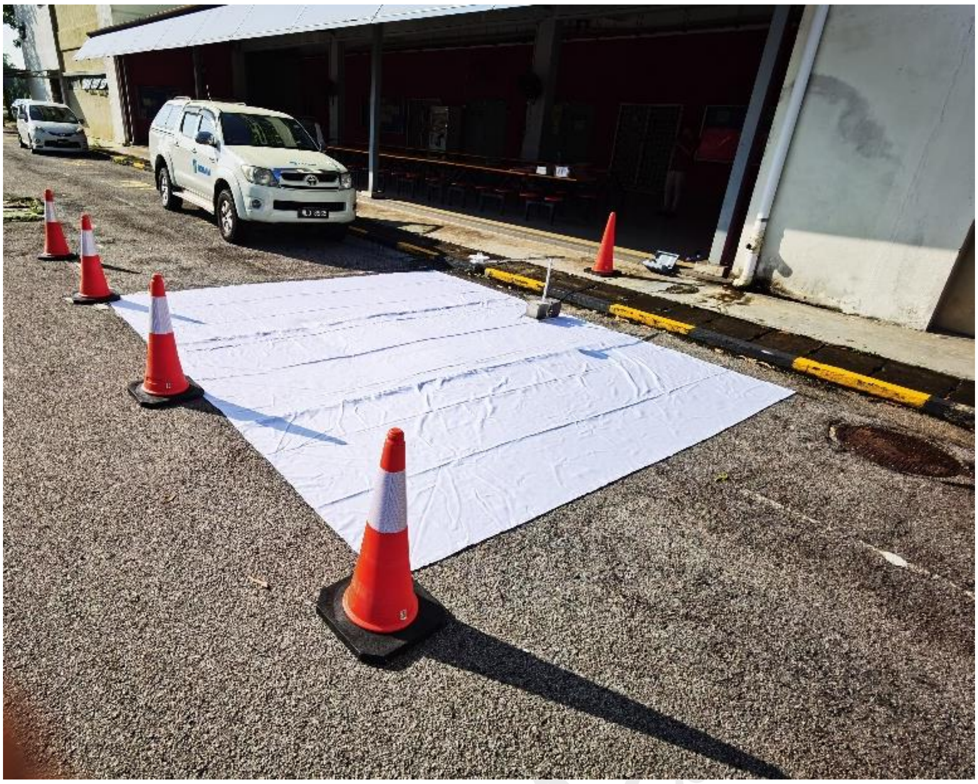

Figure 3.7: White colour surface.

Figure 3.8: Black colour surface.

Figure 3.9: Setup of pyranometer with cylindrical curtain shade.

Besides that, RGB histogram method was proposed by Hilal and Peiman (2016) to determine the albedo value for concrete samples. Hence, to validate the obtained results from field protocol test, RGB method was also implemented in this study. The luminance value of Red, Green and Blue (RGB) histogram for all selected samples were determined through Adobe Photoshop 2020 version 7.0.1. The photo for all selected samples without shadow were taken at every 15 minutes interval between 10am to 2pm. After that, the photo was imported into the software to determine its RGB value. Minimum 5 points of RGB value from each sample were collected and the average albedo value for each sample was computed (Figure 3.10). By referring to Hilal and Peiman (2016), a white paper with albedo value of 0.6 was taken as reference to determine the albedo value for the selected samples.

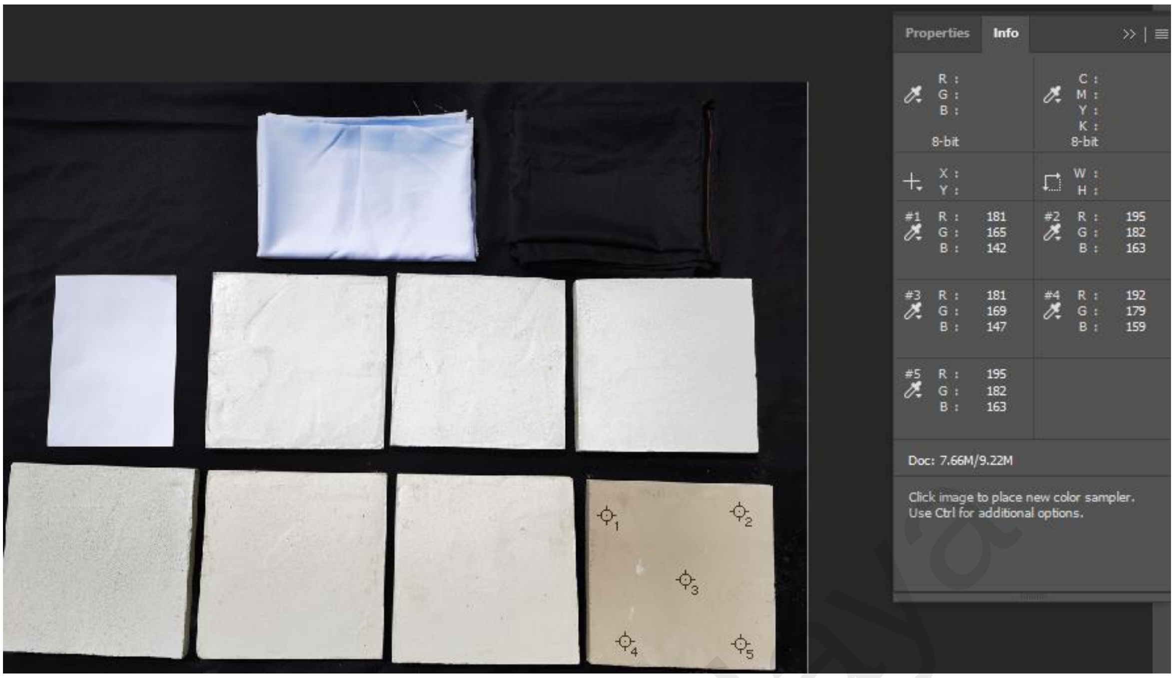

Figure 3.10: RGB analysis for sample F30-EP50.

To carry out solar reflectance test, the measurement site was located at an open space to avoid casting shadows on the samples during measurement period. The coordinate of the location was determined to be 2˚58’46’’N, 101˚44’24’’E. The overall measurement process was carried out during sufficient sunshine from period 10am to 2pm according to the standard of ASTM E1918.

CHAPTER 4: RESULTS AND DISCUSSION

4.1 General

The sections below summarize the results obtained from Phase I and Phase II of the investigation. Phase I was conducted to select the desired mortar mixtures with the help of result from RSM analysis. The selection of mortar mixtures is based on targeted density in the range of 1400-1600kg/m^3 and targeted strength greater than 5.17MPa. For these mixtures, the properties of water retention, sorptivity, sound absorption and solar reflectance of selected mortar mixtures were carried out in Phase II to address the research objectives.

4.2 Phase I

4.2.1 Flow diameter

Figure 4.1 gives the flow diameter of mortars containing EV and EP as sand replacement with GGBS as the cement replacement, whereas Figure 4.2 gives the corresponding flow diameter of mortars with fly ash as cement replacement.

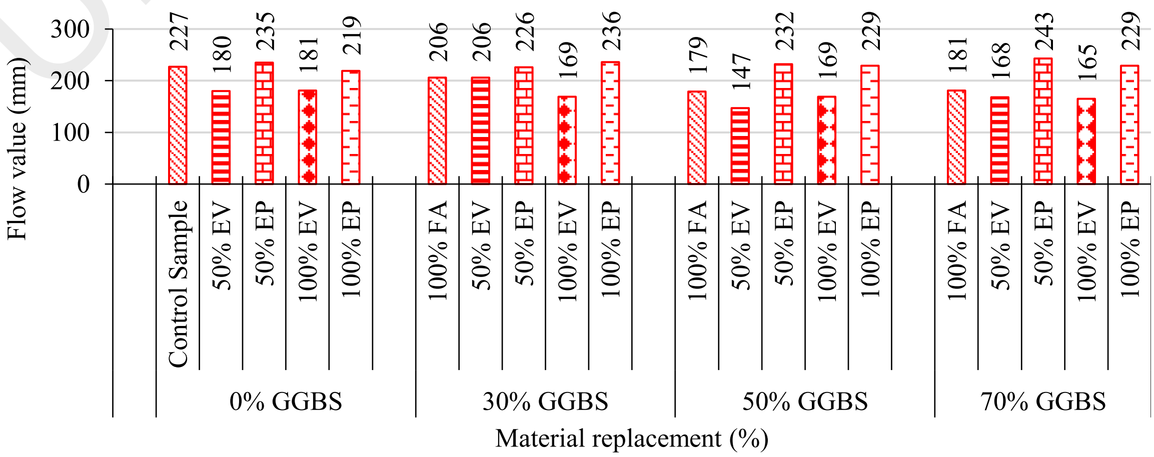

Figure 4.1: Flow value of GGBS mortar containing EV and EP as sand replacement.

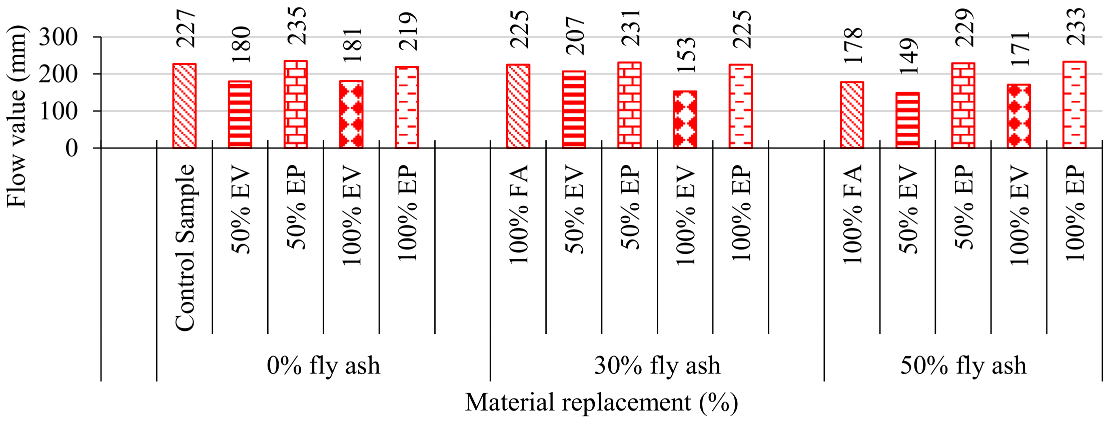

Figure 4.2: Flow value of fly ash mortar containing EV and EP as sand replacement.

As sand replacement, it appears that EP had more positive influence on the flow diameter of mortar compared to the use of EV. Regardless of the type of binder (cement or GGBS/cement or fly ash/cement), the samples containing EP consistently gave higher flow diameter range (215 mm-243 mm) than the corresponding EV samples (149 mm-207 mm). In the case of 50% EP as sand replacement, the improvement in the flow diameter is most obvious, which was about 7% higher than control mortar as observed in Table 4.1. The inclusion of saturated EP could increase workability of mortar due to the increased air content within the mixture (Rashad, 2016a; Lu et al., 2018) as well as smoother surface of the EP particle compared to normal sand. Also, the reduced viscosity of fresh mortar could be achieved with the use of EP, thereby improving the flow of the mortar (Law et al., 2018). However, generally the flow diameter was reduced when EP content was increased from 50% to 100%. This could be attributed to the small particle size of EP which had larger surface area than sand. Hence, this increased the water demand as well as amount of cement paste to coat the EP particles within the mix. Thus, the flow was reduced when EP was adopted as complete sand replacement.

Table 4.1: Reduction of flow value compared to control mortar

Sample		Flow value (mm)	Reduction (%)
0% GGBS	Control	227	-
	50% EV	180	20.7
	50% EP	235	-3.5*
	100% EV	181	20.3
	100% EP	219	3.5
30% GGBS	100% FA	206	9.3
	50% EV	206	9.3
	50% EP	226	0.4
	100% EV	169	25.6
	100% EP	236	-4.0*
50% GGBS	100% FA	179	21.1
	50% EV	147	35.2
	50% EP	232	-2.2*
	100% EV	169	25.6
	100% EP	229	-0.9*
70% GGBS	100% FA	181	20.3
	50% EV	168	26.0
	50% EP	243	-7.0*
	100% EV	165	27.3
	100% EP	229	-0.9*
30% fly ash	100% FA	225	0.9
	50% EV	207	8.8
	50% EP	231	-1.8*
	100% EV	153	32.6
	100% EP	225	0.9
50% fly ash	100% FA	178	21.6
	50% EV	149	34.4
	50% EP	229	-0.9*
	100% EV	171	24.7
	100% EP	233	-2.6*

* Negative symbol '-' denotes flow value is higher than control mortar

On the other hand, the flow diameter of mortar was decreased in the presence of EV as shown in Table 4.1. Insufficient water added (based on water absorption of EV) could be one of the reasons causing the low workability of mortar containing EV. Previous research (Schackow et al., 2014; Koksal et al., 2015) had suggested to soak EV in water for longer period, such as at least 1 hour or 24 hours prior to mixing. This was to ensure that EV is fully saturated for mixing. This also explains the difference in observation whereby improved workability in EV mortar was reported in previous research (Mo et al., 2018).

In general, in mortar mixtures without the lightweight aggregate, inclusion of high volume GGBS and fly ash as partial cement replacement resulted in lower flow values. Despite this, it could be clearly seen from Figure 4.1 and Figure 4.2 that when GGBS and fly ash were used along with the lightweight aggregate, there are some synergistic effects observed. It can be seen that when EP was incorporated, its positive influence on workability was able to offset the reducing effect of the high volume GGBS and fly ash. As a result, most mortar mixtures (with GGBS or fly ash) containing EP had similar, if not higher flow diameter than the control mortar. Besides that, the reduction in workability due to the use of EV could be decreased in the presence of GGBS and fly ash. For instance, among the studied replacement level, when GGBS and fly ash were used at 30% respectively, the flow diameter obtained for the mortars with 50% EV was close to the corresponding ones without EV. However, when GGBS and fly ash were used at 50% respectively, lowest flow diameter value was obtained for mortar with 50% EV (147mm and 149mm respectively).

In overall, the mortar prepared with the combination of either GGBS or fly ash with EP as sand replacement can be categorized as soft mortar (flow value greater than 200mm), while most of the mortar combinations of either GGBS or fly ash with EV as sand replacement can be classified as plastic mortar (flow value within range 140mm to 200mm) in accordance with ASTM C1437. Hence, it is clear that the use of EP is more beneficial compared to EV in terms of enhancing the flow of mortar, as well as allowing the use of high volume of GGBS and fly ash in the mortar.

4.2.2 Density

The density of all mortars blended with GGBS and fly ash is given in Figure 4.3 and Figure 4.4, respectively. The density of the control mortar without any replacement materials was about 2200 kg/m^3 and a reduction in density of up to 6% was obtained in the presence of either 70% of GGBS (G70-0) or 50% of fly ash (F50-0) as high-volume cement replacement. This reduction is associated with the lower specific gravity of GGBS and fly ash compared to cement.

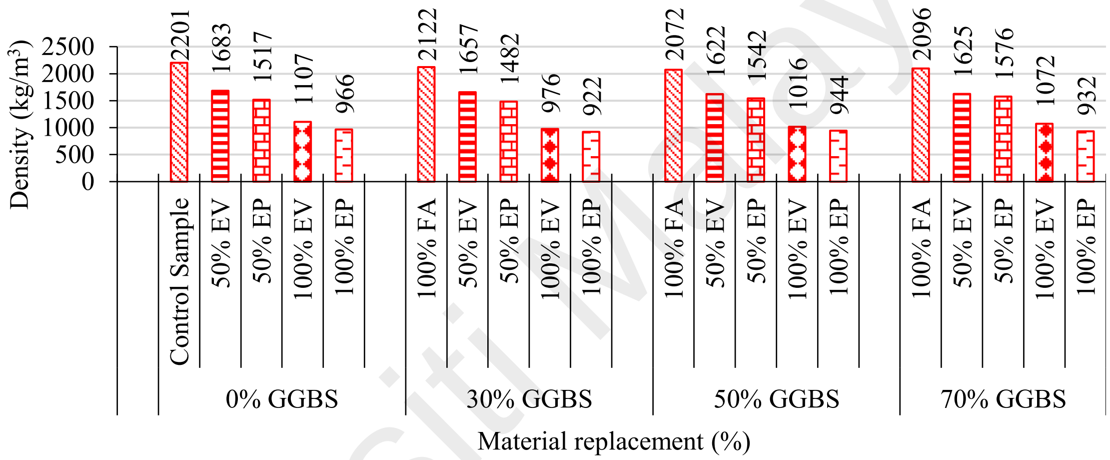

Figure 4.3: 28-day density of GGBS-blended mortar.

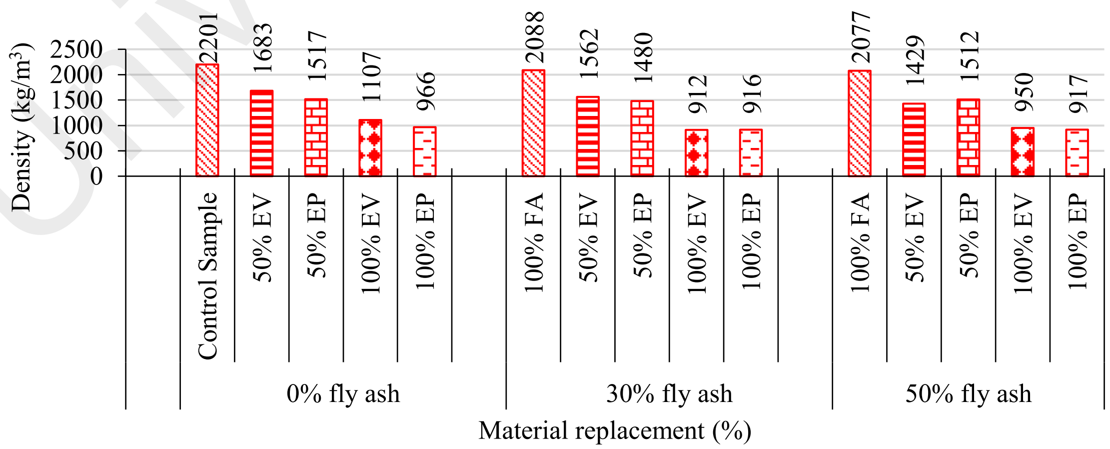

Figure 4.4: 28-day density of fly ash-blended mortar.

As summarized in Table 4.2, when sand was replaced by 50% and 100% of EV, about 24% and 50% reduction in density could be observed for the plain cement mortar. Similar trend in the density reduction could also be observed for the case of mortars containing EP, albeit to a slightly higher extent. The density of mortars containing 50% and 100% of EP can be reduced up to 31% and 56%, respectively. Similarly, past research works (Sengul, et al., 2011; Schackow, et al., 2014; Rashad, 2016a) reported that when the replacement level of sand by either EV or EP was increased, the unit weight of the cement-based products decreased significantly. The lightweight nature of the materials with low specific gravity and high porosity is the main contributing factor in reducing the density of the mortars (Turkmen and Kantarci., 2007; Koksal et al., 2015; Rashad, 2016b; Rozycka and Pichor, 2016). In short, a significant reduction in mortar density could be achieved with full replacement of sand with either EV or EP. When the lightweight aggregate was used in mortars blended with the SCM, similar observation was generally found, indicating minimal influence of the SCM on the density of lightweight aggregate mortars.

Table 4.2: Reduction of density compared to control mortar

Sample		Density (kg/m^3)	Reduction (%)
0% GGBS	**Control**	2201	-
	50% EV	1683	23.5
	50% EP	1517	31.1
	100% EV	1107	49.7
	100% EP	966	56.1
30% GGBS	**100% FA**	2122	3.6
	50% EV	1657	24.7
	50% EP	1482	32.7
	100% EV	976	55.7
	100% EP	922	58.1
50% GGBS	**100% FA**	2072	5.9
	50% EV	1622	26.3
	50% EP	1542	29.9
	100% EV	1016	53.8
	100% EP	944	57.1
70% GGBS	**100% FA**	2096	4.8
	50% EV	1625	26.2
	50% EP	1576	28.4
	100% EV	1072	51.3
	100% EP	932	57.7
30% fly ash	**100% FA**	2088	5.1
	50% EV	1562	29.0
	50% EP	1480	32.8
	100% EV	912	58.6
	100% EP	916	58.4
50% fly ash	**100% FA**	2077	5.6
	50% EV	1429	35.1
	50% EP	1512	31.3
	100% EV	950	56.8
	100% EP	917	58.3

Mortar density as low as in the range of 900–1100 kg/m^3 (classified as Class D1.2) could be achieved when the lightweight aggregate was used as complete sand replacement, whereas density in the range of 1400-1700 kg/m^3 (classified as Class D1.8) was attained with 50% of sand replacement. This was in line with previous reports whereby density below 1300kg/m^3 was found when vermiculite was used to replace sand as high as 60% (Schackow et al., 2014). Hence, the mortars containing EV and EP produced in this study can be considered as lightweight mortars based on BS EN 206-1.

4.2.3 Compressive Strength

Figure 4.5 and Figure 4.6 show the effect of sand replacement with the lightweight aggregate in GGBS and fly ash blended mortars, respectively. The compressive strength of mortar was reduced by up to 58% when the cement replacement by GGBS was increased from 0% to 70%. These results correspond well to those reported by Oner and Akyuz (2007) and Bilim and Atis (2012). This is known to be attributed to the slower hydraulic activity of GGBS compared to cement. The fly ash-blended mortar demonstrated similar trend when the cement content was reduced from 100% to 50%, as reflected with the 59% reduction in the 28-day compressive strength. This is likely due to the dilution effect and slower pozzolanic reaction of the fly ash. Nevertheless, it should be noted that the used of GGBS is more beneficial compared to that for fly ash, as higher compressive strength could still be obtained even at higher replacement levels.

In addition, slight improvement in compressive strength was found when the GGBS content was increased from 30% to 50% in either 50% EP or 100% EV mortar. This was probably due to the finer GGBS particles which improved the packing density and densified the overall cement matrix (Oner and Akyuz, 2007; Thakur et al., 2016; Xie et al., 2019). Hence, this encourages the use of lesser amount of cement towards producing a more sustainable cement mortar.

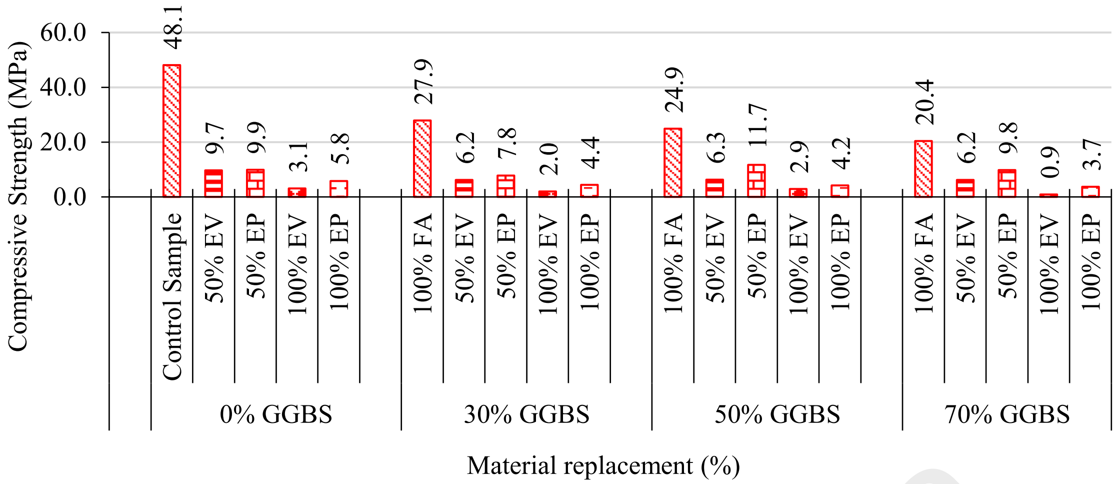

Figure 4.5: 28-day strength of GGBS-blended mortar.

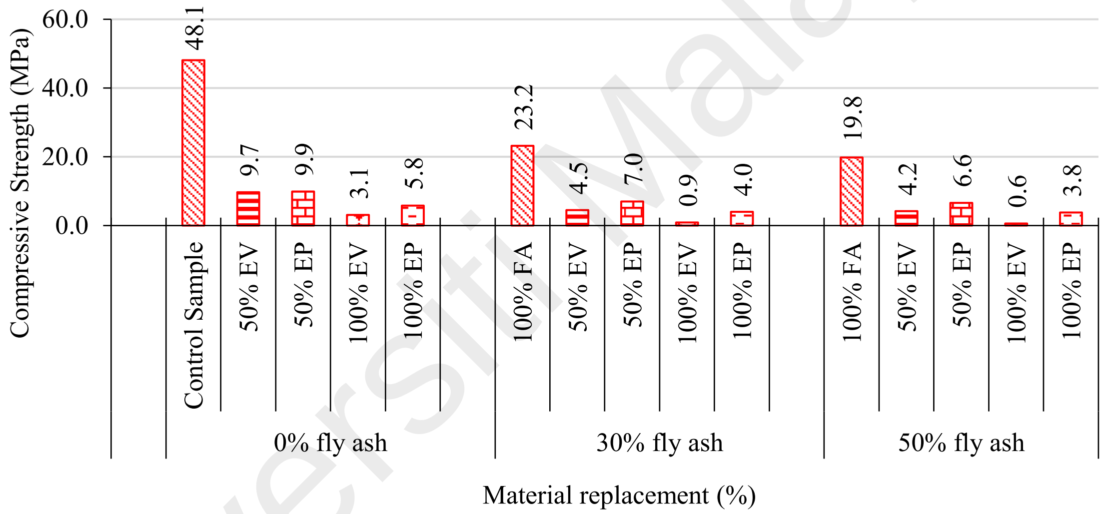

Figure 4.6: 28-day strength of fly ash-blended mortar.

In terms of the use of lightweight aggregate, when lightweight aggregate was used at 50% and 100% sand replacement, the compressive strength was decreased significantly by up to 80%-88% and 80%-94%, respectively as summarized in Table 4.3. This can be attributed to the low inherent strength of the EV and EP which contained high porosity, resulting in reduction of its mechanical properties (Rashad, 2016a). In addition, the lightweight aggregate had greater fineness and therefore surface area, thus requiring higher amount of cement paste to coat the aggregates compared to sand. Nevertheless, the results clearly highlighted that the mortar containing 50% of EP had higher compressive strength than the corresponding of mortar with similar content of EV as shown in Table 4.3. This could be due to the difference in particles size between EP and EV whereby the fineness is greater for EP. Hence, the fine particles of EP in the samples could exhibit pozzolanic reactivity and this could enhance the strength properties (Turkmen and Kantarci, 2007).

Table 4.3: Reduction of compressive strength compared to control mortar

Sample		Compressive strength (MPa)	Reduction (%)
0% GGBS	Control	48.1	-
	50% EV	9.7	79.8
	50% EP	9.9	79.4
	100% EV	3.1	93.6
	100% EP	5.8	87.9
30% GGBS	100% FA	27.9	42.0
	50% EV	6.2	87.1
	50% EP	7.8	83.8
	100% EV	2.0	95.8
	100% EP	4.4	90.9
50% GGBS	100% FA	24.9	48.2
	50% EV	6.3	86.9
	50% EP	11.7	75.7
	100% EV	2.9	94.0
	100% EP	4.2	91.3
70% GGBS	100% FA	20.4	57.6
	50% EV	6.2	87.1
	50% EP	9.8	79.6
	100% EV	0.9	98.1
	100% EP	3.7	92.3
30% fly ash	100% FA	23.2	51.8
	50% EV	4.5	90.6
	50% EP	7.0	85.4
	100% EV	0.9	98.1
	100% EP	4.0	91.7
50% fly ash	100% FA	19.8	58.8
	50% EV	4.2	91.3
	50% EP	6.6	86.3
	100% EV	0.6	98.8
	100% EP	3.8	92.1

By refer to the Table 4.3, low compressive strength (<3.5 MPa) was found for the mortars containing 100% EV, which represents a significant strength reduction of close to 95% compared to the mortars without EV. The compressive strength was even lower

(<1.0 MPa) for 100% EV in SCM-blended mortars. In contrast, in the SCM-blended mortars containing EP, the compressive strength obtained was in the range of 3.7-4.6 MPa. The corresponding compressive strength reduction was lower at about 80% compared to the SCM-blended mortars without EP. This demonstrates the use of SCM was more beneficial in reducing the strength decrease in EP mortars. A possible reason for this occurrence is the improved lightweight aggregate-matrix bonding due to the use of SCM such as GGBS and fly ash (Mo et al., 2017). This helps to reduce the compressive strength decrease associated with high EP contents. Hence, in order to obtain adequate compressive strength of lightweight aggregate mortar, EP is a more suitable choice as the lightweight fine aggregate compared to EV.

In general, mortars prepared with maximum amount of 50% EP can be classified as type N as all mortars (cement or SCM-blended) attained the minimum requirement of 5.17 MPa according to ASTM C270. For the use of 50% EV, only the cement and GGBS-blended mortars could be classified as type N. Fly ash-blended mortar containing 50% of EV can only be categorized as type O, as do all mortars containing 100% EP and cement mortar (no SCM) with 100% EV. SCM-blended mortars with 100% EV studied in this research is not recommended for use due to the low compressive strength.

4.2.4 RSM modelling and analysis

The density and compressive strength of mortar were analyzed through RSM and the design matrix of the variables were summarized in the code units as shown in Table 4.4 to Table 4.7 along with the actual (experimental values) and estimated value of all responses. Based on the RSM, a full quadratic model was employed for each factor and the coefficients of all parameters were given by the regression equation. Analyses of the variance (ANOVA) of the response surface models for all variables are presented in Table 4.5 to Table 4.8. P value approached in this study was employed for hypothesis testing, where “Prob > F” less than 0.05 denotes that the RSM model is statistically significant (Kumar and Baskar, 2014; Awolusi et al., 2019).

Table 4.4: Actual and predicted values for GGBS mortar with EP

Run	**Code factor**		**Flow (mm)**		**Density (kg/m^3)**		**Strength (MPa)**	
	A	**B**	**Actual**	**Predicted**	**Actual**	**Predicted**	**Actual**	**Predicted**
1	0	0	223	226	1410	1421	7.5	7.9
2	0	1	233	224	904	869	4.6	3.9
3	-1	-1	227	224	2201	2191	48.1	33.8
4	1	0	243	230	1576	1505	9.8	6.5
5	0	-1	201	199	2087	2064	23.9	23.3
6	-1	0	235	237	1517	1531	9.9	9.6
7	1	-1	181	189	2096	2131	20.4	17.1
8	1	1	229	241	932	970	3.7	3.4
9	-1	1	219	220	966	962	5.8	5.0
10	0	0	223	226	1410	1421	7.5	7.9
11	0	0	223	226	1410	1421	7.5	7.9
12	0	0	223	226	1410	1421	7.5	7.9
13	0	0	223	226	1410	1421	7.5	7.9
Residual SD			7.071		30.664		4.56	
COV (%)			3.90		2.59		8.29	
R^2			0.822		0.995		0.937	

Table 4.5: Actual and predicted values for GGBS mortar with EV

Run	Code factor		Flow (mm)		Density (kg/m^3)		Strength (MPa)	
	A	B	Actual	Predicted	Actual	Predicted	Actual	Predicted
1	0	0	194	188	1578	1576	6.1	5.2
2	0	1	174	173	957	991	0.9	0.7
3	-1	-1	227	215	2201	2207	48.1	44.5
4	1	0	168	176	1625	1628	6.2	4.7
5	0	-1	201	203	2087	2070	23.9	23.3
6	-1	0	180	201	1683	1695	9.7	11.8
7	1	-1	181	191	2096	2105	20.4	25.4
8	1	1	165	161	1072	1060	0.9	0.5
9	-1	1	181	186	1107	1093	3.1	1.89
10	0	0	194	188	1578	1576	6.1	5.2
11	0	0	194	188	1578	1576	6.1	5.2
12	0	0	194	188	1578	1576	6.1	5.2
13	0	0	194	188	1578	1576	6.1	5.2
Residual SD			9.414		13.73		2.14	
COV (%)			5.11		1.07		8.86	
R^2			0.707		0.998		0.987	

Table 4.6: Actual and predicted values for fly ash mortar with EP

Run	Code factor		Flow (mm)		Density (kg/m^3)		Strength (MPa)	
	A	B	Actual	Predicted	Actual	Predicted	Actual	Predicted
1	0	0	238	239	1408	1415	8.1	8.7
2	0	1	240	237	913	877	4.3	5.0
3	-1	-1	227	222	2201	2185	48.1	41.7
4	1	0	229	228	1512	1470	6.6	7.2
5	0	-1	200	206	2047	2052	21.6	22.4
6	-1	0	235	239	1517	1529	9.9	12.27
7	1	-1	178	178	2077	2089	19.8	17.7
8	1	1	233	242	917	951	3.8	4.2
9	-1	1	219	221	966	972	5.8	6.5
10	0	0	238	239	1408	1415	8.1	8.7
11	0	0	238	239	1408	1415	8.1	8.7
12	0	0	238	239	1408	1415	8.1	8.7
13	0	0	238	239	1408	1415	8.1	8.7
Residual SD			4.011		21.460		2.234	
COV (%)			1.93		1.82		4.23	
R^2			0.966		0.997		0.996	

Table 4.7: Actual and predicted values for fly ash mortar with EV

Run	Code factor		Flow (mm)		Density (kg/m^3)		Strength (MPa)	
	A	B	Actual	Predicted	Actual	Predicted	Actual	Predicted
1	0	0	192	186	1354	1367	3.9	3.6
2	0	1	177	174	932	891	0.7	0.7
3	-1	-1	227	214	2201	2239	48.1	47.0
4	1	0	149	171	1429	1428	4.2	3.2
5	0	-1	200	199	2047	2008	21.6	19.6
6	-1	0	180	201	1683	1607	9.7	11.1
7	1	-1	178	184	2077	2077	19.8	22.2
8	1	1	171	159	950	943	0.6	0.5
9	-1	1	181	189	1107	1140	3.1	2.7
10	0	0	192	186	1354	1367	3.9	3.6
11	0	0	192	186	1354	1367	3.9	3.6
12	0	0	192	186	1354	1367	3.9	3.6
13	0	0	192	186	1354	1367	3.9	3.6
Residual SD			11.78		33.583		1.149	
COV (%)			6.66		2.84		7.25	
R^2			0.600		0.994		0.995	

4.2.4.1 GGBS mortar with EP as sand replacement

For GGBS mortar containing EP as sand replacement, the ANOVA of flow diameter, density and strength are shown in Table 4.8. The flow results showed that the GGBS level effect ($p = 0.2273$) and the quadratic GGBS level effect ($p = 0.2304$) were statistically not significant at the stipulated level of 5%, which means that the significant factors of confidence level for both of these effects are lesser than 95% ($P<0.05$) in terms of probability value. Hence, null hypothesis should be considered in this case. The effect of EP content ($p = 0.0114$), quadratic EP content effect ($p = 0.0224$) and the effect of interaction of GGBS level and EP content ($p = 0.0142$) were statistically significant. Similarly, for density, only the quadratic of GGBS effect ($p = 0.0043$) were significant and other effects are insignificant.

Table 4.8: Analysis of variance (ANOVA) for flow, density and strength for GGBS with EP samples by RSM model

Sources	Flow (mm)				
	$\sum X$	D_f	$\bar{X}$	F value	p value
Model	2418.01	5	483.60	6.48	0.0147
A-GGBS	130.67	1	130.67	1.75	0.2273
B-EP	864.00	1	864.00	11.58	0.0114
AB	784.00	1	784.00	10.51	0.0142
A^2	128.75	1	128.75	1.73	0.2304
B^2	635.80	1	635.80	8.52	0.0224
Residual	522.30	7	74.61	-	-
Lack of fit	522.30	3	174.10	-	-
Pure Error	0.0000	4	0.0000	-	-
Total	2940.31	12			

Sources	Density (kg/m^3)				
	$\sum X$	D_f	$\bar{X}$	F value	p value
Model	2188000	5	437600	295.28	<0.0001
A-GGBS	1066.67	1	1066.67	0.7197	0.4243
B-EP	2138000	1	2138000	1442.88	<0.0001
AB	1260.25	1	1260.25	0.8503	0.3871
A^2	25618.55	1	25618.55	17.29	0.0043
B^2	5670.27	1	5670.27	3.83	0.0914
Residual	10374.53	7	1482.08	-	-
Lack of fit	10374.53	3	3458.18	-	-
Pure Error	0.0000	4	0.0000	-	-
Total	2198000	12			

Sources	Strength (MPa)				
	$\sum X$	D_f	$\bar{X}$	F value	p value
Model	0.1208	2	0.0604	75.43	<0.0001
A-GGBS	0.0056	1	0.0056	7.01	0.0244
B-EP	0.1152	1	0.1152	143.84	<0.0001
AB	-	-	-	-	-
A^2	-	-	-	-	-
B^2	-	-	-	-	-
Residual	0.0080	10	0.008	-	-
Lack of fit	0.0080	6	0.0013	-	-
Pure Error	0.0000	4	0.0000	-	-
Total	0.1288	12			

$\sum X$ = Sum of square; D_f = Degrees of freedom; $\bar{X}$ = Mean square

For the analysis of variance for strength in this mixture, effects of GGBS level (p = 0.0244) and EP content (p < 0.0001) were significant. Equation (4.1) to Equation (4.3) gives the final mathematical models in terms of actual factors. Since the maximum to minimum ratio for strength response was high, inverse square root transformation was adopted to achieve adjusted R^2 of 0.925. Figure 4.7 illustrated the effect of contour plot and response from RSM model for the variables of flow, density and strength in this mixture.

$$\text{Flow} = 223.943 - 0.923\text{A} + 0.567\text{B} + 0.008\text{AB} + 0.006A^2 - 0.006B^2 \quad \text{……. (4.1)}$$

$$\text{Density} = 2191.187 - 6.392\text{A} - 14.107\text{B} + 0.010\text{AB} + 0.079A^2 + 0.018B^2 \quad \text{..... (4.2)}$$

$$\text{Strength} = \left[\frac{1}{0.172+0.001A+0.003B}\right]^2 \quad \text{........ (4.3)}$$

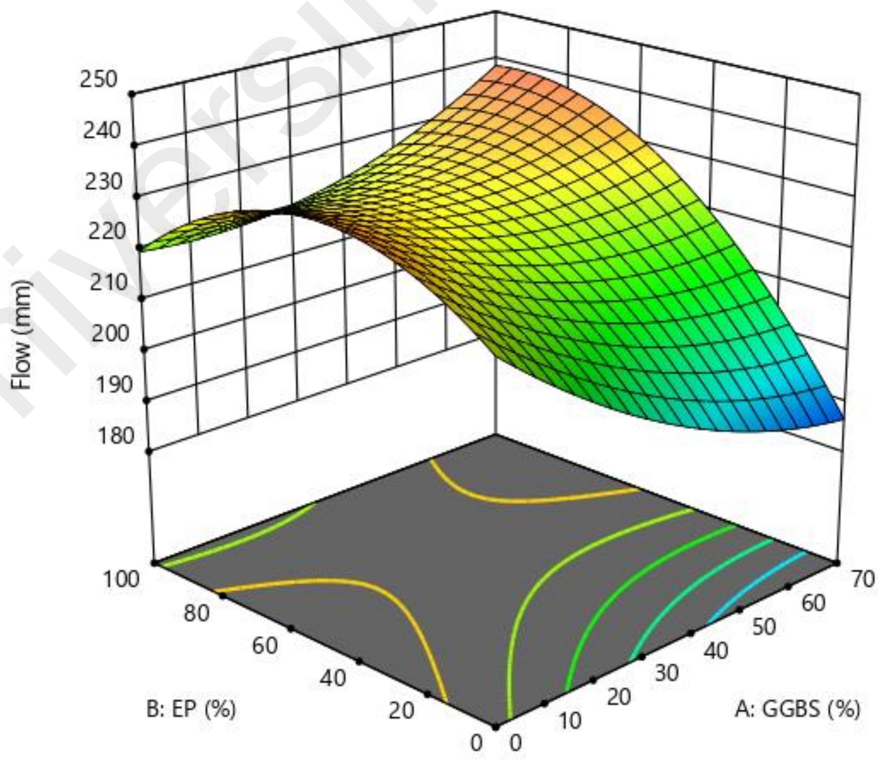

(a)

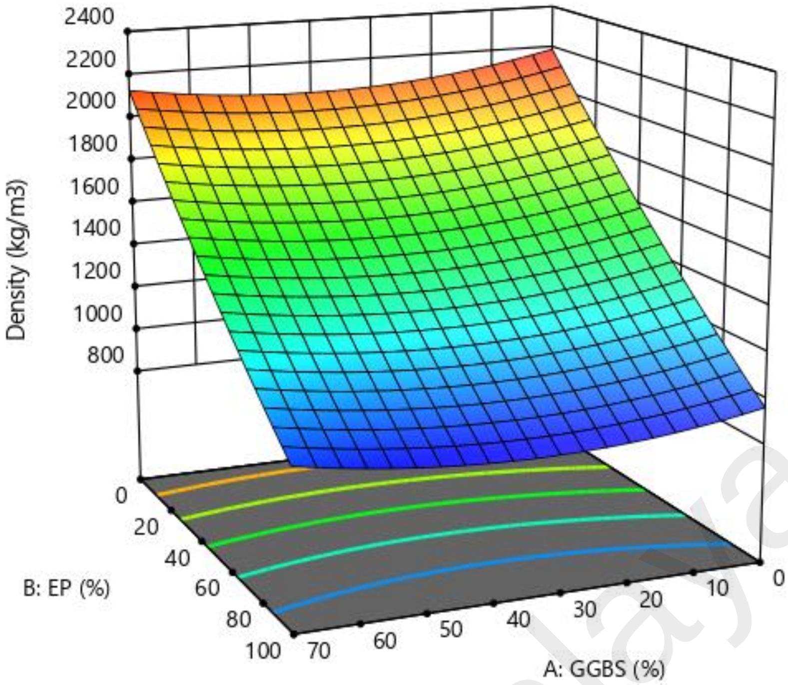

(b)

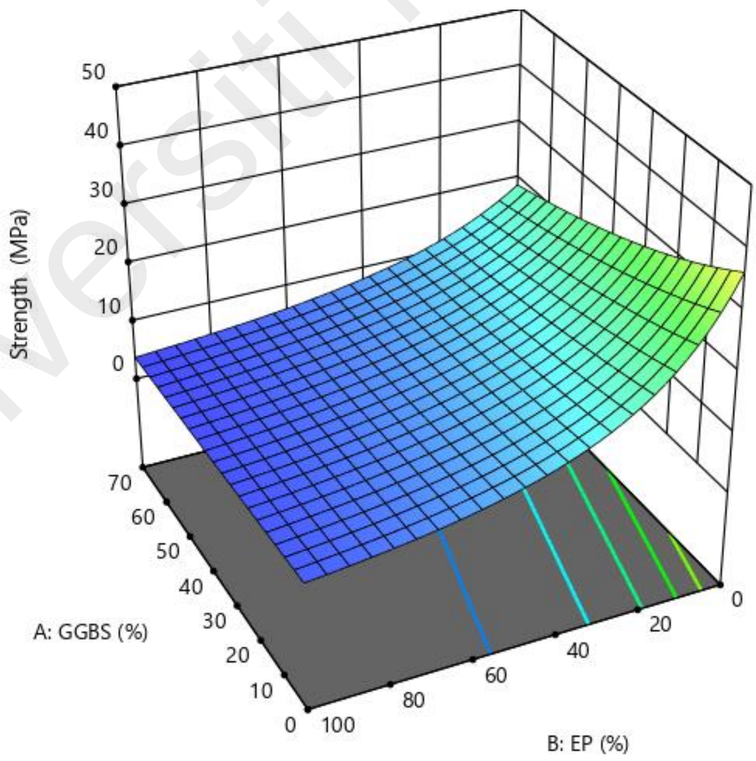

(c)

Figure 4.7: Contour plot and response surface of flow, density and strength for GGBS mortar with EP.

4.2.4.2 GGBS mortar with EV as sand replacement

Table 4.9 shows the ANOVA results for GGBS mortar with EV as sand replacement. In this mixture, the effects of GGBS level (p = 0.0104) and EV content (p = 0.0036) were statistically significant to the stipulated level for flow value. For the case of density, the effect of GGBS level (p = 0.0021), effect of EV content (p < 0.0001), quadratic effect of the GGBS level (p < 0.001) and EV content (p = 0.0029) were significant yet the effect of interaction between GGBS level with EV content (p = 0.0791) was not statistically significant at the stipulated level. Hence, null hypothesis was considered for the combination effect of GGBS with EV. The analysis of variance output for strength showed similar trend as that for the density as shown in Table 4.9. However, only the effect of interaction between GGBS level with EV content (p = 0.2867) and quadratic effect of EV content (p = 0.1194) were found not statistically significant for the strength of mortar.

Table 4.9: Analysis of variance (ANOVA) for flow, density and strength for GGBS with EV samples by RSM model

Sources	**Flow (mm)**				
	$\sum$ **X**	**D_f**	$\bar{X}$	**F value**	**p value**
Model	2232.83	2	1116.42	12.09	0.0021
A-GGBS	912.67	1	912.67	9.88	0.0104
B-EV	1320.17	1	1320.17	14.30	0.0036
AB	-	-	-	-	-
A^2	-	-	-	-	-
B^2	-	-	-	-	-
Residual	923.47	10	92.35	-	-
Lack of fit	923.47	6	153.91	-	-
Pure Error	0.0000	4	0.0000	-	-
Total	3156.31	12			

Sources	Density (kg/m^3)				
	$\sum X$	D_f	$\bar{X}$	F value	p value
Model	1787000	5	357400	1230.95	<0.0001
A-GGBS	6534.00	1	6534.00	22.50	0.0021
B-EV	1758000	1	1758000	6055.56	<0.0001
AB	1225.00	1	1225.00	4.22	0.0791
A^2	20492.62	1	20492.62	70.58	<0.0001
B^2	5809.20	1	5809.20	20.01	0.0029
Residual	2032.47	7	290.35	-	-
Lack of fit	2032.7	3	677.49	-	-
Pure Error	0.0000	4	0.0000	-	-
Total	1789000	12			

Sources	Strength (MPa)				
	$\sum X$	D_f	$\bar{X}$	F value	p value
Model	15.37	5	3.07	113.81	<0.0001
A-GGBS	1.08	1	1.08	39.89	0.0004
B-EV	13.93	1	13.93	515.85	<0.0001
AB	0.0359	1	0.0359	1.33	0.2867
A^2	0.3169	1	0.3169	11.74	0.0110
B^2	0.0849	1	0.0849	3.14	0.1194
Residual	0.1890	7	0.0270	-	-
Lack of fit	0.1890	3	0.0630	-	-
Pure Error	0.0000	4	0.0000	-	-
Total	15.56	12			

$\sum X$ = Sum of square; D_f = Degrees of freedom; $\bar{X}$ = Mean square

The final mathematical models in term of actual factors for estimation of the flow (mm), density (kg/m^3) and strength (MPa) of the mortar are given through Equation (4.4), (4.5) and (4.6). Figure 4.8 shows the contour plot and response for the variable of flow, density and strength of this mixture from the RSM model.

$$\text{Flow} = 215.397 - 0.352A - 0.297B \quad (4.4)$$

$$\text{Density} = 2207.213 - 6.365A - 9.342B + 0.010AB + 0.070A^2 - 0.018B^2 \quad (4.5)$$

$$\text{Strength} = e^{3.796-0.029A-0.0216B-0.0001AB+0.0003A^2-0.0001B^2} \quad (4.6)$$

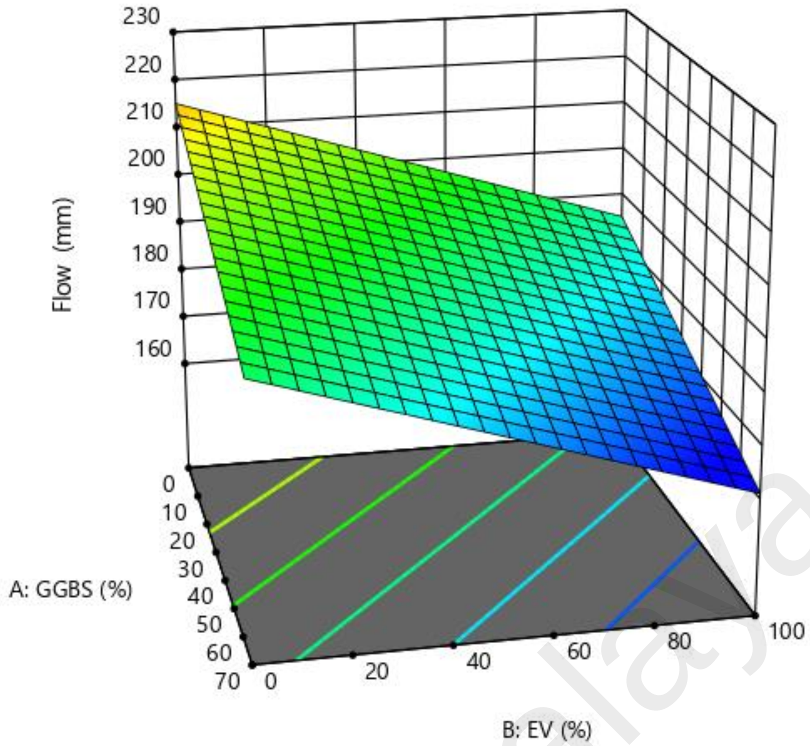

Flow (mm)
230
220
210
200
190
180
170
160
A: GGBS (%)
0
10
20
30
40
50
60
70
B: EV (%)
0
20
40
60
80
100

(a)

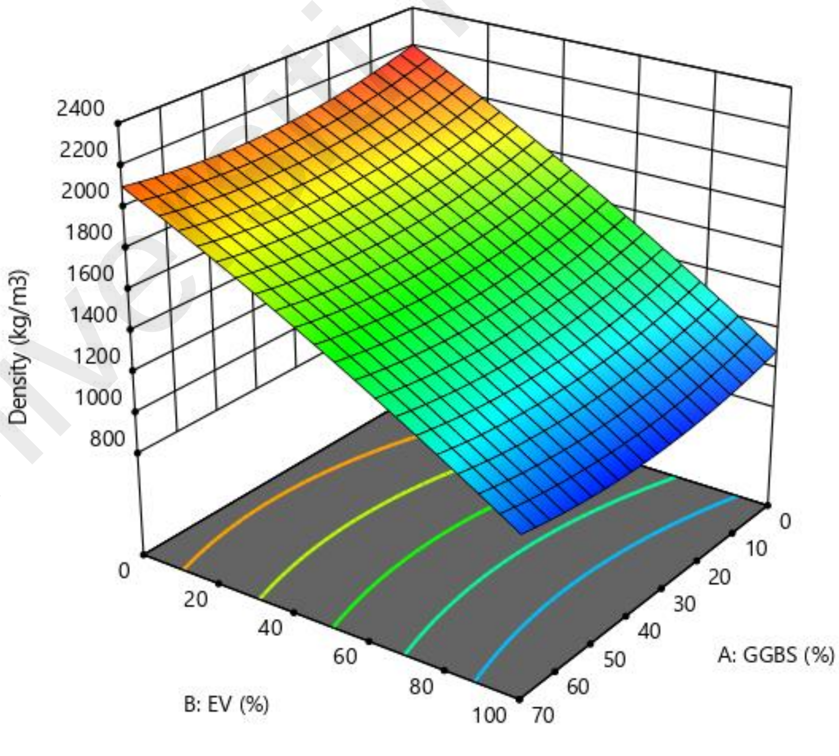

Density (kg/m3)
2400
2200
2000
1800
1600
1400
1200
1000
800
B: EV (%)
0
20
40
60
80
100
A: GGBS (%)
0
10
20
30
40
50
60
70

(b)

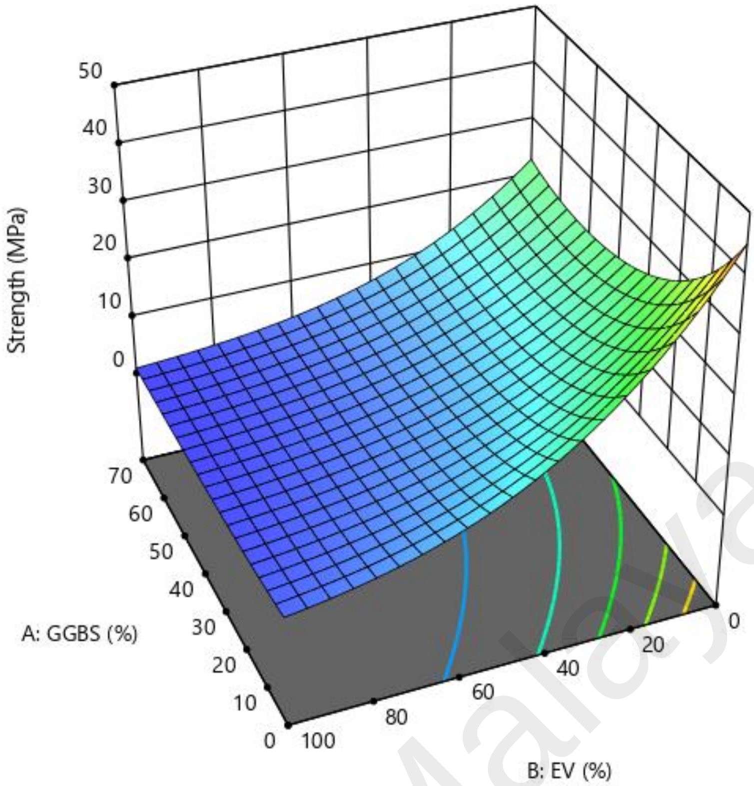

(c)

Figure 4.8: Contour plot and response surface of flow, density and strength for GGBS mortar with EV.

4.2.4.3 Fly ash mortar with EP as sand replacement

Table 4.10 summarizes the analysis output of flow, density and strength for fly ash mortar containing EP based on the RSM analysis. For flow diameter, the effects of fly ash level ($p = 0.0066$), EP content ($p < 0.0001$), quadratic effect of EP content ($p = 0.0003$) and the interaction of fly ash level with EP content ($p = 0.0002$) were statistically significant within the stipulated level of 5%, while only the quadratic effect of fly ash ($p = 0.0613$) was not statistically significant, which denotes that the significant factor of confidence level for this effect is lesser than 95%. When considering the effect on density, the analysis output shows that only the effect of interaction between fly ash with EP ($p = 0.2047$) was not statistically significant while the effect of fly ash level, EP content, quadratic effect of fly ash level and quadratic effect of EP content were all significant as shown in Table 4.10. Only the quadratic effect of fly ash content (p = 0.1917) was not significant for the case of the strength of mortar, while other effects were all statistically significant to the stipulated level of 5%.

Table 4.10: Analysis of variance (ANOVA) for flow, density and strength for fly ash with EP samples by RSM model

Sources	Flow (mm)				
	$\sum X$	D_f	$\bar{X}$	F value	p value
Model	3937.12	5	787.42	40.87	<0.0001
A-fly ash	280.17	1	280.17	14.54	0.0066
B-EP	1261.50	1	1261.50	65.47	<0.0001
AB	992.25	1	992.25	51.50	0.0002
A^2	95.47	1	95.47	4.95	0.0613
B^2	882.90	1	882.90	45.82	0.0003
Residual	134.88	7	19.27	-	-
Lack of fit	134.88	3	44.96	-	-
Pure Error	0.0000	4	0.0000	-	-
Total	4072.00	12			

Sources	Density (kg/m^3)				
	$\sum X$	D_f	$\bar{X}$	F value	p value
Model	2123000	5	424700	590.63	<0.0001
A-fly ash	5280.67	1	5280.67	7.34	0.0302
B-EP	2076000	1	2076000	2886.62	<0.0001
AB	1406.25	1	1406.25	1.96	0.2047
A^2	19568.08	1	19568.08	27.21	0.0012
B^2	6814.58	1	6814.58	9.48	0.0179
Residual	5033.38	7	719.05	-	-
Lack of fit	5033.38	3	1677.79	-	-
Pure Error	0.0000	4	0.0000	-	-
Total	2129000	12			

Sources	Strength (MPa)				
	$\sum$ X	D_f	$\bar{X}$	F value	p value
Model	0.0565	5	0.0113	389.38	<0.0001
A-fly ash	0.0049	1	0.0049	167.79	<0.0001
B-EP	0.0505	1	0.0505	1739.94	<0.0001
AB	0.0009	1	0.0009	32.07	0.0008
A^2	0.0001	1	0.0001	2.09	0.1917
B^2	0.0002	1	0.0002	6.84	0.0346
Residual	0.0002	7	0.0000	-	-
Lack of fit	0.0002	3	0.0001	-	-
Pure Error	0.0000	4	0.0000	-	-
Total	0.0567	12			

$\sum$ X = Sum of square; D_f = Degrees of freedom; $\bar{X}$ = Mean square

Equation (4.7) to Equation (4.9) presented the final mathematical models in term of actual factors for estimating the flow, density and strength of the mortar mix. Figure 4.9 showed the contour plot and response for the variables of flow, density and strength of the mix based on the RSM model. Similar as the trend observed in the corresponding GGBS mixtures containing EP, high volume replacement of fly ash and EP content reduced the overall density and compressive strength.

$$\text{Flow} = 222.290 - 0.433\text{A} + 0.690\text{B} + 0.013\text{AB} - 0.009A^2 - 0.007B^2 \quad (4.7)$$

$$\text{Density} = 2184.807 - 8.670\text{A} - 14.125\text{B} + 0.015\text{AB} + 0.135A^2 + 0.020B^2 \quad (4.8)$$

$$\text{Strength} = \frac{1}{0.024+0.001A+0.001B+0.00001AB-0.000007A^2+0.000003B^2} \quad (4.9)$$

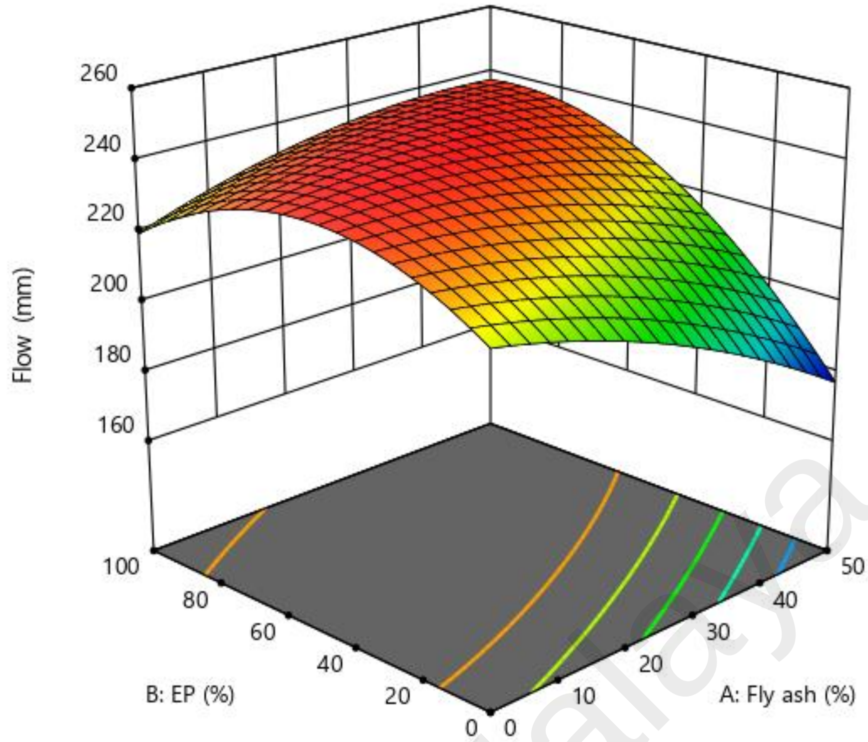

Flow (mm)
260
240
220
200
180
160
100
80
60
40
20
0
B: EP (%)
0
10
20
30
40
50
A: Fly ash (%)

(a)

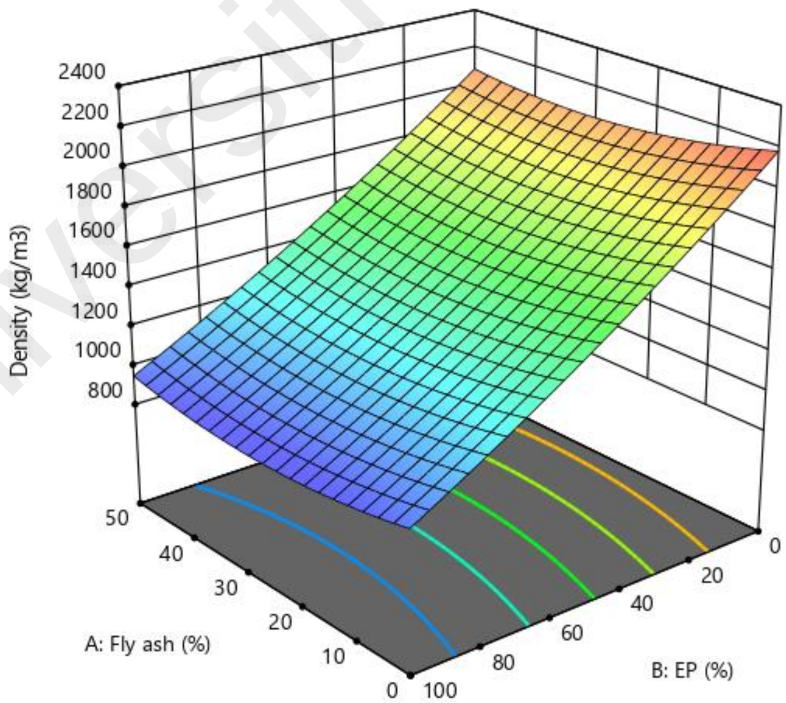

Density (kg/m3)
2400
2200
2000
1800
1600
1400
1200
1000
800
50
40
30
20
10
0
A: Fly ash (%)
100
80
60
40
20
0
B: EP (%)

(b)

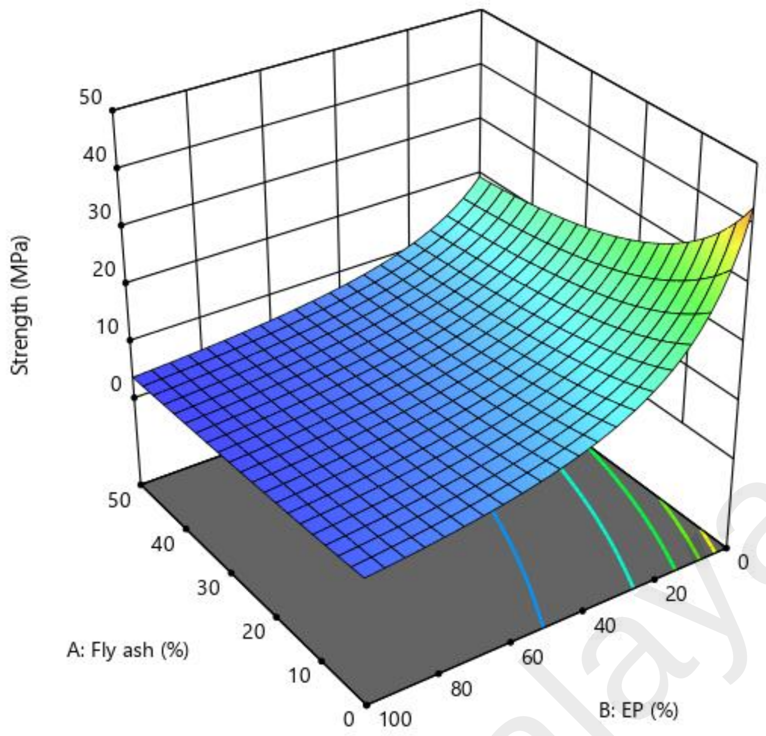

(c)

Figure 4.9: Contour plot and response surface of flow, density and strength for fly ash mortar with EP.

4.2.4.4 Fly ash mortar with EV as sand replacement

Table 4.11 summarizes the ANOVA for all 3 responses in the mixture containing fly ash with EV as sand replacement. From the RSM analysis, it was found that the effects of fly ash level ($p = 0.0143$) and EV content ($p = 0.0315$) on the flow of the mortar were statistically significant. Similar trend was found for the density, whereby the effect of fly ash level ($p = 0.0012$), effect of EV content ($p < 0.0001$), quadratic effect of fly ash level ($p = 0.0006$) and quadratic effect of EV content ($p = 0.0130$) were statistically significant at the stipulated level of 5%. However, the interaction between fly ash level and EV content ($p =0.7057$) was not statistically significant on the density of mortar. Therefore, null hypothesis was required for this effect due to larger probability value. In terms of the mortar strength, only the quadratic effect of EV content ($p = 0.9300$) was found to be not statistically significant, while the other effects, namely fly ash level ($p < 0.0001$), EV content ($p < 0.0001$), interaction of fly ash level with EV content ($p = 0.0137$) and quadratic effect of fly ash level ($p = 0.0002$) were statistically significant.

Table 4.11: Analysis of variance (ANOVA) for flow, density and strength for fly ash with EV samples by RSM model

Sources	Flow (mm)				
	$\sum X$	D_f	$\bar{X}$	F value	p value
Model	2312.67	2	156.33	7.50	0.0103
A-fly ash	1350.00	1	1350.00	8.75	0.0143
B-EV	962.67	1	962.67	6.24	0.0315
AB	-	-	-	-	-
A^2	-	-	-	-	-
B^2	-	-	-	-	-
Residual	1542.41	10	154.24	-	-
Lack of fit	152.41	6	257.07	-	-
Pure Error	0.0000	4	0.0000	-	-
Total	3855.08	12			

Sources	Density (kg/m^3)				
	$\sum X$	D_f	$\bar{X}$	F value	p value
Model	2029000	5	405800	230.78	<0.0001
A-fly ash	47704.17	1	47704.17	27.13	0.0012
B-EV	1855000	1	1855000	1054.92	<0.0001
AB	272.25	1	272.25	0.1548	0.7057
A^2	62128.57	1	62128.57	35.34	0.0006
B^2	19248.74	1	19248.74	10.95	0.0130
Residual	12307.77	7	1758.25	-	-
Lack of fit	12307.77	3	4102.59	-	-
Pure Error	0.0000	4	0.0000	-	-
Total	2041000	12			

Sources	Strength (MPa)				
	$\sum X$	D_f	$\bar{X}$	F value	p value
Model	18.43	5	3.69	276.42	<0.0001
A-fly ash	1.89	1	1.89	141.67	<0.0001
B-EV	15.58	1	15.58	1168.11	<0.0001
AB	0.1424	1	0.1424	10.68	0.0137
A^2	0.6958	1	0.6958	52.18	0.0002
B^2	0.0001	1	0.0001	0.0083	0.9300
Residual	0.0933	7	0.0133	-	-
Lack of fit	0.0933	3	0.0311	-	-
Pure Error	0.0000	4	0.0000	-	-
Total	18.52	12			

$\sum X$ = Sum of square; D_f = Degrees of freedom; $\bar{X}$ = Mean square

From RSM analysis, equations (4.10), (4.11) and (4.12) were obtained in terms of actual factors to predict the flow, density and strength of the mix. The contour plot and response of each variable in this mixture were shown in Figure 4.10. Similar as the observation in GGBS mortar containing EV, the fly ash level and EV content were found to have more significant effect individually on the properties of this mortar.

$$\text{Flow} = 214.051 - 0.600\text{A} - 0.253\text{B} \quad (4.10)$$

$$\text{Density} = 2239.244 - 15.235\text{A} - 14.294\text{A} - 0.007\text{AB} + 0.240A^2 + 0.033B^2 \quad (4.11)$$

$$\text{Strength} = e^{3.850-0.055A-0.029B-0.0002AB+0.0008A^2+0.000003B^2} \quad (4.12)$$

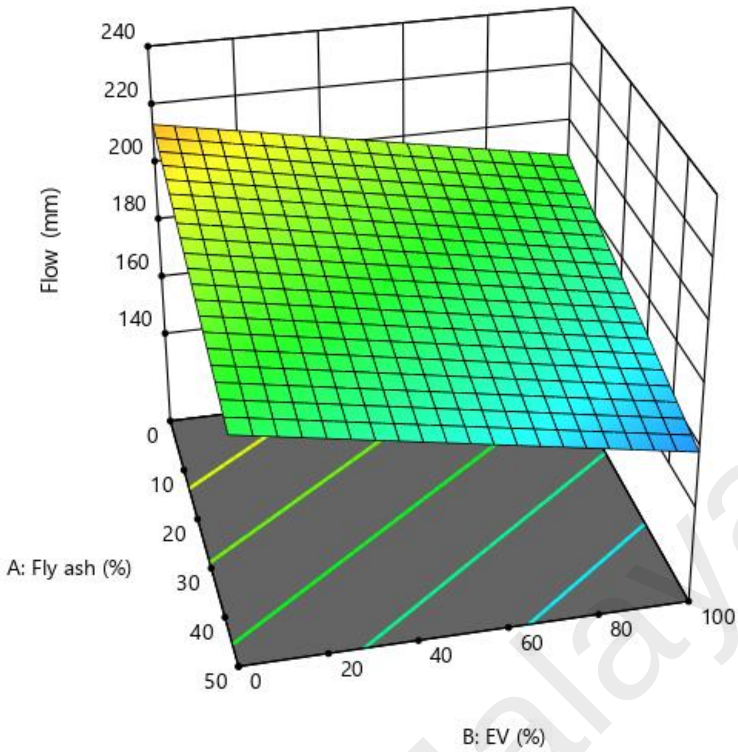

240
220
200
180
160
140
Flow (mm)
0
10
20
30
40
50
A: Fly ash (%)
0
20
40
60
80
100
B: EV (%)

(a)

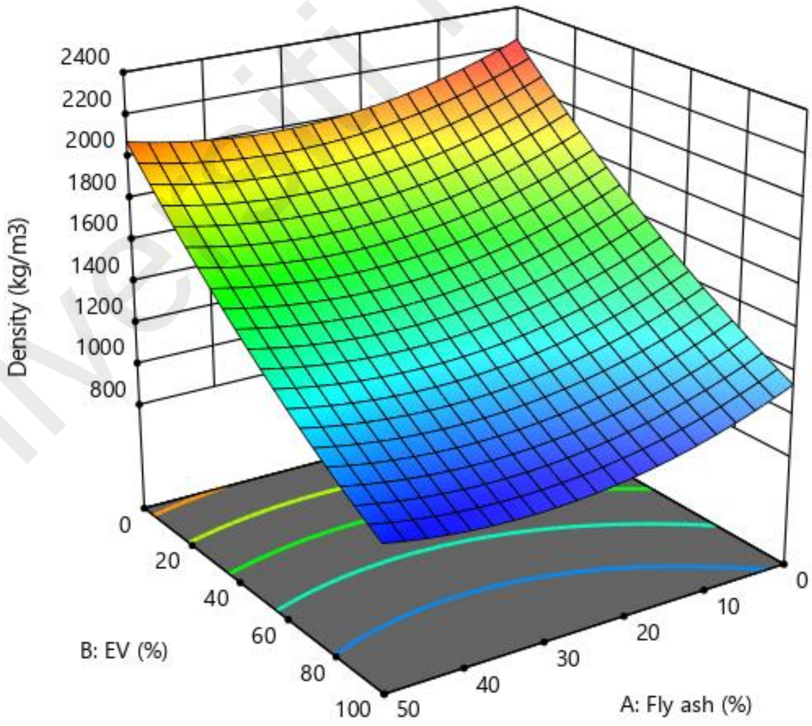

2400
2200
2000
1800
1600
1400
1200
1000
800
Density (kg/m3)
0
20
40
60
80
100
B: EV (%)
50
40
30
20
10
0
A: Fly ash (%)

(b)

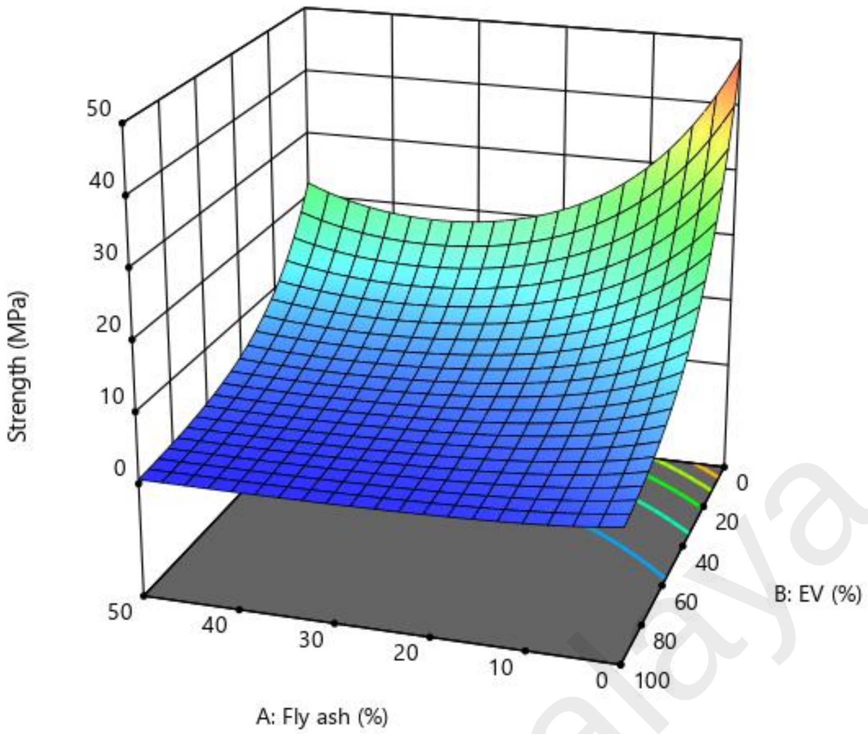

(c)

Figure 4.10: Contour plot and response surface of flow, density and strength for fly ash mortar with EV.

4.2.4.5 Validation of experiment

The overall model of all mixtures was statistically significant for chosen significant level of 5% (Kumar and Baskar, 2014). The experimental values of flow, density and strength of the mortars were used to validate the calculated statistical models. For validation of mortar mixtures containing GGBS with either EP or EV as sand replacement, the constituent of 35% GGBS with 50% of EP or EV content were taken, whereas 25% fly ash with 50% of EP or EV content were adopted for the validation analysis in the fly ash mortar mixtures. It can be seen from Table 4.12 that the experimental values agreed well with the predicted values, and this validates the calculated response surface models (Kumar and Baskar, 2014).

Table 4.12: Validation of the responses surface model for different types of samples

Properties / Mix types	Flow (mm)			Density (kg/m^3)			Strength (MPa)		
	C	D	Diff.	C	D	Diff.	C	D	Diff.
GGBS with EP mix	223	226	-1.35	1410	1421	-0.78	7.5	7.9	-5.3
GGBS with EV mix	194	188	3.09	1578	1576	0.13	6.1	5.2	14.8
Fly ash with EP mix	238	239	-0.42	1408	1415	-0.50	8.1	8.7	-7.4
Fly ash with EV mix	192	186	3.13	1354	1367	-0.96	3.9	3.6	7.7

C = Experiment Results D = RSM Prediction Diff. = Differences (%)

4.3 Phase II

Table 4.13 summarizes the comparison between experimental results and RSM analysis. The accuracy of density prediction from RSM analysis as high as 95% was obtained for SCM mortar mixed with selected lightweight fine aggregate. Whereas, when evaluated in terms of compressive strength, the accuracy as high as 87% was obtained for all combination mix containing SCM with EP as sand replacement. However, the accuracy of RSM prediction was reduced to 69% especially for EV mortar in the absence of SCM. In overall, the combination mix such like control, G0-EV50, G30-EV50, G0-EP50, G30-EP50 and F30-EP50 are achieved with the targeted density (in the range of 1400-1600kg/m^3) and strength ($\geq$ 5.17MPa) for both experimental data and RSM analysis. Hence, these samples were selected to further evaluated at Phase II.

Table 4.13: Comparison result between experimental data and RSM analysis

Properties / Mix types	Density (kg/m^3)			Strength (MPa)		
	C	D	Diff.	C	D	Diff.
Control	2201	-	-	48.1	-	-
G0-EV50	1683	1694	-0.7	9.7	12.7	-30.9
G30-EV50	1657	1582	4.5	6.2	6.4	-3.2
G0-EP50	1517	1531	-0.9	9.9	10.4	-5.1
G30-EP50	1482	1425	3.9	7.8	8.8	-12.8
F30-EP50	1480	1412	4.6	7.0	7.7	-10.0

C = Experiment Results D = RSM Prediction Diff. = Differences (%)

4.3.1 Fresh properties (flow diameter and water retention)

Figure 4.11 presents the flow value of selected samples in Phase II. As discussed in section 4.2.1, all mortars containing EP with different types of binder (cement + GGBS/cement + fly ash/cement) had higher flow diameter range (220mm-235mm) than the corresponding EV mortar sample (185mm-195mm). The trend of the results is in line with the results obtained from Phase I. Hence, it can be verified that the mortar containing EP as sand replacement with or without SCM (GGBS/fly ash) is categorized as soft mortar (flow value > 200mm), while the mortar with 50% EV can only be classified as plastic mortar (flow value within 140mm to 200mm) in accordance with ASTM C1437.

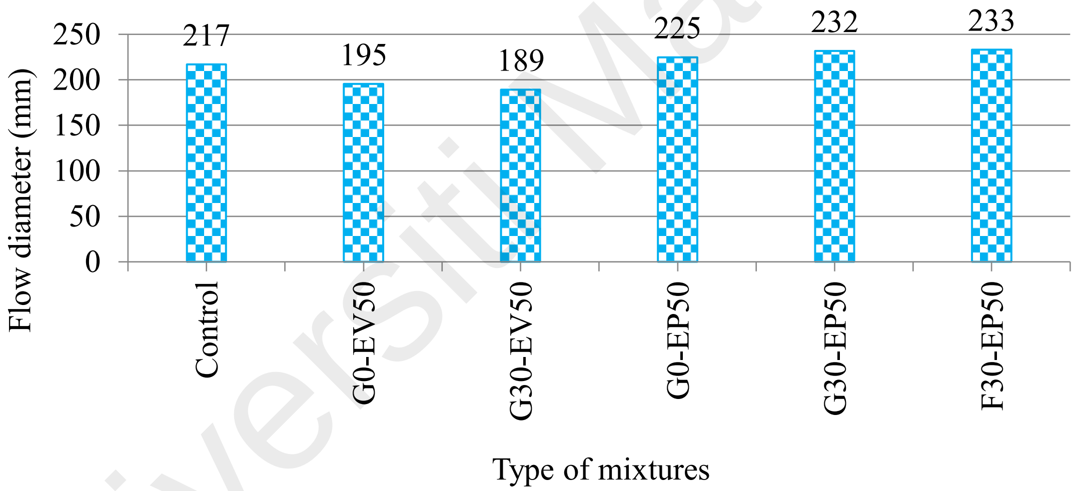

Figure 4.11: Flow value of selected samples.

Figure 4.12 shows the results of the water retention capacity of the fresh mortar samples. With regards to the effect of cement replacement in the fresh lightweight mortar, there was only minimal effect on the water retention when the SCM (GGBS or fly ash) was adopted as partial cement replacement. As compared to G0-EV50 and G0-EP50, there was no significant difference in the water retention value when 30% of GGBS or fly ash was used in EV or EP mortar (91.3% to 92.8%). However, the water retention capacity of these mortars seemed to be influenced by the type and content of aggregates used (Carrajola et al., 2021). For example, mortar mixed with 50% of EP and EV as lightweight aggregate exhibited slightly higher water retention value (91.3% and 92.8%, respectively) than the control mortar (90.6%). This could be mainly attributed to the porous structure of EV and EP mortar which retained more water and improved the water molecules bonding in the mixture. Furthermore, the internal cavities of the lightweight aggregate could be partially saturated with water due to the 30-minutes pre-soaking of the lightweight aggregate in water prior to mixing. Hence, an adequate amount of EV or EP in mortar is useful to enhance the water retention and ensure limited water loss.

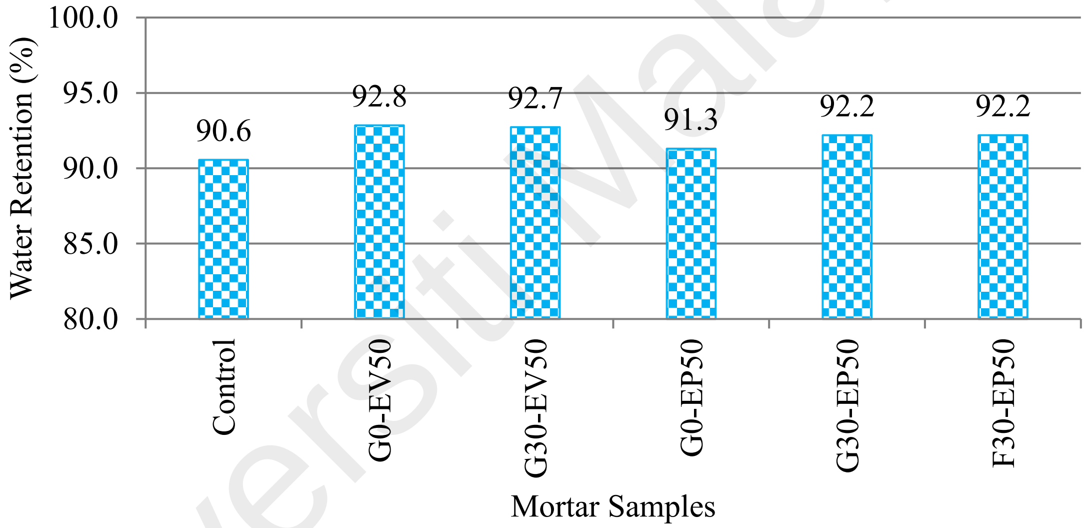

Figure 4.12: Water retention value of selected samples.

This is in line with previous works where 20% recycled concrete aggregates (Neno et al., 2014) and 50% crushed sanitary ware aggregates (Lucas et al., 2016) were utilized as sand replacement in mortar, recording the higher water retentivity of 89.3% and 75.4%, respectively compared to the control sample (< 72.7%). Similarly, in the use of pre-soaked woodchips as sand replacement in mortar, it was reported that the water retention was about 25% higher compared to that for conventional mortar when 63% sand (by volume) was replaced. The high hygroscopicity of woodchips than sand increased the capacity of water retention in the mixture (Nakarai et al. 2019). In addition, it was highlighted that water retention value as high as 86% was obtained when 25% lightweight expanded polystyrene or cork was used as sand replacement in mortar (Oliveira et al., 2013).

In short, the obtained water retention results in this research are in the range of 90% to 93%. These types of mortars are suitable to be used as rendering for concrete block due to its adequate water retentivity (>85%) which can resist high shrinkage rate or extensive cracking (Suryakanta, 2017).

4.3.2 Density

The density of all mortar samples in Phase II is presented in Table 4.14. There is only a maximum of 6% difference in the density found in samples compared to that obtained in Phase I and estimation from the RSM, indicating the consistency in producing the lightweight mortar. As discussed in section 4.2.2, the choice of materials used in mortar samples influenced its overall density. For example, the reduction in density is clearly highlighted in the samples containing the lightweight aggregate, namely G0-EV50 and G0-EP50 compared to the control mortar (Table 4.14). This was similarly pointed out in past researchers when incorporating more than 50% EP (Oktay et al., 2015; Rozycka et al., 2016) or EV (Karatas et al., 2019; Mo et al., 2018) as sand replacement in concrete or mortar samples. The density reduction as high as 65% could be achieved in these past findings. The reduction of density in mortar or concrete sample was attributed to the use of lightweight aggregate (either EP or EV) which are porous structure and has lower specific gravity (0.70 and 1.01, respectively for EP and EV) than sand (2.65). Also, the porous structure and high water absorption capacity of lightweight aggregate could cause density reduction due to increase number of internal cavities in mortar or concrete matrix (Kou et al., 2009; Lv et al., 2015; Bisht and Ramana, 2017).

Table 4.14: Differences in density between Phase II with Phase I and RSM prediction

Sample	**Density (kg/m^3)**			**Difference with Phase I (%)**	**Difference with RSM (%)**
	Phase I	**Phase II**	**RSM**		
Control	2201	2151	-	2.3	-
G0-EV50	1683	1592	1694	5.4	6.0
G30-EV50	1657	1575	1582	4.9	0.4
G0-EP50	1517	1452	1531	4.3	5.2
G30-EP50	1482	1460	1425	1.5	-2.5
F30-EP50	1480	1415	1412	4.4	-0.2

In this research, the use of SCM (either fly ash or GGBS) as partial cement replacement in mortar sample did not have significant influence on the density of mortar. Only a maximum of 3% density reduction was found in mortar containing fly ash or GGBS, corresponding well with the observed maximum 6% reduction found from Phase I. The slight reduction can be attributed to the lower specific gravity of fly ash (2.5) and GGBS (2.9) than cement (3.15). In short, it is verified that the selected mortar samples in Phase II achieved the target density (in the range of 1400kg/m^3 to 1600kg/m^3). The mortar samples are classified as Class D1.6 according to BS EN 206-1.

4.3.3 Compressive strength

Figure 4.13 shows the crack pattern of lightweight mortar after the 28 days compressive strength test. There is no negative impact on the crack pattern for the mortars mixed with 50% lightweight aggregate (EP or EV) and incorporated with 30% SCM (GGBS or fly ash) as cement replacement. In terms of compressive strength of cement mortar as shown in Table 4.15, there is only a maximum of 9% difference was found by comparing results between Phase II with Phase I, verifying the accuracy and consistency of the experimental results.

Figure 4.13: Crack pattern of lightweight mortars.

Table 4.15: Difference of strength between Phase II with Phase I

Sample	Compressive strength (MPa)		Difference (%)
	Phase I	Phase II	
Control	48.1	45.3	-6.2
G0-EV50	9.7	8.9	-9.0
G30-EV50	6.2	5.8	-8.6
G0-EP50	9.9	9.5	-4.2
G30-EP50	7.8	8.3	6.0
F30-EP50	7.0	7.6	7.9

Concerning the effect of sand replacement, the use of lightweight aggregate (EP and EV) in mortar is the main factor which caused the reduction of strength. This was also highlighted in previous works where about 40% to 65% of sand was replaced by either EP or EV in mortar or concrete sample resulted in strength reduction in the range of 31% to 85% (Sengul et al., 2011; Schackow et al., 2014; Oktay et al., 2015; Mo et al., 2018; Karatas et al., 2019). It was similarly reported that when 30% to 50% of crumb rubber was used as sand replacement in mortar or concrete sample, strength reduction as high as 78% could be found (Yu and Zhu, 2016; ; Si et al., 2018; Zahid Hossain et al., 2019). The reduction in strength for these mortars or concretes was generally attributed to the use lightweight aggregates which are more porous (Sengul et al., 2011; Oktay et al., 2015) and could increase the internal cavities in the mixture.

On the other hand, by using 30% of GGBS as cement replacement in EP and EV mortars, the strength loss was increased by about 13% and 35%, respectively compared to sample without GGBS. Previous research works highlighted similar trends whereby when 45% to 70% of cement was replaced by GGBS, the strength loss as high as 20% was found for mortar (Lim et al., 2012; Ling and Poon, 2014) and concrete samples (Thakur et al., 2016; Xie et al, 2020). The reduction of strength is likely due to the slow hydraulic activity of GGBS than cement (Oner and Akyuz, 2007; Bilim and Atis, 2012). In addition, strength reduction associated with GGBS can be attributed to the effect of cement content dilution with GGBS which is more significant particularly at higher cement replacement level (Oner and Akyuz, 2007; Thakur et al., 2016; Chowdary et al., 2017; Xie et al., 2020).

Similarly, with the use of 30% fly ash as cement replacement in EP mortar (F30-EP50), strength loss increased up to 20% compared the corresponding sample without fly ash. The obtained result is in line with past research when 50% of fly ash was used as cement replacement in blended mortar, where strength reduction could be up to 34% (He et al., 2019). This was due to the dilution effect and slower pozzolanic reaction of fly ash than cement which required longer time for strength gain. Unlike GGBS, fly ash is not a hydraulic material. Hence, by replacing the cement content with high amount of fly ash, the depletion of calcium hydroxide caused fly ash to be less effective in contributing to the strength development by the pozzolanic reaction (Gholampour and Ozbakkaloglu, 2017).

Nevertheless, all samples prepared in Phase II are verified to have similar performance as determined in Phase I. These mortars can be categorized as mortar type

N according to ASTM C270 as the minimum compressive strength requirement of 5.17MPa was achieved.

4.3.4 Sorptivity

Sorptivity refers to the transportation of water in porous structure of matrix due to the surface tension acting in capillaries action. As the number of pores in the mortar or concrete reduced, the sorptivity coefficient decreased significantly due to low capillary sorption. Table 4.16 summarizes the sorptivity of the selected mortars in Phase II. Obviously, the control mortar had the lowest sorptivity coefficient (0.336mm.min$^{-0.5}$). This is because sand is denser and less porous compared to EV or EP. The control mortar is therefore denser and has lesser capillary pores. Figure 4.14 shows the appearance of samples after the completion of sorptivity test. It can be seen that the water level due to capillary action is lower for the control mortar compared to the other lightweight mortar samples, justifying the lower sorptivity coefficient obtained for the control mortar.

Table 4.16: Average value of sorptivity coefficient with the standard deviation

Sample	**Average sorptivity coefficient (mm.min$^{-0.5}$)**	**Standard deviation**
Control	0.336	0.001
G0-EV50	0.999	0.022
G30-EV50	1.399	0.097
G0-EP50	1.101	0.090
G30-EP50	0.947	0.215
F30-EP50	1.298	0.068

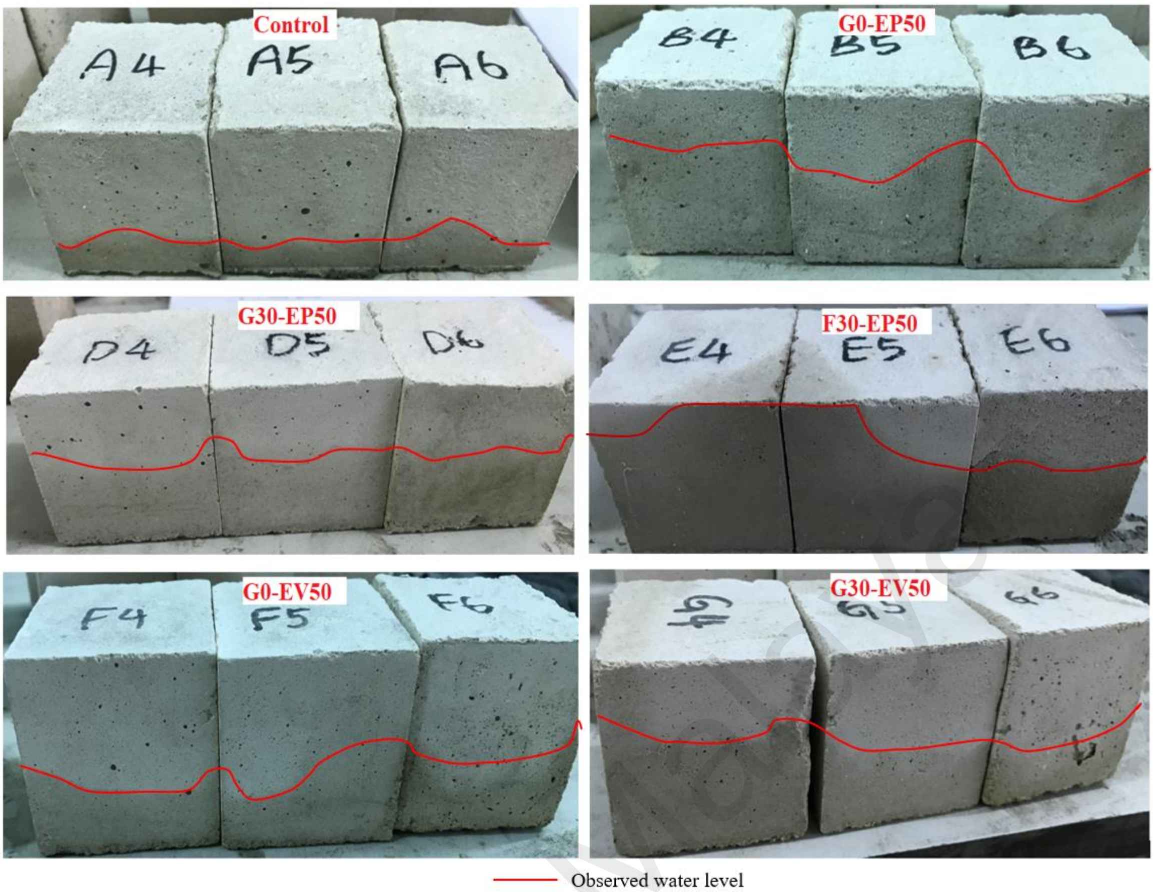

Figure 4.14: Appearance of mortars after completion of sorptivity test.

The reduction of sorptivity (from 1.101mm.min$^{-0.5}$ to 0.947mm.min$^{-0.5}$) was found when the GGBS content in EP mortar was increased from 0% to 30%. This can be attributed to finer particles of GGBS which reduced the tendency of capillary absorption as more pores can be filled by the inclusion of GGBS in the mixture (Mohan and Mini, 2018). This was in line with previous works when 10% silica fume was introduced as cement replacement in lightweight expanded clay concrete as the sorptivity coefficient was decreased up to 50% compared to the concrete without silica fume (Muhammad and Chen, 2019; Muhammad et al., 2019). However, the opposite trend in the results was observed when fly ash was used as cement replacement in EP mortar. The sorptivity coefficient for F30-EP50 (1.298 mm.min$^{-0.5}$) was higher than G30-EP50 (0.947 mm.min$^{-0.5}$). As suggested with the reduced compressive strength of the lightweight mortar due to fly ash, there could be more pores, as the dominating cement dilution effect could cause the fly ash to be less reacted and with lesser pozzolanic reactions, there are less C-S-H gels formed. Besides that, the incomplete hydration process of fly ash in EP mortar could be due to the air curing method used in this research. Since fly ash is known to be sensitive to curing, the air curing may limit the pre refinement effect of the fly ash.

By partially replacing sand with either EP or EV, the mortar samples of G0-EP50 and G0-EV50 exhibit similar sorptivity of 1.101 mm.min$^{-0.5}$ and 0.999 mm.min$^{-0.5}$, respectively, which was about 3 times higher than that for the control. Both EP and EV have low specific gravity with high water absorption than sand, which likely result in high sorptivity (Silva et al., 2010; Schackow et al., 2014; Rozycka and Pichor, 2016; Rashad, 2016a). The highly porous microstructure of EP was the main reason which caused the EP mortar to absorb more water and increase the sorptivity coefficient (Rozycka and Pichor, 2016 and Lu et al., 2018). Similarly, in the case for EV mortar, the porous and soft structure of EV increased the number of internal cavities in the matrix (Silva et al, 2010; Schackow et al., 2014). In addition, insufficient water for hydration in EV mortar could create more pores due to weak bonding between EV with cement paste (Gencel et al., 2021). Hence, more water will be absorbed in EV mortar than that corresponding with control. This is in line with previous work where the sorptivity coefficient was increased by about 50% when 75% sand was replaced by lightweight polyethylene terephthalate aggregates in cement mortar (Choi et al., 2009).

4.3.5 Sound absorption

In building materials, sound absorption refers to the amount of energy removed from the sound wave as the wave pass through a given material such as plastering mortar or concrete block wall. Generally, the sound absorption coefficient (in the range of 0 to

1) is used to evaluate the sound absorption efficient of the materials. Higher coefficient (close to 1) indicates that sound energy is completely absorbed by the materials used and this means that the noise can be controlled. Hence, in order to improve the noise absorption of cement-based materials, nowadays high volume of lightweight aggregate introduced (Bashar et al., 2012; Mohammed et al., 2012; Arenas et al., 2013). This is because lightweight aggregate such as EV, EP, expanded clay and crumb rubber have the characteristics of low self-weight with porous structure which can contribute to absorb more sound or noise when used as part of building materials for rendering purpose. In this way, the use of acoustic insulation materials such as acoustic foam and fiberglass cotton can be minimized.

Figure 4.15 shows the graph of sound absorption coefficient versus frequency for the selected mortars in Phase II. Compared to control mortar (density about 2151kg/m^3), the higher sound absorption coefficient value in the range of 0.23 to 0.26 (at frequency between 400Hz to 500Hz) was obtained for all the lightweight mortars (density about 1400kg/m^3 to 1600kg/m^3). This was attributed to the inclusion of EP and EV which are porous than sand and this created more voids in the matrix to improve the acoustic performance. Similar trend of results was reported by Mohammed et al. (2012) as the obtained absorption coefficient was 0.23 (frequency range of 100 – 5000Hz) when 50% of crumb rubber was used as sand replacement in hollow concrete block (density about 1500kg/m^3).

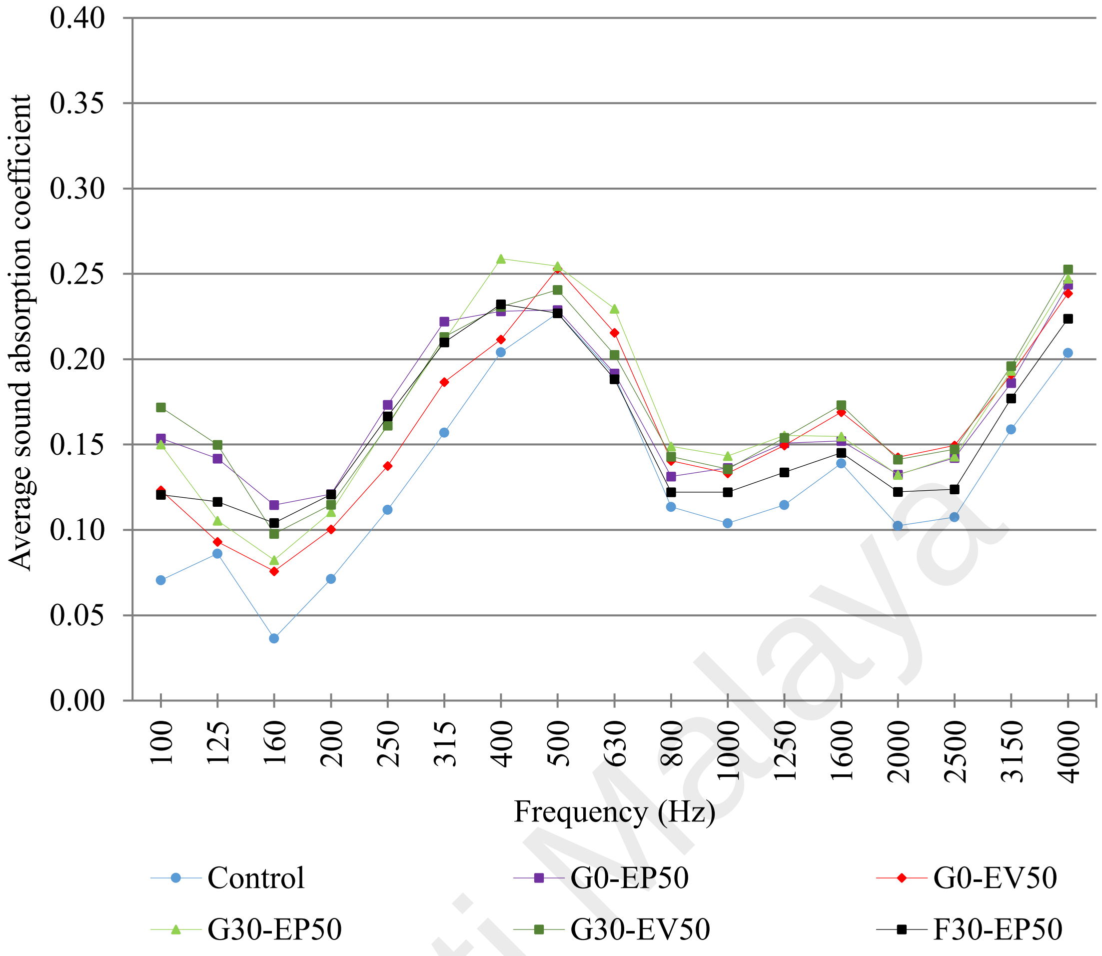

Figure 4.15: Sound absorption coefficient for Phase II samples.

However, it is difficult to compare the acoustic performance of materials based on sound absorption coefficient values at different frequency range. Hence, the noise reduction coefficient (NRC) is computed for further analysis. Table 4.17 shows the NRC value for the selected mortars. The NRC value for all lightweight mortars is in the range of 0.16 to 0.17 and higher than the control mortar (NRC about 0.14). The obtained results correspond well with past research works for lightweight concrete and cement mortar containing crumb rubber. It was reported that sound absorption for concrete was improved by about 71% when crumb rubber was used up to 50% sand replacement (Ling et al., 2010; Mohammed et al., 2012). Shah et al. (2021) also reported that the NRC value of cement mortar increased from 0.096 to 0.102 when the crumb rubber content as sand replacement was increased from 50% to 100%. This was due to the formation of porosity in crumb rubber mortar or concrete created from the trapped air between cement paste and aggregate surface. Similar observation was reported when using bottom ash as sand replacement in concrete. For example, NRC as high as 0.25 and 0.59 was obtained when 60% (Leiva et al., 2012) and 80% (Arenas et al., 2013) of bottom ash was used as sand replacement in concrete. The improvement of NRC was also attributed to the porous nature and lower specific gravity of bottom ash aggregate.

Table 4.17: NRC for selected mortar samples

Sample	NRC
Control	0.14
G0-EV50	0.17
G30-EV50	0.17
G0-EP50	0.17
G30-EP50	0.17
F30-EP50	0.16

Besides that, the smaller particle size of the lightweight aggregates (EP and EV) compared to sand could be another reason which increased the NRC. In separate research using EV aggregate, pervious concrete with smaller size EV had a higher NRC of 0.35 compared to larger-size EV which recorded NRC of 0.28 (Carbajo et al., 2015). It was reasoned that the smaller aggregate size could create higher flow resistivity and narrower pore structure in mixture and enhanced the attenuation.

4.3.6 Solar reflectance

The solar reflectance index (SRI) is the measurement of material's ability to reject or reflect the solar heat. This is an important parameter to be evaluated in view of understanding the potential of a material for applications related to solar heat an building energy conversation. Generally, bright or white coloured surface of cement-based materials have higher SRI than those in materials with darker coloured surface. Compared to a darker coloured surface, bright or white coloured surface of cement-based materials have the benefit of reflect solar radiation and reduce the room temperature when applied in the building materials for exterior wall.

Figure 4.16 shows the appearance and color of the selected mortar samples. The sample G0-EP100 has the "whitest" appearance compared to the other samples. Hence, this mixture was additionally investigated for the solar reflectance for comparison purpose. Figure 4.17 summarizes the comparison of SRI between RGB histogram with the field protocol measurement of the mortar samples. From the analysis, G0-EP100 has the highest SRI value, which was about 0.61 and 0.65 for protocol measurement and RGB histogram, respectively. The obtained result is in line with literature whereby the solar reflectance for white concrete tile was in the range of 0.65 and 0.80 (Kultur and Turkeri, 2012). However, the albedo value obtained by other researchers for white tarp sample was slightly lower compared to this research, which was about 0.50 (Sailor et al., 2006). This was probably due to the type of samples used and locality where the weather differs between countries.

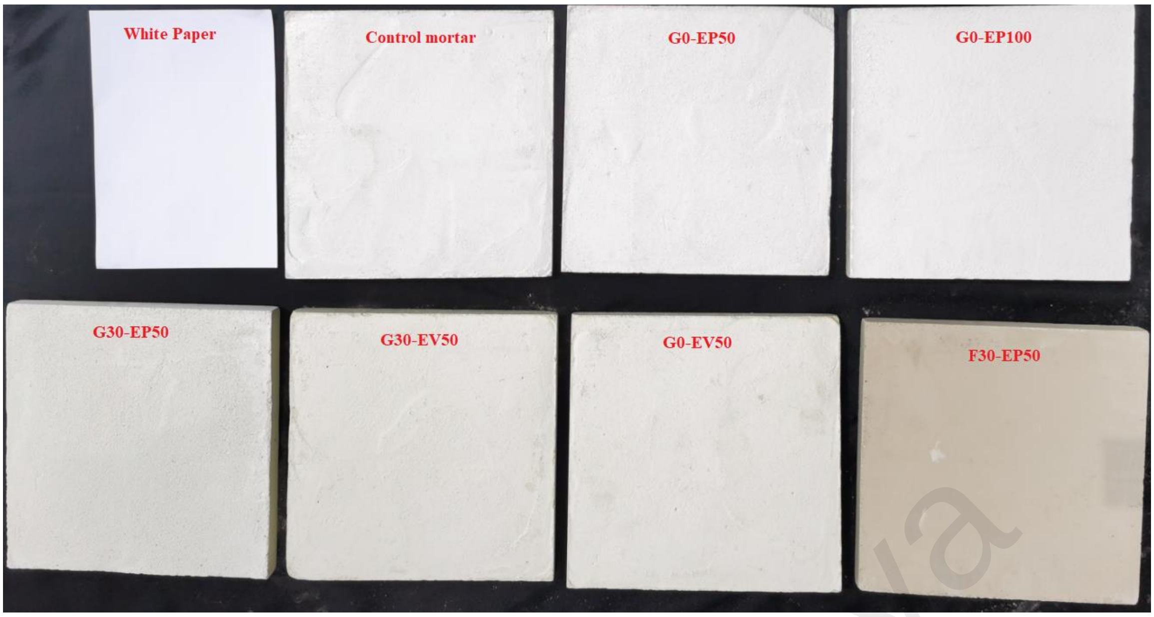

Figure 4.16: Appearance of the mortar samples in solar reflectance test.

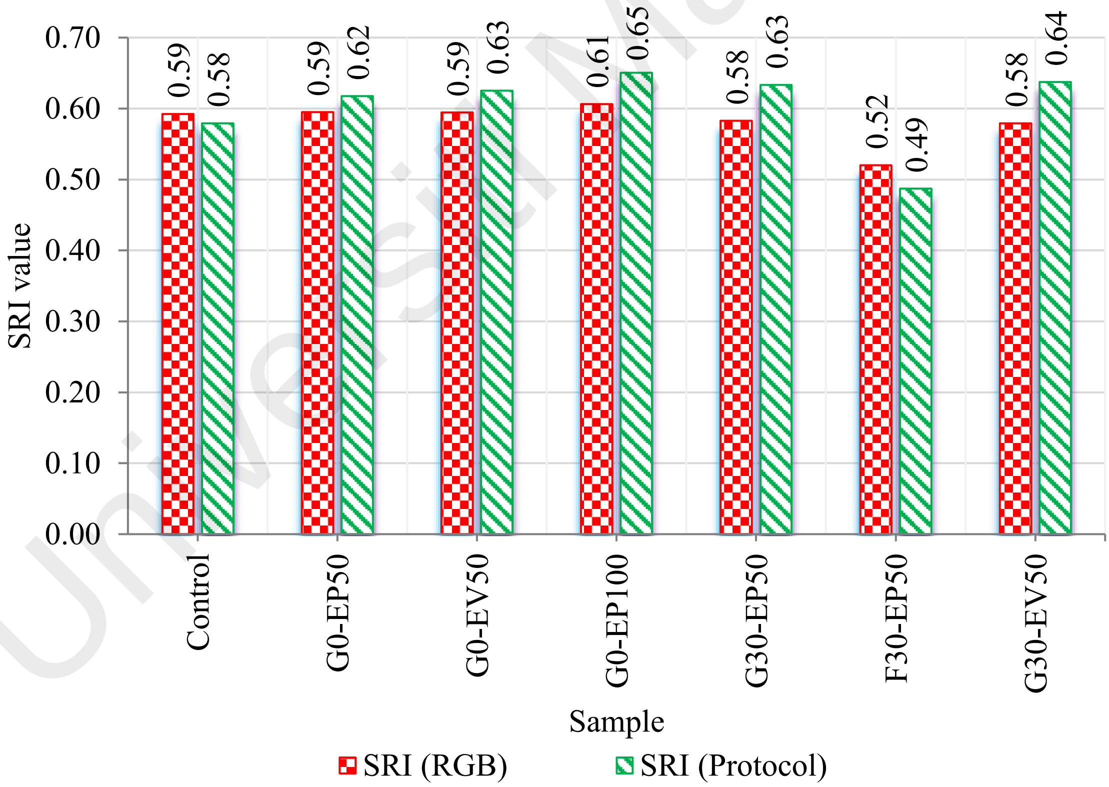

Figure 4.17: Comparison between SRI value from RGB histogram analysis with protocol measurement.

There is little influence on the solar reflectance due to the type of lightweight aggregates (EP or EV) and the use of GGBS. However, the SRI value was reduced when 30% of fly ash was adopted as cement replacement in EP mortar. The SRI value was reduced from 0.63 to 0.49 by using protocol measurement and decreased from 0.58 to 0.52 when analyzed through RGB histogram. This is likely due to the brownish color of fly ash which caused mortar sample to turn light brownish in color. This is in agreement with the works of Dornelles et al. (2015) where the solar reflectance value was reduced significantly from 0.90 to 0.54 when the roof coating was changed from white to dark-yellow color. Similarly, it was reported that SRI for basalt rock concrete was reduced from 0.59 to 0.54 when the darker concrete was produced by changing the fine aggregate from beach sand to brown sand (Levison and Akbari, 2002). Furthermore, Nickholas Anting et al. (2014) revealed that the used of waste light grey tiles as coating materials for asphalt pavement could lower down the surface temperature up to 8.5% when compared to uncoated asphalt pavement. This was attributed to the bright colour of the coating materials on asphalt pavement which resulted in higher reflectance properties than the uncoated asphalt pavement. It was reported previously that by incorporating 30% of POFA as cement replacement in foamed concrete, the surface temperature was slightly increased by up to 3% due to blackish colour of POFA than cement (Jhatial et al., 2020c). This is because darker or black colour surface will absorb most of the solar radiation (or reduced the solar reflectance) and caused the surface temperature increased. Hence, it can be concluded that the appearance of sample is the main factor influencing the solar reflectance properties.

By comparing the SRI value between RGB histogram with protocol measurement, not more than 10% difference was found for the mortar samples. This suggests that the RGB histogram can be an alternative method to evaluate the SRI for sample, particularly for lab-scale size samples which are much smaller. However, further investigation is recommended to further verify the accuracy of the method.

In short, G0-EP100 shows the best performance in reflecting solar radiation compared to other samples. This is then followed by G30-EV50, G30-EP50, G0-EV50 and G0-EP50, whereby the SRI was about 0.62 to 0.64 from protocol measurement and range between 0.58 to 0.59 based on RGB histogram. However, for the purpose of good solar radiation reflectance, the use of fly ash in the mortar is not suggested as it may darken the color of the produced mortar.

CHAPTER 5: CONCLUSION & RECOMMENDATIONS

5.1 Conclusion

The research involves 2 phases: in Phase I, the influence of SCM (fly ash and GGBS) and lightweight aggregate (EP and EV) on the density and strength of mortars were evaluated; in Phase II, selected lightweight mortar mixtures were further evaluated for their key properties and functional properties. Based on the research, the following conclusions can be drawn based on the individual objectives set out in the study:

i) Objective 1: To determine the optimum combination of high volume SCM (GGBS and fly ash) and lightweight fine aggregate in cement mortar

Mortar density as low as in the range 900-1000kg/m^3 can be obtained when EP and EV was used as complete sand replacement while density in the range of 1400 kg/m^3 to 1700kg/m^3 was achieved when 50% of EP and EV was used. Basically, inclusion of lightweight aggregate in mortar caused significant reduction in compressive strength. However, through the use of SCM, the strength reduction could be limited especially for EP mortar. The mathematical equation used to predict the density and compressive strength of the lightweight mortar mixtures were also proposed through RSM. In overall, samples such as control, G0-EV50, G30-EV50, G0-EP50, G30-EP50 and F30-EP50 are achieved with the targeted density (in the range of 1400 kg/m^3 to 1600kg/m^3) and targeted strength (≥5.17MPa). Hence, these mortars are considered as optimum mixes in this study.

ii) Objective 2: To evaluate the influence of SCM (GGBS and fly ash) and lightweight fine aggregate on the key properties of cement mortar.

All selected mortars containing EP as sand replacement (G0-EP50, G30-EP50 and F30-EP50) are categorized as soft mortar due to the higher flow diameter (220mm-235mm) obtained compared to that of the corresponding to EV (185mm-195mm) mortar. Water retention value as high as 90% could be obtained for all selected mortars. Hence, these types of mortars are suitable to be used as rendering for construction work. In terms of strength and density, all the selected mortar can be categorized as Mortar Type N (≥ 5.17MPa) with Density Class D1.6 (1400kg/m^3 to 1600m^3) according to ASTM C270 and BS EN 206-1. Among the selected lightweight aggregate mortar samples, G30-EP50 (30% GGBS in 50% EP mortar) is considered as the best to be used due to the adequate strength (8.3MPa), flow (232mm) and lowest sorptivity coefficient (0.947 mm.$min^{-0.5}$).

iii) Objective 3: To assess the functional properties (sound absorption and solar reflectance) of the lightweight cement mortar.

Among all the selected lightweight mortars, the mortar containing 30% GGBS as cement replacement and 50% EP as sand replacement exhibited the highest sound absorption of 0.26 at frequency about 400Hz. In terms of NRC, lightweight aggregate mortar with EP and EV was 0.16 - 0.17 and represents an improvement compared to the control. This indicates the beneficial effect in using the lightweight aggregate for better sound absorption properties. Among the selected lightweight aggregate mortar samples, G0-EP100 (100% expanded perlite with only cement) has the best performance in reflecting solar radiation (SRI of 0.65). This is followed by G30-EV50, G30-EP50, G0-EV50, G0-EP50 and control with only slightly lower but similar SRI of 0.62 to 0.64. F30-EP50 exhibited the lowest

SRI of 0.49 due to the brownish color of fly ash compared to the lighter colour of white cement and GGBS.

Among the mortar investigated in this research, the lightweight cement mortar mixed with 30% GGBS as partial cement replacement and 50% EP as partial sand replacement (G30-EP50) is considered as the best performing mix in achieving the research objectives.

5.2 Recommendations

Considering the positive performance of the lightweight aggregate mortar in application specific to rendering application, there are certain aspects of research can that be carried out in future, these includes:

- Development of rendering / thermal mortar mixtures using lightweight aggregate and SCM
- Assessment of the adhesive and shrinkage properties of the lightweight cement mortar to ensure suitable usage for rendering purpose.
- Investigate the vapour and water transmission properties of the lightweight cement mortars to ensure suitable usage of rendering.

REFERENCE

Abdul Rahman, S.S. & Bahu, G.K. (2016). An experimental investigation on lightweight cement concrete using vermiculite minerals. *International Journal of Innovative Research in Science, Engineering and Technology,* 5 (2), 2389-2392, http:// doi:10.15680/ijirset.2016.0502156.

Akbari, H., Levinson, R, Stern, S. (2008). Procedure for measuring the solar reflectance of flat or curved roofing assemblies. *Solar Energy*, 82 (7), 648-655, https://doi.org/10.1016/j.solener.2008.01.001.

Ali, M.B., Saidur, R. & Hossain, M.S. (2011). A review on emission analysis in cement industries. *Renewable and Sustainable Energy Reviews,* 15 (5), 2552-2261, https://doi.org/10.1016/j.rser.2011.02.014.

Allameh-Haery, H., Kisi, E., Pineda, J., Prasad Suwal, L. & Fiedler, T. (2017). Elastic properties of green expanded perlite particle compacts. *Powder Technology,* 310, 329-342, https://doi.org/10.1016/j.powtec.2017.01.045.

Amato, I. (2013). Green cement: Concrete solutions. *International Weekly Journal of Science*, 494, 300-301, https://doi.org/10.1038/494300a.

American Society for Testing and Materials (ASTM – C270). (2014). Standard specification for mortar for unit mansonry. American Society. USA.

Ampol, W., Vanchai, S., Behzad, N., Jay, S. & Chindaprasirt, P. (2018). Mechanical and thermal properties of lightweight geopolymer mortar incorporating crumb rubber. *Journal of Clean Production,* 195, 1069-1080, https://doi.org/10.1016/j.jclepro.2018.06.003.

Arenas, C., Leiva, C., Vilches, L.F., Cifuentes, H. (2013). Use of co-combustion bottom ash to design an acoustic absorbing materials for highway noise barrier. *Waste Management,* 33 (11), 2316-2321, https://doi.org/10.1016/j.wasman.2013.07.008.

Arenas, C., Leiva, C., Vilches, L.F., Cifuentes, H., Rodriguez-Galan, M. (2015). Technical specifications for highway noise barriers made of coal bottom ash-based sound absorbing concrete. *Construction and Building Materials,* 95, 585-591, https://doi.org/10.1016/j.conbuildmat.2015.07.107.

ASTM International Designation: (C91/C91M). (2018). Standard specification for masonry cement. American Society. West Conshohocken.

ASTM International Designation: (ASTM C 1437). (2015). Standard test method for flow of hydraulic cement mortar. American Society.

ASTM International Designation: (ASTM C 1585). (2004). Standard test method for measurement of rate of absorption of water by hydraulic cement concretes. American Society.

ASTM International Designation: (ASTM E1918). (2016). Standard test method for measuring solar reflectance of horizontal and low sloped surfaces in the field. American Society. West Conshohocken.

ASTM International Designation: (C 618-19). (2019). Standard specification for coal fly ash and raw or calcined natural pozzolan for use. American Society. West Conshohocken.

Awolusi, T.F., Oke, O.L., Akinkurolere, O.O., & Sojobi, A.O. (2019). Application of response surface methodology: Predicting and optimizing the properties of concrete containing steel fibre extracted from waste tires with limestone powder as filler. *Cases Studies in Construction Materials*, 10, e00212, https://doi.org/10.1016/j.cscm.2018.e00212.

Bakhtiyari, S., Allahverdi, A. & Rais-Ghasemi, M. (2014). A case study on modifying the fire resistance of self-compacting concrete with expanded perlite aggregate and zeolite powder additives. *Asian Journal of Civil Engineering (Building and housing),* 15 (3), 339-349, https://www.sid.ir/en/journal/ViewPaper.aspx?id=353382.

Bashar, S.M., Khandaker, M.A.H., Ting, J.E.S., Wong, G. & Abdullahi, M. (2012). Properties of crumb rubber hollow concrete block. *Journal of Clean Production.* 23 (1), 57-67, https://doi.org/10.1016/j.jclepro.2011.10.035.

Bashar, S.M. & Musa, A. (2018). Mechanical performance of roller compacted concrete pavement containing crumb rubber and nano silica. *Construction and Building Materials,* 159, 234-251, https://doi.org/10.1016/j.conbuildmat.2017.10.098.

Benli, A., Karatas, M. & Bakir, Y. (2017). An experimental study of different curing regimes on the mechanical properties and sorptivity of self-compacting mortars with fly ash and silica fume. *Construction and Building Materials,* 144, 552-562, https://doi.org/10.1016/j.conbuildmat.2017.03.228.

Bilim, C. & Atis, C.D. (2012). Alkali activation of mortars containing different replacement levels of ground granulated blast furnace slag. *Construction and Building Materials.* 28 (1), 708-712, https://doi.org/10.1016/j.conbuildmat.2011.10.018.

Bisht, K. & Ramana, P.V. (2017). Evaluation of mechanical and durability properties of crumb rubber concrete. *Construction and Building Materials,* 155, 811-817, https://doi.org/10.1016/j.conbuildmat.2017.08.131.

Borges, A., Flores-Colen, I. & Brito, J.D. (2018). Physical and mechanical performance of cement-based renders with different content of fly ash, expanded cork granules and expanded clay. *Construction and Building Materials.* 191, 535-543, https://doi.org/10.1016/j.conbuildmat.2018.10.043.

Braga, M., Brito, J.D. & Veiga, R. (2012). Incorporation of fine concrete aggregates in mortars. *Construction and Building Materials.* 36, 960-968, https://doi.org/10.1016/j.conbuildmat.2012.06.031.

Branco, F.G. & Godinho, L. (2013). On the use of lightweight mortars for the minimization of impact sound transmission. *Construction and Building Materials.* 45. 184-191, https://doi.org/10.1016/j.conbuildmat.2013.04.001.

British Standard (BS 5628-1). (1992).Code of practice for use of masonry – Part 1: Structural use of unreinforced masonry. Committee: B/525.

British Standard (BS EN 1097-6). (2013). Tests for mechanical and physical properties of aggregates. Determination of the particle density and water absorption. Committee: B/502/6.

British Standard (BS EN 933-1). (2012). Tests for geometrical properties of aggregates. Determination of the particle size distribution. Sieving method. Committee: B/502/6.

British Standard (BS EN 12390-3). (2002). Testing hardened concrete – Part 3: Compressive strength of test concrete. United Kingdom.

Bristish Standard (BS 4551). (1998). Method of testing mortars, screeds and plaster: Part 1: Physical testing.

Bristish Standard (BS EN 15167-1). (2006). Ground granulated blast furnace slag for use in concrete, mortar and grout - Part 1: Definitions, specifications and conformity criteria. United Kingdom.

Bristish Standard (BS EN 206-1). (2000). Concrete - Part 1: Specification, performance, production and conformity. United Kingdom.

Carbajo, J., Esquerdo-Lioret, T.V., Ramis, J., Nadal-Gisbert, A.V. & Denia, F.D. (2015). Acoustic properties of porous concrete made from arlite and vermiculite lightweight aggregates. *Materials De Construction,* 65 (320), e072, http://dx.doi.org/10.3989/mc.2015.01115.

Carrajola, R., Hawreen, A. Flores-Colen, I. & Brito, J.D. (2021). Fresh properties of cement-based thermal renders with fly ash, air lime and lightweight aggregates. *Journal of Building Engineering,* 34, 101868, https://doi.org/10.1016/j.jobe.2020.101868.

Cerulli, T., Pistolesi, C., Maltese, C. & Salvioni, D. (2003). Durability of traditional plasters with respect to blast furnace slag-based plaster. *Cement and Concrete Research,* 33 (9), 1375-1383, https://doi.org/10.1016/S0008-8846(03)00072-3.

Chen, J., Zhou, Z., Wu, J.T., Hou, S.G. & Liu, M.C. (2019). Field and laboratory measurement of albedo and heat tranfer for pavement materials. *Construction and Building Materials,* 202, 46-57, https://doi.org/10.1016/j.conbuildmat.2019.01.028.

Chen, B. & Liu, J. (2008). Experimental application of mineral admixures in lightweight concrete with high strength and workability. *Construction and Building Materials,* 22 (6), 1108-1113, https://doi.org/10.1016/j.conbuildmat.2007.03.001.

Cheeerarot, R. & Jaturapitakkul, C. (2004). A study of disposed fly ash from landfill to replace portland cement. *Waste Management,* 24 (7), 701-709, https://doi.org/10.1016/j.wasman.2004.02.003.

Chin, M.Y., Rahman, M.R., Cherlene, Y.W.P. & Anita W.M.C. (2020). The curing time effect on the strength of ground granulated blast furnace slag (GGBFS) mortar. *Construction and Building Materials,* 260, 120622, https://doi.org/10.1016/j.conbuildmat.2020.120622.

Chindaprasirt, P., Buapa, N. & Cao, H.T. (2005). Mixed cement containing fly ash for masonry and plastering work. *Construction and Building Materials,* 19 (8), 612-618, https://doi.org/10.1016/j.conbuildmat.2005.01.009.

Choi, Y.W., Moon, D.J., Kim, Y.J. & Lachemi, M. (2009). Characteristics of mortar and concrete containing fine aggregate manufactured from recycled waste polyethylene terephthalate bottles. *Construction and Building Materials,* 23 (8), 2829-2835, https://doi.org/10.1016/j.conbuildmat.2009.02.036.

Chowdary, P.L., Khutubuddin, S.K., Vinayaka, B., Saikiran, D., Induja, Y. & Narasappa, Y. (2017). An experimental study on cement replacement by GGBS in concrete. *International Journal Innovative Research in Science, Engineering and Technology,* 6 (4), 5966 – 5973, http:// doi:10.15680/ijirset.2017.0604229.

Christy, C.F. & Tensing, D. (2010). Effect of Class-F fly ash as partial replaement with cement and fine aggregate in mortar. *Indian Journal of Engineering & Materials Sciences,* 17 (2), 140-144, http://hdl.handle.net/123456789/8614.

Chung, S.Y., Pawel, S., Kim, D.J., Mohamed, E.E.M. & Mohamed, A.E. (2021). Effect of different expanded aggregates on durability-related characteristics of lightweight aggregate concrete. *Materials Characterization*, 173, 110907, https://doi.org/10.1016/j.matchar.2021.110907.

Claudio, S.K., Samuel, D.S., Orlando, A., Cristhiana, C.A. & Mauricio, M. (2020). Rendering mortars with crumb rubber: Mechanical strength, thermal and fire properties and durability behaviour. *Construction and Building Materials,* 253, 119002, https://doi.org/10.1016/j.conbuildmat.2020.119002.

Coppola, B., Courard, L., Michel, F., Incarnato, L., Scarfato P. & Maio, L. D. (2018). Hygro-thermal and durability properties of a lightweight mortar made with foamed plastic waste aggregates. *Construction and Building Materials,* 170, 200 – 206, https://doi.org/10.1016/j.conbuildmat.2018.03.083.

Damtoft, J.S., Lukasik, J., Herfort, D., Sorrentino, D. & Gartner, E.M. (2008). Sustainable development and climate change initiatives. *Cement and Concrete Research,* 38 (2), 115-127, https://doi.org/10.1016/j.cemconres.2007.09.008.

Dornelles. K., Caram, R. & Sichieri, E. (2015). Natural weathering cool coatings and its effect on solar reflectance of roof surfaces. *Energy Procedia,* 78, 1587-1592, https://doi.org/10.1016/j.egypro.2015.11.216.

Duran-Herrera, A., Juarez, C.A.,Valdez, P. & Bentz, D.P. (2011). Evaluation of sustainable high-volume fly ash concretes. *Cement & Concrete Composites,* 33 (1), 39-45, https://doi.org/10.1016/j.cemconcomp.2010.09.020.

Elmrabet, R., Harfi, A.E. & Youbi, M.S.E. (2019). Study of properties of fly ash cements. *Materials Today: Proceedings,* 13 (3), 850-856, https://doi.org/10.1016/j.matpr.2019.04.048.

Elsharief, A., Cohen, M.D. & Olek, J. (2005). Influence of lightweight aggregate on the microstructure and durability of mortar. *Cement and Concrete Research,* 35 (7), 1368-1376, https://doi.org/10.1016/j.cemconres.2004.07.011.

Ferrandiz-Mas, V., Bond, T., Garcia-Alcocel, E. & Cheeseman, C.R. (2004). Lightweight mortars containing expanded polystyrene and paper sludge ash. *Construction and Building Materials,* 61, 285-292, https://doi.org/10.1016/j.conbuildmat.2014.03.028.

Gandage, A.S., Vinayaka Rao, V.R., Sivakumar, M.V.N., Vasan, A., Venu, M. & Yaswanth, A.B. (2013). Effect of perlite on thermal conductivity of self compacting cocnrete. *Procedia – Social and Behavioral Sciences,* 104, 188-197, https://doi.org/10.1016/j.sbspro.2013.11.111.

Ganesh Babu, K., & Saradhi Babu, D. (2004). Performance of fly ash concrete containing lightweight EPS aggregates. *Cement and Concrete Composites,* 26 (6), 605-611, https://doi.org/10.1016/S0958-9465(03)00034-9.

Gencel, O., Gholampour, A., Tokay, H. & Ozbakkaloglu, T. (2021). Replacement of natural sand with expanded vermiculite in fly ash-based geopolymer mortars. *Applied Sciences,* 11 (4), 1917, https://doi.org/10.3390/app11041917.

Gesoglu, M. & Guneyisi, E. (2011). Permeability properties of self-compacting rubberized concretes. *Construction and Building Materials*, 25 (8), 3319-3326, https://doi.org/10.1016/j.conbuildmat.2011.03.021.

Ghazali, N., Muthusamy, K., Embong, R., Rahim, I.S.A., Muhamad Razali, N.F., Yahaya, F.M., Arffin, N.F. & Ahmad, S.W. (2021). Effect of fly ash as partial cement replacement on workability and compressive strength of palm oil clinker lightweight concrete. *Earth and Environmental Science,* 682, 012038, http:// doi:10.1088/1755-1315/682/1/012038.

Ghizdavet, Z., Stefan, B., Nastac, D., Vasile, O. & Bratu, M. (2016). Sound absorbing materials made by embedding crumb rubber waste in a concrete matrix. *Construction and Building Materials,* 124, 755-763, https://doi.org/10.1016/j.conbuildmat.2016.07.145.

Gholampour, A. & Ozbakkaloglu, T. (2017). Performance of sustainable concretes containing very high volume Class-F fly ash and ground granulated blast furnace slag. *Journal of Cleaner Production,* 162, 1407-1417, https://doi.org/10.1016/j.jclepro.2017.06.087.

Hawileh, R.A., Abdalla, J.A., Fardmanesh, F., Shahsana, P. & Khalili, A. (2017). Performance of reinforced concrete beams casts with different percentages of GGBS replacement to cement. *Archives of Civil and Mechanical Engineering,* 17 (3), 511-519, https://doi.org/10.1016/j.acme.2016.11.006.

He, T., Da, Y.Q., Xu, R.S. & Tang, R.H. (2019). Effect of multiple chemical activators on mechanical property of high replacement high calcium fly ash blended system. *Construction and Building Materials*, 198, 537-545, https://doi.org/10.1016/j.conbuildmat.2018.11.287.

Henlensiefken, R., Castro, J., Bentz, D., Nantung, T. & Weiss, J. (2009). Water absorption in internally cured mortar made with water-filled lightweight aggregate. *Cement and Concrete Research,* 39 (10), 883-892, https://doi.org/10.1016/j.cemconres.2009.06.009.

Herki, B.A., Khatib, J.M. & Negim, E.M. (2013). Lightweight concrete made from waste polystyrene and fly ash. *World Applied Sciences Journal,* 21 (9), 1356-1360, doi: 10.5829/idosi.wasj.2013.21.9.20213.

Hilal, E. & Peiman K. (2016). Pervious concrete pavement incorporating GGBS to alleviate pavement runoff and improve urban sustainability. *Road Materials and Pavement Design,* 19 (1), 167-181, https://doi.org/10.1080/14680629.2016.1251957.

Holmes, N., Browne, A. & Montague, C. (2014). Acoustic properties of concrete panels with crumb rubber as a fine aggregates replacement. *Construction and Building Materials,* 73, 195-204, https://doi.org/10.1016/j.conbuildmat.2014.09.107.

Hsu, S., Chi, M. & Huang, R. (2018). Effect of fineness and replacement ratio of ground fly ash on properties of blended cement mortar. *Construction and Building Materials,* 176, 250-258, https://doi.org/10.1016/j.conbuildmat.2018.05.060.

Huang, C.H., Lin, S.K., Chang, C.S. & Chen, H.J. (2013). Mix propotions and mechanical properties of concrete containing very high-volume of class F fly ash. *Construction and Building Materials,* 46, 71-78, https://doi.org/10.1016/j.conbuildmat.2013.04.016.

International Organizaion for Standardization (ISO-10534-2). (1998). Acoustics – Determination of sound absorption coefficient and impendance in impendance tubes. Part 2: Transfer-function method. Switzerland.

Jhatial, A.A., Goh, W.I., Noridah, M., Touqeer, A.R. & Abdul Razzaque, S. (2020a). Development of thermal insulating lightweight foamed concrete reinforced with polypropylene fibres. *Arabian Journal for Science and Engineering,* 45, 4067-4076, https://doi.org/10.1007/s13369-020-04382-0.

Jhatial, A.A., Goh, W.I., Samiullah, S. & Noridah, M. (2020b). Thermo-mechanical properties of various densities of foamed concrete incorporating polypropylene fibres. *Arabian Journal for Science and Engineering,* 45, 8171-8186, https://doi.org/10.1007/s13369-020-04657-6.

Jhatial, A.A., Goh, W.I., Sohu, S., Mangi, S.A. & Mastoi, A.K. (2020c). Preliminary investigation of thermal behavior of lightweight foamed concrete incorporating palm oil fuel ash and eggshell powder. *Periodica Polytechnica Civil Engineering,* 65 (1), 168-180, https://doi.org/10.3311/PPci.16498.

Karakoc, M.B., Demirboga, R., Turkmen, I., & Can, I. (2012). Effect of expanded perlite aggregate on cyclic thermal loading of HSC and artificial neural network modeling. *Scientia Iranica,* 19 (1), 41-50, https://doi.org/10.1016/j.scient.2011.11.035.

Karakoc, M.B. & Demirboga, R. (2010). HSC with expanded perlite aggregate at wet and dry curing conditions. *Journal of Materials in Civil Engineering,* 22 (12), 1252-1259, https://doi.org/10.1061/(ASCE)MT.1943-5533.0000134.

Karatas, M., Benli, A. & Toprak, H.A. (2019). Effect of incorporation of raw vermiculite as partial sand replacement on the properties of self-compacting mortars at elevated temperature. *Construction and Building Materials,* 221, 163-176, https://doi.org/10.1016/j.conbuildmat.2019.06.077.

Koksal, F., Gencel, O. & Kaya, M. (2015). Combined effect of silica fume and expanded vermiculite on properties of lightweight mortars at ambient and elevated temperatures. *Construction and Building Materials,* 88, 175-187, https://doi.org/10.1016/j.conbuildmat.2015.04.021.

Koksal, F., Mutluay, E. & Gencel, O. (2020). Characteristics of isolation mortars produced with expanded vermiculite and waste expanded polystyrene. *Construction and Building Materials,* 236, 117789, https://doi.org/10.1016/j.conbuildmat.2019.117789.

Kou, S.C., Lee, G., Poon, C.S. & Lai, W.L. (2009). Properties of lightweight aggregate concrete prepared with PVC granules derived from scraped PVC pipes. *Waste Management*, 29 (2), 621-628, https://doi.org/10.1016/j.wasman.2008.06.014.

Kultur, S. & Turkeri, N. (2012). Assessment of long term solar reflectance performance of roof coverings measured in laboratory and in field. *Building and Environment,* 48, 164-172, https://doi.org/10.1016/j.buildenv.2011.09.004.

Kumar, K. S. & Baskar, K. (2014). Responses surfaces for fresh and hardened properties of concrete with E-waste (HIPS). *Journal of Waste Management,* 517219, http://dx.doi.org/10.1155/2014/517219.

Kurt, M., Abdulkadir, C.A., Muhammed, S.G. Rustem G. & Turkay, K. (2015).The effect of fly ash to self-compactability of pumice aggregate lightweight concrete. *Indian Academy of Sciences*, 40 (4), 1343-1359, https://doi.org/10.1007/s12046-015-0337-y.

Lanzon, M & Garcia-Ruiz, P. A. (2008). Lightweight cement mortar: Advantages and inconveniences of expanded perlite and its influence on fresh and hardened state and durability. *Construction and Building Materials,* 22 (8), 1798-1806, https://doi.org/10.1016/j.conbuildmat.2007.05.006.

Lanzon, M & Garcia-Ruiz, P. A. (2009). Lightweight pozzolanic materials used in mortars: Evaluation of their influence on density, mechanical strength and water absorption. *Cement & Concrete Composites,* 31 (2), 114-119, https://doi.org/10.1016/j.cemconcomp.2008.11.003.

Law, D. S.Y.W., Aslani, F. & Ma, M.ASCE. G. (2018). Lightweight self-compacting concrete incorporating perlite, scoria and polystyrene. *Journal of Materials in Civil Engineering,* 30 (8), 04018178, https://doi.org/10.1061/(ASCE)MT.1943-5533.0002350.

Leiva, C., Vilches, L.F., Arenas, C., Delgado, S. & Fernandez-Pereira, C. (2012). Potential recycling of bottom and fly ashes in acoustic mortars and concretes. *ACI Materials Journal,* 109 (5), 529-535.

Levinson, R. & Akbari, H. (2002). Effects of comparison and exposure on the solar reflectance of portland cement concrete. *Cement and concree research,* 32 (11), 1679 – 1698, https://doi.org/10.1016/S0008-8846(02)00835-9.

Levinson, R., Akbari, H. & Berdahl, P. (2010). Measuring solar reflectance – Part 1: Defining a metric that accurately predicts solar heat gain. *Solar Energy,* 84 (9), 1717-1744, https://doi.org/10.1016/j.solener.2010.04.018.

Lim, S.K., Ling, T.C & ,Mohd, W.H. (2012). Strength properties of self-compacting mortar mixed with GGBFS. *Construction Materials,* 165 (2), 87-98, https://doi.org/10.1680/coma.10.00016.

Ling, T.C., Nor, H.M. & Lim, S.K. (2010). Using recycled waste tyres in concrete paving blocks. *Waste and Resource Management,* 163 (1), 37-45, https://doi.org/10.1680/warm.2010.163.1.37.

Ling, T.C & Poon, C.S. (2014). Feasible use of large volumes of GGBS in 100% recycles glass architectural mortar. *Cement & Concrete Composites,* 53, 350-356, https://doi.org/10.1016/j.cemconcomp.2014.05.012.

Liu, X., Chia, K.S. & Zhang, M.H. (2010). Development of lightweight concrete with high resistance to water and chloride-ion penetration. *Cement & Concrete Composites*, 32 (10), 757-766, https://doi.org/10.1016/j.cemconcomp.2010.08.005.

Lucas, J., Brito, J.D., Veiga, R. & Farnha, C. (2016). The effect of using sanitary ware as aggregates on rendering mortar's performance. *Materials and Design,* 91, 155-164, https://doi.org/10.1016/j.matdes.2015.11.086.

Lu, Z., Hanif, A., Lu, C., Liu, K. Sun, G. & Li, Z. (2018). A novel lightweight cementitious composite with enhanced thermal insulation and mechanical properties by extrusion technique. *Construction and Building Materials,* 163, 446-449, https://doi.org/10.1016/j.conbuildmat.2017.12.130.

Lv, J., Zhou, T., Du, Q. & Wu, H. (2015). Effects of rubber particles on mechanical properties of lightweight aggregate concrete. *Construction and Building Materials*, 91, 145-149, https://doi.org/10.1016/j.conbuildmat.2015.05.038.

Manuel, C.P., Antonio, S., Ines, F. & Joao, R.C. (2020). Influence of exposure to elevated temperatures on the physical and mechanical properties of cementitious thermal mortars. *Applied Sciences*, 10 (6), 2200, https://doi.org/10.3390/app10062200.

Medgar, L.M. & Martha, G.V. (2007). Solar reflectance of concretes for LEED sustainable sites credit: Heat island effect. *Research & Development Information by Portland Cement Association*, 1-94, http://www.cement.org/bookstore/profile.asp?itemid=SN2982.

Medina, N. F., Flores-Medina, D. & Hernandez-Olivares, F. (2016). Influence of fibers partially coated with rubber from tire recycling as aggregate on the acoustical properties of rubberized concrete. *Construction and Building Materials*, 129, 25-36, https://doi.org/10.1016/j.conbuildmat.2016.11.007.

Mo, K.H., Johnson Alengaram, U. & Mohd. Z.J. (2015a). Utilization of ground granulated blast furnace slag as partial cement replacement in lightweight oil palm shell concrete. *Materials and Structures*, 48, 2545-2556, https://doi.org/10.1617/s11527-014-0336-1.

Mo, K.H., Johnson Alengaram, U. & Mohd, Z.J. (2015b). Experimental investigation on the properties of lightweight concrete containing waste oil palm shell aggregate. *Procedia Engineering*, 125, 587-593, https://doi.org/10.1016/j.proeng.2015.11.065.

Mo, K.H., Johnson Alengaram, U. & Mohd, Z.J. (2015c). Compressive behaviour of lightweight oil palm shell concrete incorporating slag. *Construction and Building Materials*, 94, 263-269, https://doi.org/10.1016/j.conbuildmat.2015.06.057.

Mo, K.H., Visintin, P., Johnson Alengaram, U. & Mohd. Z.J. (2016). Prediction of the structural behaviour of oil palm shell lightweight concrete beams. *Construction and Building Materials*, 102 (1), 722-732, https://doi.org/10.1016/j.conbuildmat.2015.10.184.

Mo, K.H., Ling, T.C., Johnson Alengaram, U., Yap, S.P. & Yuen, C.W. (2017). Overview of supplementary cementitious materials usage in lightweight aggregate concrete. *Construction and Building Materials,* 139 , 403-418, https://doi.org/10.1016/j.conbuildmat.2017.02.081.

Mo, K.H., Lee, H.J., Yong, M. & Ling, T.C. (2018). Incorporation of expanded vermiculite lightweight aggregate in cement mortar. *Construction and Building Materials,* 179, 302-306, https://doi.org/10.1016/j.conbuildmat.2018.05.219.

Mohammed, B.S., Anwar Hossain, K.M., Jackson, T.E.S., Wong, G. & Abdullahi, M. (2012). Properties of crumb rubber hollow concrete block. *Journal of Cleaner Production,* 23 (1), 57-67, https://doi.org/10.1016/j.jclepro.2011.10.035.

Mohan, A & Mini, K.M. (2018). Strength and durability studies of SCC incorporating silica fume and ultra fine GGBS. *Construction and Building Materials,* 171, 919-928, https://doi.org/10.1016/j.conbuildmat.2018.03.186.

Mortar Industry Association (MIA). (2015). A Guide to BS EN 998-1 and BS EN 998-2. *Material Products Association.* Retrieved on: February 15, 2020: http://www.mortar.org.uk/documents/miadata19.pdf.

Muhammad, R.A. & Chen, B. (2019). Experimental research on the performance of lightweight concrete containing foam and expanded clay aggregate. *Composites*

Part B: Engineering, 171, 46-60, https://doi.org/10.1016/j.compositesb.2019.04.025.

Muhammad, R.A., Chen, B. & Syed, F.A.S. (2019). Investigate the influence of expanded clay aggregate and silica fume on the properties of lightweight concrete. *Construction and Building Materials*, 220, 253-266, https://doi.org/10.1016/j.conbuildmat.2019.05.171.

Munoz-Ruiperez, C., Rodriguez, A., Gonzalez, G. & Calderon, V. (2016). Lightweight masonry mortars made with expanded clay and recycled aggregates. *Construction and Building Materials*, 118, 139-145, https://doi.org/10.1016/j.conbuildmat.2016.05.065.

Munoz-Ruiperez, C., Rodriguez, A., Junco, C., Fiol, F. & Calderon, V. (2018). Durability of lightweight concrete made concurrently with waste aggregates and expand clay. *Structural Concrete*, 19 (5), 1309-1317, https://doi.org/10.1002/suco.201700209.

Muthusamy, K., Budiea, A.M.A., Azhar, N.W., Jaafar, M.S., Syed Mohsin, S.M., Arifin, N.F. & Yahaya, F.M. (2021). Durability properties of oil palm shell lightweight aggregate concrete containing fly ash as partial cement replacement. *Materials Today: Proceedings,* 41 (1), 56-60, https://doi.org/10.1016/j.matpr.2020.10.1003.

Nakarai, K., Suzuki, Y., Mori, M., Ho, L.S. Arai, A. & Kobayashi, Y. (2019). Physicomechanical properties and durability of a new lightweight porous mortar utilizing woodchips. *Journal of Cleaner Production,* 235, 158-165, https://doi.org/10.1016/j.jclepro.2019.06.244.

Neno, C., Brito, J.D., Veiga, R. (2014). Using fine recycled concrete aggregate for mortar production. *Material Research,* 17 (1), 168-177, https://doi.org/10.1590/S1516-14392013005000164.

Ngohpok, C., Sata, V., Satiennam, T., Klungboonkrong, P. & Cjindaprosirt, P. (2018). Mechanical properties, thermal conductivity and sound absorption of pervious concrete containing recycled concrete and bottom ash aggregates. *KSCE Journal of Civil Engineering,* 22, 369-1376, https://doi.org/10.1007/s12205-017-0144-6.

Nguyen, T.B.T, Saengsoy, W. & Tangtermsirikul, S. (2018). Effect of initial moisture of wet fly ash on the workability and compressive strength of mortar and concrete. *Construction and Building Materials,* 183, 408-416, https://doi.org/10.1016/j.conbuildmat.2018.06.192.

Nickholas Anting.A.G., Fadhil, M.M.D., Ponraj, M. & Iwao, K. (2014). Thermal performance of developed coating material as cool pavement material for tropical regions. *Journal of Materials in Civil Engineering,* 26 (4), 755-760, https://doi.org/10.1061/(ASCE)MT.1943-5533.0000859.

Ofosu-Adarkwa, J., Xie, N. & Ahmed Javed, S. (2020). Forecasting CO_2 emissions of China's cement industry using a hybird Verhulst-GM (1, N) model and emissions' technical conversion. *Renewable and Sustainable Energy Reviews,* 130, 109945, https://doi.org/10.1016/j.rser.2020.109945.

Oktay, H., Yumrutas, R. & Akpolat, A. (2015). Mechanical and thermophysical properties of lightweight aggregate concretes. *Construction and Building Materials,* 96, 217-225, https://doi.org/10.1016/j.conbuildmat.2015.08.015.

Oliveira, L.A.P.D., Castro Gomes, J.P. & Nepomuceno, M.C.S. (2013). The influence of wastes materials on the rheology of rendering mortars. *Applied Rheology,* 23 (1), 15505, https://doi.org/10.3933/applrheol-23-15505.

Oner, A. & Akyuz, S. (2007). An experimental study on optimum usage of GGBS for the compressive strength of concrete. *Cement & Concrete Composites,* 29 (6), 505-514, https://doi.org/10.1016/j.cemconcomp.2007.01.001.

Palomar, I., Barluenga, G. & Puentes, J. (2015). Lime-cement mortars for coating with improved thermal and acoustic performance. *Construction and Building Materials*, 75, 306-314, https://doi.org/10.1016/j.conbuildmat.2014.11.012.

Pastor, J.M., Garcia, L.D., Quintana, S. & Pena, J. (2014). Glass reinforced concrete panels containing recycled tyres- Evaluation of the acoustic properties of for their use as sound barriers. *Construction and Building Materials*, 54, 541-549, https://doi.org/10.1016/j.conbuildmat.2013.12.040.

Penacho, P., Brito, J.D. & Veiga, M.R. (2014). Physico-mechanical and performance characterization of mortars incorporating fine glass waste aggregate. *Cement & Concrete Composites*, 50, 47-59, https://doi.org/10.1016/j.cemconcomp.2014.02.007.

Pisello, A. L. (2015). High-albedo roof coatings for reducing building cooling needs. *Eco-efficient Materials for Mitigating Building Cooling Needs*, Woodhead Publishing, 243-268, https://doi.org/10.1016/B978-1-78242-380-5.00009-1.

Prakash, R., Thenmozhi, R. & Raman, S.N. (2019). Mechanical characterisation and flexural performance of eco-friendly concrete produced with fly ash as cement replacement and coconut shell coarse aggregate. *International Journal of Environment and Sustainable Development*, 18 (2), 131-148, https://doi.org/10.1504/IJESD.2019.099491.

Prasath Kumar, V.R., Gunasekaran, K. & Shyamala, T. (2019). Characterization study on coconut shell concrete with partial replacement of cement by GGBS. *Journal of Building Engineering*, 26, 100830, https://doi.org/10.1016/j.jobe.2019.100830.

Radwan, M.K.H., Onn, C.C.O., Mo, K.H., Yap, S.P., Ng., C.G. & Yusoff, S. (2021a). Eco-mechanical performance of binary and ternary cement blends containing fly ash and slag. *Proceedings of the Institution of Civil Engineers,* 174 (1), 23-26, https://doi.org/10.1680/jensu.20.00009.

Radwan, M.K.H., Onn, C.C.O., Mo, K.H., Yap, S.P., Chin, R.J. & Lai, S.H. (2021b). Sustainable ternary cement blends with high-volume ground granulated blast furnace slag-fly ash. *Environment, Development and Sustainability,* 1-35, https://doi.org/10.1007/s10668-021-01633-4.

Rashad, A. M. (2015). A brief on high-volume Class F fly ash as cement replacement – A guide for Civil Engineer. *International Journal of Sustainable Built Environment,* 4 (1), 278-306, https://doi.org/10.1016/j.ijsbe.2015.10.002.

Rashad, A. M. (2016a). A synopsis about perlite as building materials – A best practice guide for civil engineer. *Construction and Building Materials,* 121, 338-353, https://doi.org/10.1016/j.conbuildmat.2016.06.001.

Rashad, A. M. (2016b). Vermiculite as a construction material – A short guide for civil engineer. *Construction and Building Materials,* 125, 53-62, https://doi.org/10.1016/j.conbuildmat.2016.08.019.

Reza, F & Boriboonsomsin, K. (2015). Pavements made of concrete with high solar reflectance. *Eco-efficient materials for mitigating building cooling needs*, Woodhead Publishing, 37-62, https://doi.org/10.1016/B978-1-78242-380-5.00003-0.

Rickard, W.D.A., Gluth, G.J.G. & Pistol, K. (2016). In-situ thermo-mechanical testing of fly ash geopolymer concretes made with quartz and expanded clay aggregates. *Cement and Concrete Research*, 80, 33-43, https://doi.org/10.1016/j.cemconres.2015.11.006.

Rooholamini, H., Haassani, A. & Aliha, M.R.M. (2018). Evaluating the effect of macro-synthetic fibre on the mechanical properties of roller-compacted concrete pavement using response surface methodology. *Construction and Building Materials,* 159, 517-529, https://doi.org/10.1016/j.conbuildmat.2017.11.002.

Rozycka, A. & Pichor, W. (2016). Effect of perlite waste addition on the properties of autoclaved aerated concrete. *Construction and Building Materials,* 120, 65-71, https://doi.org/10.1016/j.conbuildmat.2016.05.019.

Sabet, F.A., Libre, N.A. & Schekarchi, M. (2013). Mechanical and durability properties of self-consolidating high performance concrete incorporating natural zeolite, silica fume and fly ash. *Construction and Building Materials,* 44, 175-184, https://doi.org/10.1016/j.conbuildmat.2013.02.069.

Sahmaran, M. & Yaman, I. O. (2007). Hybrid fiber reinforced self-compacting concrete with a high-volume conarse fly ash. *Construction and Building Materials,* 21 (1), 150-156, https://doi.org/10.1016/j.conbuildmat.2005.06.032.

Sailor, D. J., Resh, K. & Segura, D. (2006). Field measurement of albedo for limited extent test surfaces. *Solar Energy,* 80 (6), 589-599, https://doi.org/10.1016/j.solener.2005.03.012.

Schackow, A., Effting, C., Folgueras, M.V., Guths, S. & Mendes, G.A. (2014). Mechanical and thermal properties of lightweight concretes with vermiculite and EPS using air-entraining agent. *Construction and Building Materials,* 57, 190-197, https://doi.org/10.1016/j.conbuildmat.2014.02.009.

Sengul, O., Azizi, S., Karaosmanoglu, F. & Ali Tasdemir, M. (2011). Effect of expanded perlite on the mechanical properties and thermal conductivity of lightweight concrete. *Energy and Buildings,* 43 (2-3), 671-676, https://doi.org/10.1016/j.enbuild.2010.11.008.

Shafigh, P., Mohd, Z.J., Hilmi, B.M. & Johnson Alengaram, U. (2013). Oil palm shell lightweight concrete containing high volume ground granulated blast furnace slag. *Construction and Building Materials*, 40, 231-238, https://doi.org/10.1016/j.conbuildmat.2012.10.007.

Shafigh, P., Mohd, A.N., Johnson Alengaram, U., Hilmi, B.M. & Mohd, Z.J (2016). Engineering properties of lightweight aggregate concrete containing limestone powder and high volume fly ash. *Journal of Cleaner Production*, 135, 148-157, https://doi.org/10.1016/j.jclepro.2016.06.082.

Shah, S.N., Mo, K.H., Yap, S.P., Putra, A. & Muhammad, N.O. (2021). Assessment of lightweight recycled crumb rubber-cement composite produced by preplaced method. *Advances in Concrete Construction*, 11 (5), 409-417, https://doi.org/10.12989/acc.2021.11.5.409.

Shaikh, F.U.A. & Supit, S.W.M. (2015). Compressive strength and durability properties of high volume fly ash (HVFA) concrete containing ultrafine fly ash (UFFA). *Construction and Building Materials,* 82, 192-205, https://doi.org/10.1016/j.conbuildmat.2015.02.068.

Shannag, M.J. (2011). Characteristics of lightweight concrete containing mineral admixtures. *Construction and Building Materials*, 25 (2), 658-662, https://doi.org/10.1016/j.conbuildmat.2010.07.025.

Si, R., Wang, J., Guo, S., Dai, Q. & Han, S. (2018). Evaluation of laboratory performance of self-consolidating concrete with recycled tire rubber. *Journal of Cleaner Production*, 180, 823-831, https://doi.org/10.1016/j.jclepro.2018.01.180.

Siddique, R. (2004). Performance characteristics of high-volume Class F fly ash concrete. *Cement and Concrete Research,* 34 (3), 487-493, https://doi.org/10.1016/j.cemconres.2003.09.002.

Siddique, R. & Bennacer, R. (2012). Use of iron and steel industry by product (GGBS) in cement paste and mortar. *Resources, Conservation and Recycling,* 69, 29-34, https://doi.org/10.1016/j.resconrec.2012.09.002.

Silva, L.M., Ribeiro, R.A., Labrincha, J.A. & Ferreira, V.M. (2010). Role of lightweight fillers on the properties of mixed-binder mortar. *Cement & Concrete Composites,* 32 (1), 19-24, https://doi.org/10.1016/j.cemconcomp.2009.07.003

.

Sindhuja, S., Saketh Raman, K. & Bhuvaneshwari, P. (2020). A review on strength characteristics of GGBS based fiber-reinforced lightweight aggregate concrete. *Materials Science and Engineering*, 872, 012135, http://doi:10.1088/1757-899X/872/1/012135.

Srivastava, V., Atul, Mehta, P.K., Satyendranath, Tripathi, M.K. (2018). Supplementary cementitious materials in construction – An attempt to reduce CO_2 emission. *Journal of Environmental Nanotechnology* 7 (2), 31-35, http:// doi:10.13074/jent.2018.06.182306.

Sugapriya, P. & Ramkrishnan, R. (2018). Crumb rubber recycling in enhancing damping properties of concrete. *Materials Science and Engineering*, 310, 012013, http:// doi:10.1088/1757-899X/310/1/012013.

Sukontasukkul, P. (2009). Use of crumb rubber to improve thermal and sound properties of pre-cast concrete panel. *Construction and Building Materials,* 23 (2), 1084-1092, https://doi.org/10.1016/j.conbuildmat.2008.05.021.

Sun, Y., Wang, K.Q. & Lee, H.S. (2021). Prediction of compressive strength development for blended cement mortar considering fly ash fineness and replacement ratio. *Construction and Building Materials,* 271, 121532, https://doi.org/10.1016/j.conbuildmat.2020.121532.

Suryakanta. (2017). 6 Important Engineering Properties of Mortar. *CIVILBLOG.ORG.* Retrieved on: October 18, 2020: https://civilblog.org/2017/06/02/6-important-engineering-properties-mortar/

Tanwar, V., Bisht, K., Ahmed Kabeer, K.I. & Ramana, P.V. (2021). Experimental investigation of mechanical properties and resistance to acid and sulphate attack of GGBS based concrete mixes with beverage glass waste as fine aggregate. *Journal of Building Engineering*, 41, 102372, https://doi.org/10.1016/j.jobe.2021.102372.

Tanyildizi, H. & Coskun, A. (2008). The effect of high temperature on compressive strength and splitting tensile strength of structural lightweight concrete containing fly ash. *Construction and Building Materials*. 22 (11), 2269-2275, https://doi.org/10.1016/j.conbuildmat.2007.07.033.

Tavasoli, S., Nili, M., & Serpoush, B. (2018). Effect of GGBS on the frost resistance of self-consolidating concrete. *Construction and Building Materials,* 165, 717-722, https://doi.org/10.1016/j.conbuildmat.2018.01.027.

Thakur, I.C., Kisku, N., Singh, J.P. & Kumar, S. (2016). Properties of concrete incorporated with GGBS. *International Journal of Research in Engineering and Technology,* 5 (8), 275 – 281, http://doi:10.15623/IJRET.2016.050846.

Tiwari, V., Shukla, A. & Bose, A. (2004). Acoustic properties of cenosphere reinforced cement and asphalt concrete. *Applied Acoustics,* 65 (3), 263-275, https://doi.org/10.1016/j.apacoust.2003.09.002.

Tommy, Y.L., Cui, H.Z., Abid, N. & Li, Z.G. (2006). The effect of air content on permeability of lightweight concrete. *Cement and Concrete Research*, 36 (10), 1874-1878, https://doi.org/10.1016/j.cemconres.2006.06.009.

Turkmen, I. & Kantarci, A. (2007). Effects of expanded perlite aggregate and different curing conditions on the physical and mechanical properties of self-compacting concrete. *Building and Environment.* 42 (6), 2378-2383, https://doi.org/10.1016/j.buildenv.2006.06.002.

Wainwright, P.J. & Rey, N. (2000). The influence of ground granulated blast furnace slag (GGBS) additions and time delay on the bleeding of concrete. *Cement and Concrete Composites*, 22 (4), 253-257, https://doi.org/10.1016/S0958-9465(00)00024-X.

Xie, J., Liu, J. Wang, J. & Huang, P. (2019). Investigation of a new lightweight green concrete containing sludge ceramsite and recycled fine aggregates. *Journal of Cleaner Production*, 235, 1240-1254, https://doi.org/10.1016/j.jclepro.2019.07.012.

Xie, J., Li, J., Lu, Z., Li, Z., Fang, C., Huang, L. & Li, L. (2019). Combination effects of rubber and silica fume on the fracture behaviour of steel-fibre recycled aggregate concrete. *Construction and Building Materials*, 202, 164-173, https://doi.org/10.1016/j.conbuildmat.2019.01.094.

Xie, J., Zhao, J., Wang, J., Huang, P. & Liu, J. (2020). Investigation of the high-temperature resistance of sludge ceramiste concrete with recycled aggregates and GGBS and its application in hollow blocks. *Journal of Building Engineering*, 34, 101954, https://doi.org/10.1016/j.jobe.2020.101954.

Yan, B.F. & Lee, S.H. (2017). Measurement of reflected solar radiation of urban pavement materials. *Journal of Technology*, 32 (1), 1-11.

Yang, K., Jung, Y., Cho, M. & Tae, S. (2014). Effect of supplementary cementitious materials on reduction of CO_2 emissions from concrete. *Journal of Cleaner Production*, 103, 774-783, https://doi.org/10.1016/j.jclepro.2014.03.018.

Yoon, S., Monteiro, P.J.M., Macphee, D.E.M., Glasser, F.P. & Mohammed, S.E.I. (2014). Statistical evaluation of the mechanical properties of high-volume class F-fly ash concretes. *Construction and Building Materials*, 54, 432-442, https://doi.org/10.1016/j.conbuildmat.2013.12.077.

Yu, Y. & Zhu, H. (2016). Influence of rubber size on properties of crumb rubber mortars. *Multidisciplinary Digital Publishing Institute*, 9 (7), 527, https://doi.org/10.3390/ma9070527.

Zahid Hossain, F.M., Shahjalal, Md., Kamrul, I., Mohammad, T., Shahria Alam, M. (2019). Mechanical properties of recycled aggregate concrete containing crumb rubber and polypropylene fiber. *Construction and Building Materials*, 225, 983-996, https://doi.org/10.1016/j.conbuildmat.2019.07.245.

Zhang, T., Gao, P., Gao, P., Wei, J. & Yu, Q. (2013). Effectiveness of novel and traditional methods to incorporate industrial wastes in cementitious materials -An Review. *Resources, Conservation and Recycling*, 74, 134-143, https://doi.org/10.1016/j.resconrec.2013.03.003.

LIST OF PUBLICATION

Tie, T.S., Mo, K.H., Azma, P., Loo, S.C., Johnson Alengaram, U. & Ling, T.C. (2020). Sound absorption performance of modified concrete: A review. *Journal of Building Engineering.* 30, 101219, https://doi.org/10.1016/j.jobe.2020.101219.

Tie, T.S., Mo, K.H., Johnson Alengaram, U., Senthil Kumar, K. & Ling, T.C. (2020). Study on the use of lightweight expanded perlite and vermiculite aggregates in blended cement mortars. *European Journal of Environment and Civil Engineering,* https://doi.org/10.1080/19648189.2020.1806934.